

# Large scale RNAi screen in *Tribolium* reveals novel genes involved in dorsoventral pattern formation

## In a u g u r a l - D i s s e r t a t i o n

zur  
Erlangung des Doktorgrades  
der Mathematisch-Naturwissenschaftlichen Fakultät  
der Universität zu Köln



vorgelegt von

Muhammad Salim Din Muhammad

aus Afghanistan

Köln, 2018

**Berichterstatter:**

**Prof. Dr. Siegfried Roth**

**PD Dr. Michael Kroiher**

**Vorsitzender der Prüfungskommission:**

**Prof. Dr. Ute Höcker**

**Prüfungsdatum:**

**27.02.2018**

# Table of Contents

---

<b>1. Abstract</b>	5
<b>2. Zusammenfassung</b>	6
<b>3. Introduction</b>	8
3.1 Emerging model organism <i>Tribolium castaneum</i>	8
3.2 Evolution of dorsoventral patterning mechanism	9
3.3 Dorsoventral axis formation in <i>Drosophila melanogaster</i>	10
3.3.1 Establishment of dorsoventral asymmetry during oogenesis	10
3.3.2 Establishment of embryonic DV patterning	11
3.3.3 Dorsal morphogen gradient formation	13
3.4 Dorsoventral patterning in <i>Tribolium castaneum</i>	15
<b>4. Aim of the Thesis</b>	19
<b>5. Material and Methods</b>	20
5.1 iBeetle RNAi screening	22
5.2 Embryonic RNA isolation	25
5.3 cDNA synthesis	25
5.4 Polymerase chain reaction (PCR)	25
5.5 Double stranded RNA synthesis	26
5.6 DIG labeled probes synthesis	27
5.7 Fixation of embryos	27
5.8 <i>In situ</i> hybridization (ISH)	27
5.9 Double <i>in situ</i> hybridization (D-ISH)	28
5.10 Antibody staining	29
5.11 Microscopy and photos processing	29
5.12 Phylogenetic analysis	29
5.13 Quantitative reverse transcription PCR (qRT-PCR)	30
<b>6. Results</b>	31
6.1 The iBeetle large scale RNA interference screen	31
6.2 Re-screening and selection of the iBeetle candidates	34
6.3 iB-09824 (TC032710) anionic trypsin-2-like serine protease	36
6.4 iB-07888 (TC011067) serine protease P125	39
6.5 iB-06699 (TC034678) Leukocyte elastase inhibitor	50
6.6 iB-06774 <i>spatzle</i> (ligand of the Toll receptor)	57

<b>7. Discussion.....</b>	<b>62</b>
7.1 Novel DV patterning genes identified in the iBeetle screen .....	62
7.2 iB-06774 <i>Spaetzle</i> functions as a ligand for the <i>Toll</i> receptor.....	63
7.3 iB-09824 and iB-07888 act upstream of Toll signaling .....	65
7.4 iB-06699 regulates the activity of the protease cascade.....	68
7.5 Spatial and temporal regulation of Dorsal target genes.....	69
<b>8. Conclusion and Future Outlook .....</b>	<b>72</b>
<b>9. Supplementary Information .....</b>	<b>73</b>
<b>10. References .....</b>	<b>86</b>
<b>11. Acknowledgements.....</b>	<b>91</b>
<b>12. Erklärung.....</b>	<b>92</b>
<b>13. Curriculum Vitae .....</b>	<b>93</b>



# 1. Abstract

---

The detailed knowledge about dorsoventral (DV) axis formation in *Drosophila melanogaster* provides an excellent platform for comparative studies of embryonic DV patterning within insects. In *Drosophila*, the ventral activation of Toll-receptor initiates the nuclear uptake of the transcription factor NF- $\kappa$ B/Dorsal resulting in a stable nuclear Dorsal gradient, which regulates zygotic target genes like the mesodermal gene *twist* and the neuroectodermal gene *short gastrulation (sog)* in a concentration dependent manner. In the red flour beetle *Tribolium castaneum*, NF- $\kappa$ B/Dorsal also forms a nuclear concentration gradient. This gradient, however, is highly dynamic due, to positive and negative feedback loops. Both *Tc-Toll* and the inhibitor *Tc-cactus* are activated zygotically by Toll signaling.

In the past, the investigation of DV patterning genes in *T. castaneum* was based on a candidate gene approach. Through this comparative approach, only genes which were known to have a DV function in *D. melanogaster* were investigated in *T. castaneum*, which leads to biased conserved gene function analysis. Hence, novel DV patterning genes in *T. castaneum* that are not present in *D. melanogaster*, could not be identified through a candidate gene approach. Therefore, I have participated in a large scale RNAi screen (the iBeetle screen Phase-II). The unbiased iBeetle RNAi screen provided an excellent platform to overcome the limitations of the candidate gene approach and revealed novel DV patterning genes in *T. castaneum*.

In the course of a large scale RNAi screen in *T. castaneum*, we have identified three novel DV patterning genes (two serine proteases and one serpin inhibitor) and the Toll ligand Spaetzle. The newly identified genes act upstream of Toll signaling and regulate the activity of NF- $\kappa$ B/Dorsal gradient formation and the activation of zygotic target genes. Knockdown of both iB-09824 (anionic trypsin-2-like serine protease) and iB-06774 (*spaetzle*) produced *Toll*-like dorsalized phenotype, whereas knockdown of iB-06699 (leukocyte elastase inhibitor-like) revealed ventralized phenotype. In addition, another positive feedback element, a new serine protease (iB-07888) was identified in the iBeetle screen. iB-07888 is likely to act upstream of *Toll* within the protease cascade activating the Toll ligand Spaetzle. The expression of this gene is activated ventrally during early blastoderm stage in a broad domain along the entire egg length. After iB-07888 knockdown, *Tc-twist*, *Tc-sim* and *Tc-cactus* lack early expression and are activated only during early gastrulation. This corresponds to a delayed formation of the nuclear Dorsal gradient. In contrast to *Tc-twist* *Tc-sim* and *Tc-cactus*, the expression of *Tc-sog* is completely lost in most knockdown embryos. This suggests that the new protease affects the timing of Dorsal gradient formation. Taken together, our results indicate that the Dorsal target genes in *T. castaneum* are activated in a temporal sequence to define their spatial expression domains at different time points. We propose that in contrast to *D. melanogaster*, where several Dorsal target genes are activated simultaneously in a concentration dependent manner, the *Tribolium* NF- $\kappa$ B Dorsal gradient acts by a temporal shift to regulate its zygotic target genes in a time-dependent manner.

## 2. Zusammenfassung

---

Das tiefgehende Verständnis der dorsoventralen (DV) Achsenbildung in *Drosophila melanogaster* bildet eine ausgezeichnete Grundlage für vergleichende Studien der embryonalen DV Musterbildung in Insekten. In *Drosophila* führt die ventrale Aktivierung des Toll-Rezeptors zur Translokation des Transkriptionsfaktors NF- $\kappa$ B/Dorsal in den Nukleus, wodurch ein stabiler nukleärer Dorsal Gradient gebildet wird. Dies wiederum führt zu der konzentrationsabhängigen Aktivierung zygotischer Zielgene, wie z.B. des mesodermalen Gens *twist* oder des neuroektodermalen Gens *short gastrulation (sog)*. Im rotbraunen Reismehlkäfer *Tribolium castaneum* bildet NF- $\kappa$ B/Dorsal ebenfalls einen nukleären Konzentrationsgradienten. Der Toll-Signalweg führt dort jedoch zur zygotischen Aktivierung des Rezeptors *Tc-Toll* und des Inhibitors *Tc-cactus*. Aufgrund dieser positiven und negativen Rückkopplungsmechanismen ist der NF- $\kappa$ B/Dorsal Gradient in *T. castaneum* sehr dynamisch.

Die Analyse der DV Musterbildungsgene wurde in *T. castaneum* bisher mithilfe eines Kandidatengenansatzes durchgeführt. Dieser vergleichende Ansatz führte zu einer einseitigen Betrachtung des DV Systems in *T. castaneum*, da nur Gene analysiert wurden, deren Funktion in *D. melanogaster* konserviert sind. Ein Kandidatengenansatz ist somit nicht geeignet bisher unbekannte Gene zu identifizieren, die in *T. castaneum*, aber nicht in *D. melanogaster* eine Funktion in der DV Musterbildung übernehmen. Daher habe ich an einem großangelegten RNAi Screen mitgearbeitet (iBeetle Screen, Phase-II). Der iBeetle-Screen ist sehr gut geeignet, die Limitationen des Kandidatengenansatzes zu überwinden, und führte aufgrund seines unvoreingenommenen Designs zu der Entdeckung neuer DV Musterbildungsgene in *T. castaneum*.

Im Verlauf des iBeetle Screens konnten wir sowohl drei bisher unbekannte DV Musterbildungsgene (zwei Serin-Proteasen und einen Serpin-Inhibitor), als auch den *Toll* Liganden *spätzle* identifizieren. Die neu identifizierten Gene sind dem Toll-Signalweg vorgeschaltet und beeinflussen die Bildung des NF- $\kappa$ B/Dorsal Gradienten und die Regulation seiner zygotischen Zielgene. Sowohl die Reduktion der Aktivität von iB-09824 (anionische Trypsin-2-ähnliche Serin-Protease), als auch von iB-06774 (*spätzle*) führen zu *Toll* ähnlichen, dorsalisierten Phänotypen. Die Verminderung des Genprodukts von iB-06699 (Leukozyten Elastase-Inhibitor-ähnlich) hingegen führte zu ventralisierten Phänotypen. Es wurde zudem auch eine neue Serin-Protease (iB-07888) entdeckt, die Bestandteil eines positiven Rückkopplungsmechanismus ist. iB-07888 agiert wahrscheinlich vorgeschaltet zu *Toll*, in der Proteasekaskade, die zur Aktivierung des *Toll* Liganden *spätzle* führt. Das Gen wird initial während des frühen Blastoderms entlang des gesamten Eies auf der ventralen Seite exprimiert. Eine Verminderung der Genaktivität von iB-07888 führt zu dem Verlust der frühen Expression von *Tc-twist*, *Tc-sim* und *Tc-cactus*. Sie werden erst während der frühen Gastrulation aktiviert. Dies ist im Einklang mit der verzögerten Bildung des nukleären Dorsal Gradienten. Im Gegensatz dazu ist jedoch in den meisten RNAi-Embryonen überhaupt keine Expression von *Tc-sog* mehr nachweisbar. Diese Beobachtungen deuten daraufhin, dass die neue Protease den Zeitpunkt der Bildung des Dorsal-Gradienten beeinflusst. Zusammengefasst führen unsere Ergebnisse zu der Annahme, dass die Zielgene von Dorsal in *T. castaneum* in einer temporalen Sequenz aktiviert werden, um die räumlichen

Expressionsdomänen zu verschiedenen Zeitpunkten zu bilden. Wir postulieren, dass im Gegensatz zu *D. melanogaster*, wo konzentrationsabhängig mehrere Zielgene simultan aktiviert werden, der NF- $\kappa$ B/Dorsal Gradienten in *Tribolium* seine zygotischen Zielgene mithilfe einer temporalen Verschiebung zeitabhängig reguliert.

### 3. Introduction

---

**“A study of the effects of genes during development is as essential for an understanding of evolution as are the study of mutation and that of selection”**

**Julian Huxley, *Evolution: The Modern Synthesis* (1942)**

One of the most fascinating questions in developmental biology is how does a group of identical cells specify different cell fates and well-defined anterior-posterior (AP) and dorsal-ventral (DV) pattern formation during embryogenesis. The identification of several genes in major signaling pathways by the famous Heidelberg-Screen, delivered a comprehensive platform for better understanding of the developmental processes involved in embryonic pattern formation in *Drosophila melanogaster* (Nüsslein-Volhard and Wieschaus, 1980). For a long time, research on developmental genetics was limited to just two invertebrate model organisms, *D. melanogaster* and *Caenorhabditis elegans* (Sommer, 2009). However, the availability of the genome sequences in recent times and the development of new genetic tools, including forward and reverse genetics, allowed researchers to conduct gene function analyses in new model organisms. The successful application of RNA interference (RNAi) technology in other arthropods created a solid platform for comparative studies of the gene network evolution and embryonic pattern formation within insects (Anderson and Irvine, 2009; Sommer, 2009). Comparative analyses between closely related species of the same taxa are needed to investigate the evolution and mechanisms of embryonic pattern formation. Here we compare the well-studied traditional model organism *D. melanogaster* with an emerging model organism *Tribolium castaneum* (Sommer, 2009; Lynch and Roth, 2011).

#### 3.1 Emerging model organism *Tribolium castaneum*

The advancement of molecular genetic tools and the increasing availability of the whole genome sequences of non-drosophilid arthropod model organisms have revolutionized the field of evolutionary developmental biology (Evo-Devo). Recently, several non-drosophilid arthropod model organisms (*T. castaneum*, *Nasonia vitripennis*, *Oncopeltus fasciatus* etc.) have been used for comparative studies to investigate the evolution of developmental patterning mechanisms (Sachs et al., 2015; Lynch and Roth, 2011). Nevertheless, the red flour beetle, *T. castaneum* is leading the way and emerging as a model organism in many aspects. The availability of the whole genome sequence (Richards et al., 2008), its ancestral short mode of embryogenesis (Lynch et al., 2011), the presence of two extra-embryonic membranes (van der Zee et al., 2005), highly efficient systemic parental RNAi response (Schmitt-Engel et al., 2015; Bucher et al., 2002) and other tools for live imaging and insertional mutagenesis (Benton et al., 2013; Trauner et al., 2009) made *T. castaneum* one of the most powerful model systems for comparative studies. Therefore, we have selected *T. castaneum* as a model organism to investigate the evolution of embryonic DV patterning mechanism within insects.

### 3.2 Evolution of dorsoventral patterning mechanism

Despite differences in the body shapes and modes of embryogenesis, most of the signaling pathways necessary for establishing pattern formations are evolutionarily conserved in different organisms (Lynch and Roth, 2011). For instance, the establishment of DV patterning by Chordin-BMP signaling was found to be highly conserved between invertebrate and vertebrate model organisms (Lynch and Roth, 2011; De Robertis, 2008). Regardless of these highly conserved processes for embryonic axial patterning, several evolutionary novelties emerged during evolution. For instance, the importance of BMP signaling for embryonic DV patterning was gradually reduced and taken over by Toll signaling during insect evolution (Sachs et al., 2015; Lynch and Roth, 2011). Besides, Toll signaling has a conserved ancestral role in innate immunity in a wide range of animals from hydra to humans and its function in DV patterning appears to be an evolutionary novelty of insects (Sachs et al., 2015).

In *Drosophila*, Toll signaling generates the ventral cell fates by activating genes like *twist*, while the dorsal cell fates are specified by restricting the BMP signaling to the dorsal side through activation of *sog* and inhibition of *dpp* (Figure 1). In contrast to *Drosophila*, Toll signaling in *Tribolium* doesn't function directly as a repressor of BMP signaling but it restricts the BMP signaling on the dorsal side only by activating *sog* (Sachs et al., 2015; Lynch and Roth, 2011). BMP signaling has extended function in DV pattern formation in more basally branched insects such as *Nasonia* and *Oncopeltus*. In *Nasonia*, Toll signaling is essential only to establish the ventral cell fates, while the expression domains of the ventrally expressed genes are demarcated by BMP signaling. In *Oncopeltus*, BMP signaling is essential for cell fates specification along the DV axis, while the role of Toll signaling is limited only to polarize the BMP signaling (Sachs et al., 2015).

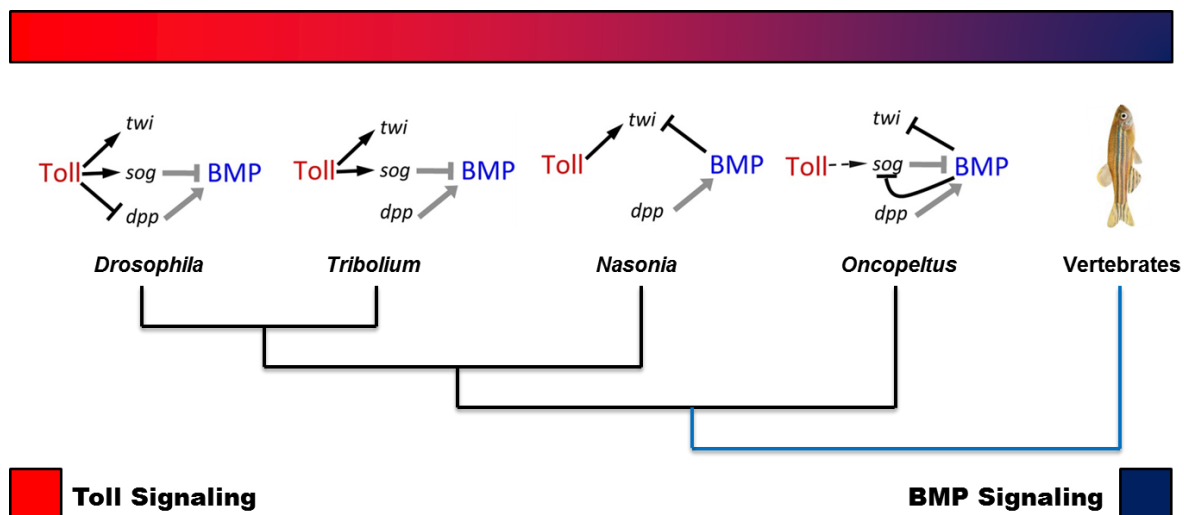


**Figure 1. Evolution of Toll and BMP signaling for dorsoventral pattern formation.**

In *Drosophila*, Toll signaling activates genes like *twist* and *sog* to generate the ventral cell fates while it restricts the BMP signaling to the dorsal side by activation of *sog* and inhibition of BMP ligand *dpp*. In *Tribolium*, Toll signaling restricts the BMP signaling to the dorsal side only by activation of *sog*. BMP signaling is more important in basally branched insects. In *Nasonia*, Toll signaling activates only *twist* while the expression domains are generated by BMP signaling. In *Oncopeltus*, the function of Toll signaling is only to polarize the BMP signaling. Moreover, the BMP signaling is required to establish the dorsoventral axis of the zebrafish embryo (Langdon and Mullins, 2011). Modified from Sachs et al., 2015

### 3.3 Dorsoventral axis formation in *Drosophila melanogaster*

Dorsoventral axis formation is established by three major signaling pathways in *D. melanogaster*. The initial symmetry-breaking event occurs during oogenesis by EGF signaling followed by the activation of a protease cascade during early embryogenesis. The activated protease cascade leads to the initiation of Toll signaling at the ventral side of the embryo and subsequently the establishment of BMP signaling to the dorsal side of the embryo (Stein and Stevens, 2014; Moussian and Roth, 2005).

#### 3.3.1 Establishment of dorsoventral asymmetry during oogenesis

In *D. melanogaster*, the nurse-cell-oocyte complex is surrounded by an epithelium of somatic follicle cells which plays a crucial role in establishment of the DV axis of the future embryo (Figure 2). The DV symmetry of the egg chamber breaks when the oocyte nucleus migrates from its initial posterior position towards the anterior-dorsal side of the egg chamber (Stein and Stevens, 2014; Roth and Lynch, 2009). Several observations, such as laser ablation studies, experiments with binuclear *Drosophila* oocytes and the inhibition of nuclear migration have shown that the position of the oocyte nucleus is necessary to determine the DV polarity of the egg chamber (Roth and Lynch, 2009; Roth, 2003; Roth et al, 1999; Montell et al., 1991). *gurken* mRNA which encodes for Transforming Growth Factor  $\alpha$  (TGF- $\alpha$ ) like molecule accumulates adjacent to the asymmetrically positioned oocyte nucleus (Figure 2). The localized expression of Gurken protein leads to the activation of epidermal growth factor receptor (EGFR) in the nearby follicle cells. The asymmetric activation of EGFR signaling defines the dorsal side of the follicular epithelium and restricts the expression of the sulfotransferase encoding gene *pipe* to the ventral side. The confined expression of *pipe* in the ventral follicle cells together with other factors such as *slalom*, *windbeutel* and *nudel* modifies the extra cellular matrix (ECM) and subsequently activates a protease cascade in the perivitelline space (Moussian and Roth, 2005).

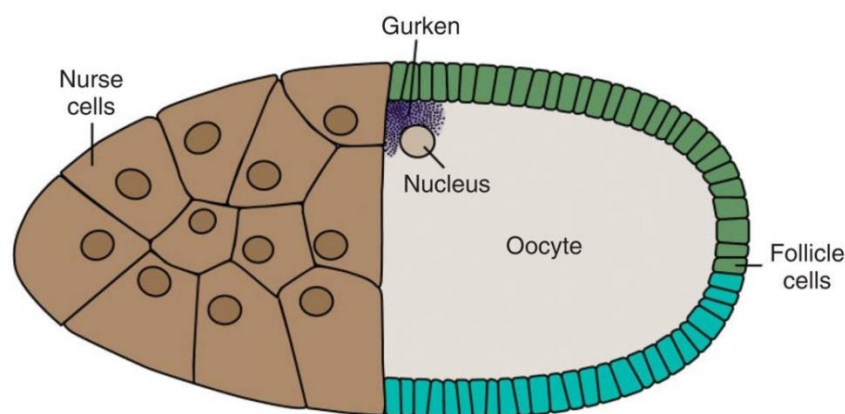


**Figure 2. Model for the ventrally restricted expression of Pipe in the follicular epithelium.**

Schematic drawing of the *Drosophila* egg chamber at stage 10 during oogenesis. *gurken* RNA is localized adjacent to the asymmetrically positioned oocyte nucleus. Localized Gurken protein activates epidermal growth factor receptor (EGFR) in the adjacent follicle cells. EGF signaling at the dorsal follicle cells (green) restricts *pipe* expression to the ventral follicle cells (blue). Reproduced from Stein and Stevens, 2014.

### 3.3.2 Establishment of embryonic DV patterning

The confined expression of *pipe* in the ventral follicular epithelium during *Drosophila* oogenesis is essential to establish the DV polarity of the future embryo. The follicular factors (*pipe*, *slalom*, *windbeutel* and *nudel*) modify the extracellular matrix and subsequently activate the downstream serine protease cascade in the perivitelline space. The protease cascade includes serine proteases like *gastrulation defective* (GD), *snake* and *easter* which function in the perivitelline space to activate the Toll ligand Spaetzle (Figure 3) (Moussian and Roth, 2005).

The autocatalytic serine protease *nudel*, which is expressed in the follicular epithelium during oogenesis, triggers the activation of protease cascade. Ventrally localized GD, through *pipe*-dependent ventral cue, facilitates the processing of Easter by activated Snake protein (Stein and Stevens, 2014; Stein et al., 2013). Subsequently, the function of the activated Easter is spatially restricted to the ventral side of the perivitelline space by an inhibitor known as *serpin27A* (Stein and Stevens, 2014; Hashimoto et al., 2003; Ligoxygakis et al., 2003). Furthermore, Seele an endoplasmic reticulum-resident saposin like protein is necessary for secretion of Easter to the perivitelline space for its processing and activity (Stein et al., 2010). The *pipe*-dependent ventrally restricted processing of Easter is a key step to activate the Toll pathway and establish the DV polarity of the embryo (Figure 3) (Cho et al., 2010).

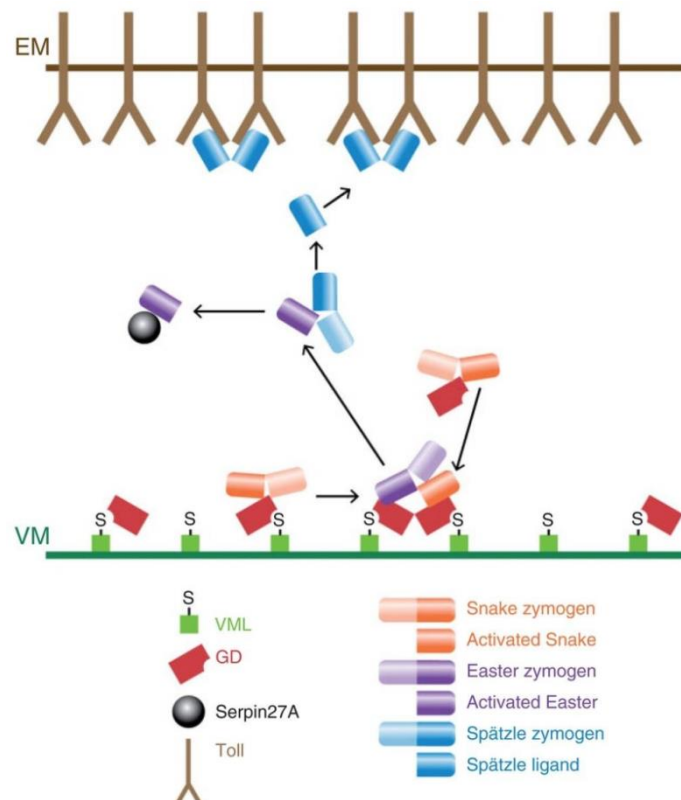


**Figure 3. Activation of the Toll ligand Spaetzle in the perivitelline space.**

GD processes and activates Snake which in turns leads the activation of Easter. GD association with Pipe-sulfated VML promotes the interaction between the activated Snake and the Easter zymogen which ultimately leads to Easter processing. The activated Easter processes the Toll ligand Spaetzle and the Toll signaling is initiated. The function of Easter is spatially regulated by Serpin27A Reproduced from Stein and Stevens, 2014.



The ventrally triggered protease cascade leads to the activation of the Toll receptor ligand Spaetzle. After egg deposition, the activated Spaetzle binds to the Toll receptors which are present in the plasma membrane of the embryo (Lynch and Roth, 2011). Once the processed Spaetzle activates the Toll receptor, it leads to the recruitment of heterotrimeric complex of MyD88-Tube-Pelle through an adaptor protein known as Weckle (Stein and Stevens, 2014; Valanne et al., 2011). The formation of the heterotrimeric complex of MyD88-Tube-Pelle leads to the phosphorylation, ubiquitination and subsequently degradation of Cactus inhibitor. In the absence of signaling, Cactus binds to the NF- $\kappa$ B transcription factor Dorsal, restricting its activity and translocation into the nuclei (Lynch and Roth, 2011; Valanne et al., 2011). Besides the inhibitory function of *cactus*, recent study has shown a new function of *cactus* in promoting Toll signaling and Dorsal nuclear localization in *D. melanogaster* embryo (Cardoso et al., 2017). Nevertheless, the degradation of Cactus inhibitor allows the NF- $\kappa$ B transcription factor Dorsal to translocate into the nuclei (Figure 4). In addition to the degradation of Cactus inhibitor, the phosphorylation of Dorsal is also necessary for the translocation into the nuclei. For nuclear entry, Dorsal interacts with the nuclear transport machinery which includes factors like *tamo*, *Drosophila nuclear transport factor-2* (DNTF-2) and *members-only* (Mbo). This leads to the establishment of a ventral-to-dorsal nuclear Dorsal gradient formation which regulates the transcription of different target genes in a concentration dependent manner (Moussian and Roth, 2005).

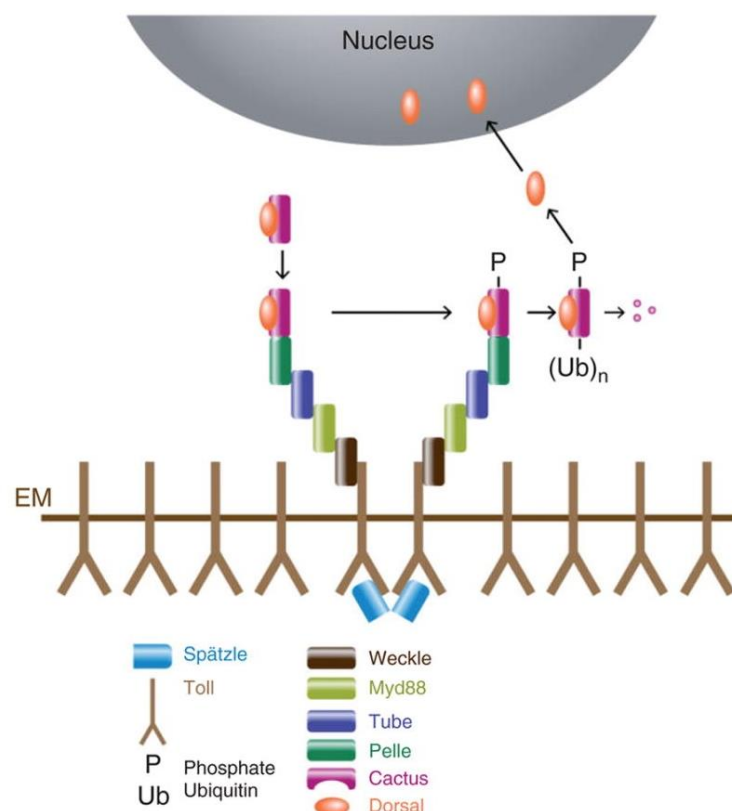


**Figure 4. Activation of the Toll pathway and nuclear localization of the Dorsal protein.**

The activated Spaetzle binds to the Toll receptor which leads to the recruitment of heterotrimeric complex of MyD88-Tube-Pelle through an adaptor protein known as Weckle. This recruitment leads to the degradation of Cactus inhibitor and allows the Dorsal protein to translocate in to the nuclei. Reproduced from Stein and Stevens, 2014



### 3.3.3 Dorsal morphogen gradient formation

The ventrally localized activation of Toll signaling leads to the formation of a nuclear concentration gradient of the NF- $\kappa$ B Dorsal transcription factor. The establishment of the nuclear Dorsal gradient is a key event to pattern the expression of different target genes and specify different cell fates along the DV axis of *Drosophila* embryo. Strong nuclear Dorsal localization is present in the ventral most region of the embryo, while in the dorsal side of the embryo, *cactus* inhibits the nuclear localization of Dorsal transcription factor which remains in the cytoplasm (Moussian and Roth, 2005; Roth et al., 1989).

The nuclear Dorsal gradient forms at syncytical blastoderm stage, during the nuclear division cycles 10 to 14. In contrast to the stability of the nuclear Dorsal gradient's width, the nuclear Dorsal gradient is dynamic and varies during each nuclear division cycle. The nuclear Dorsal concentration rises to a higher level during interphase, reduces to a low level during mitosis and subsequently rises again at the next interphase (Stein and Stevens, 2014; Reeves et al., 2012; Rushlow and Shvartsman, 2012; Kanodia et al., 2009; Liberman et al., 2009). The expression of Dorsal target genes also corresponds to the dynamics of the Dorsal gradient during each nuclear division cycle. For instance, the expression of *snail* increases during cycle 13, disappears briefly during mitosis and subsequently rises again during nuclear division cycle 14 (Reeves et al., 2012; Rushlow and Shvartsman, 2012). Nevertheless, NF- $\kappa$ B nuclear Dorsal transcription factor acts as a morphogen and differentially regulates about 60-70 different zygotic target genes along the dorsoventral axis in a concentration-dependent manner (Hong et al., 2008).

The regulation of different zygotic Dorsal target genes can be classified into three large categories (Types I, II and III) based on their expression domains and response to the nuclear Dorsal gradient level (Figure 5) (Reeves et al., 2012). A large number of zygotic target genes (Type I genes), such as *twist* (*twi*) and *snail* (*sna*) is expressed ventrally (18-20 cells, 20%), where the highest level of nuclear Dorsal is present and which is required to specify the presumptive mesoderm (Hong et al., 2008; Moussian and Roth, 2005; Roth et al., 1989). Type II genes such as *ventral nervous system defective* (*vnd*) and *rhomboid* (*rho*) are expressed in the ventrolateral region of the embryo and specify the neurogenic ectoderm and require the intermediate levels of nuclear Dorsal concentration. Lowest concentration of nuclear Dorsal gradient regulates Type III genes in broad lateral region of the embryo. Expression of the Type III genes is essential for establishment of dorsal ectoderm and extraembryonic amnioserosa. Type III genes are further subdivided into two classes, Type III<sup>+</sup> genes such as *short gastrulation* (*sog*) which are activated by Dorsal and Type III<sup>-</sup> genes like *zerknüllt* (*zen*) and *decapentaplegic* (*dpp*) which are repressed by Dorsal transcription factor (Reeves et al., 2012; Reeves and Stathopoulos, 2009; Moussian and Roth, 2005).

Furthermore, the ventral activation of BMP inhibitor *sog* and the restricted expression of BMP ligand *dpp* and metalloprotease *tolloid* (*tld*) by NF- $\kappa$ B/Dorsal, establishes a BMP signaling gradient at the dorsal side (Lynch and Roth, 2011; O'Connor et al., 2006). Therefore, Toll signaling not only patterns the ventral half of the embryo, but also indirectly

controls the patterning of the dorsal half of the *D. melanogaster* embryo through BMP signaling (Sachs et al., 2015).

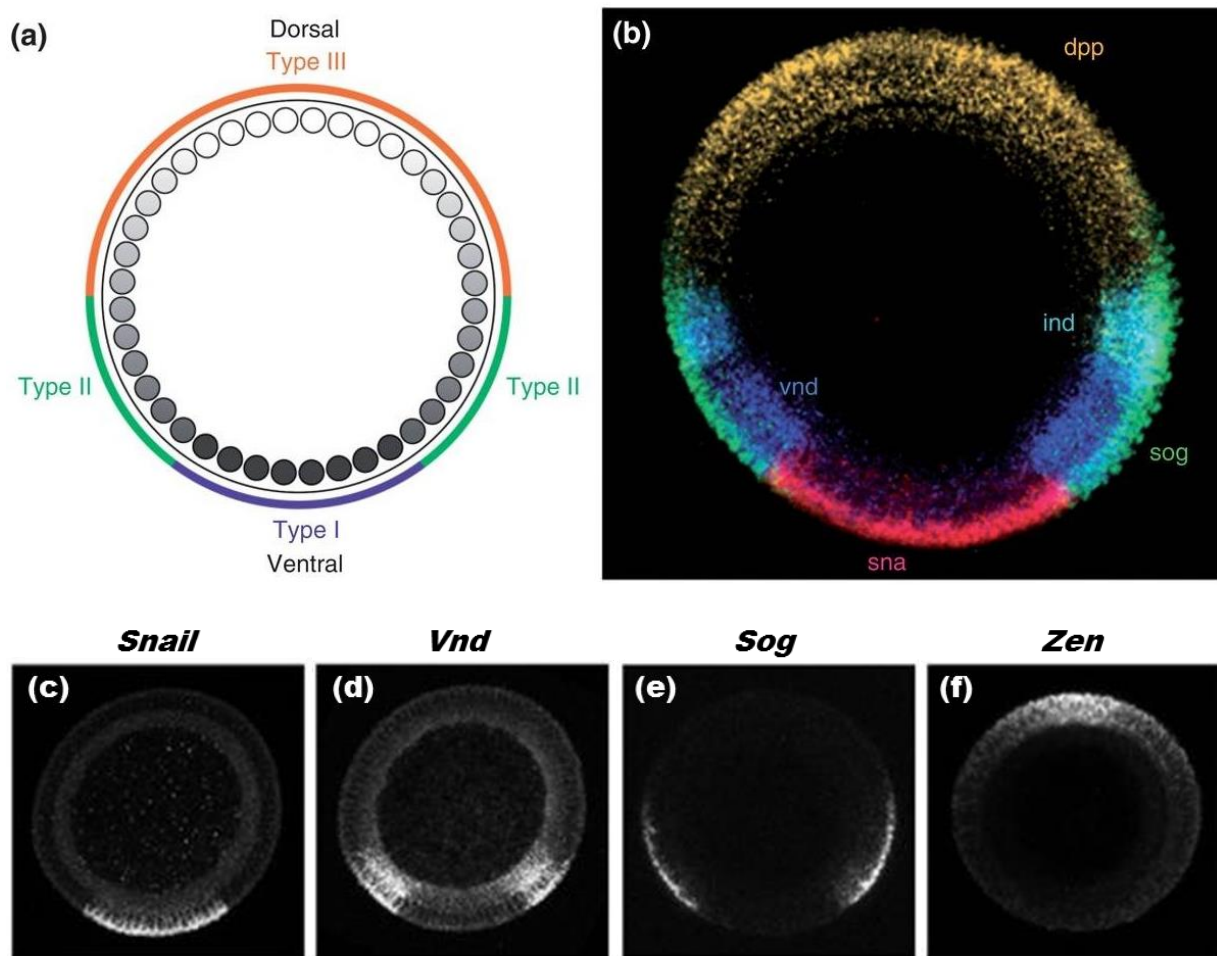


**Figure 5. Nuclear Dorsal gradient and differential genes regulation along the dorsoventral axis.**

(a) Diagram showing the level of nuclear Dorsal gradient along the DV axis. Filled grey circles indicate the nuclear dorsal gradient concentration. Colors on the outside circle show the types of Dorsal-dependent genes expression. Type I genes are expressed in the ventral-most region and require high nuclear Dorsal gradient. Expression of Type II genes in the lateral neuroectoderm region requires intermediate level of nuclear Dorsal. Type III genes which require low level of nuclear Dorsal are regulated in broad lateral region of the embryo, while genes which require no nuclear Dorsal are transcribed in the dorsal region. (b) Expression domains of different Dorsal-dependent target genes i.e. *snail* (Type I), *ventral nervous system defective* (Type II), *intermediate neuroblasts defective* (Type II), *short gastrulation* (Type III), and *decapentaplegic* (Type III). (c-f) Single expression patterns of different Dorsal-dependent genes in wild-type embryos at nuclear cycle 14. Pictures (a-b) reproduced from Stein and Stevens, 2014. Pictures (c-f) are reproduced and modified from Reeves et al., 2012

### 3.4 Dorsoventral patterning in *Tribolium castaneum*

DV pattern formation in *T. castaneum* is established through the same processes like *D. melanogaster*. However, many striking differences were identified in *Tribolium* compared to *Drosophila* DV patterning (Lynch and Roth, 2011). Major components of the three signaling pathways, which define the DV axis in *Drosophila* (EGF signaling, Toll signaling and BMP signaling), were analyzed in *T. castaneum* (Figure 7). Like in *Drosophila*, the asymmetric localization of the oocyte nucleus breaks the DV symmetry of the *Tribolium* egg chamber during late stages of oogenesis. In contrast to *Drosophila*, where *gurken* mRNA is localized adjacent to the asymmetric positioned oocyte nucleus, *gurken* mRNA in *Tribolium* is present uniformly in the oocyte. EGF receptor is expressed in the somatic follicular epithelium in *Tribolium*. However, experiments with cross-reactive antibody against dpERK showed that the activated MAPK accumulates in the follicular epithelium surrounding the location of oocyte nucleus (Lynch et al., 2010). Furthermore, functional analysis of EGF signaling after knockdown of its components (ligand and EGF receptor) by parental RNAi showed strong DV patterning defects in *Tribolium*. Surprisingly, none of the known target components of EGF signaling in *Drosophila*, showed an asymmetric expression pattern or DV patterning defects in *Tribolium*. Therefore, it is not clear how the maternally established DV asymmetries during oogenesis are transferred into embryonic DV patterning. Nevertheless, the asymmetric activation of EGF signaling in the follicular epithelium suggests that like in *Drosophila*, the EGF pathway is required to establish DV polarity of the *Tribolium* egg chamber through germline-to-soma signaling (Lynch and Roth, 2011; Lynch et al., 2010).

Toll signaling in *Tribolium* is initiated at the ventral side of the embryo and generates different cell fates along the DV axis of the embryo (Nunes da Fonseca et al., 2008; Maxton-Küchenmeister et al., 1999). The loss of Toll signaling after parental RNAi leads to dorsalized phenotypes in *Tribolium*. *Toll* knockdown embryos lack DV asymmetry and the border between serosa and germ rudiment becomes rotationally symmetric and straight (Figure 6). Therefore like in *Drosophila*, the Toll pathway is necessary to establish the embryonic DV patterning in *T. castaneum* (Nunes da Fonseca et al., 2008).

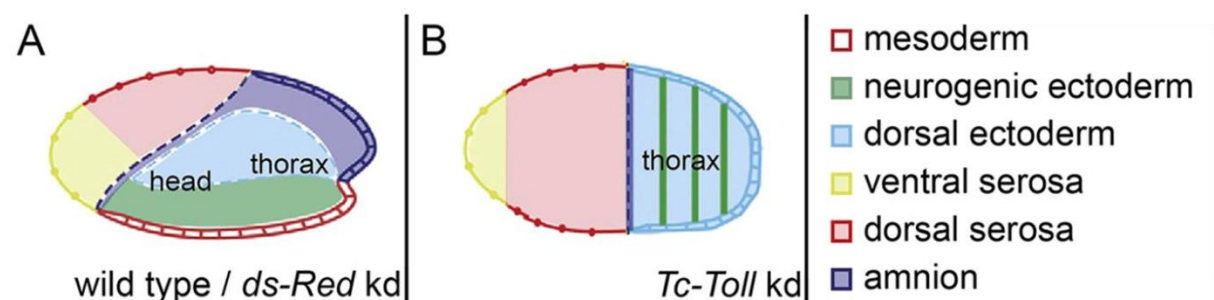


**Figure 6. Schematic drawings of wild-type and *Toll* knockdown embryos fate maps.**

(A) Fate map of wild-type embryo (B) Fate map of *Toll* knockdown embryo. *Tc-Toll* knockdown embryos are dorsalized and the border between serosa and germ rudiment becomes straight. In contrast to wild-type, mesoderm and neurogenic ectoderm is absent while dorsal ectoderm is expanded in *Tc-Toll* knockdown embryo. Modified from Stappert et al., 2016.

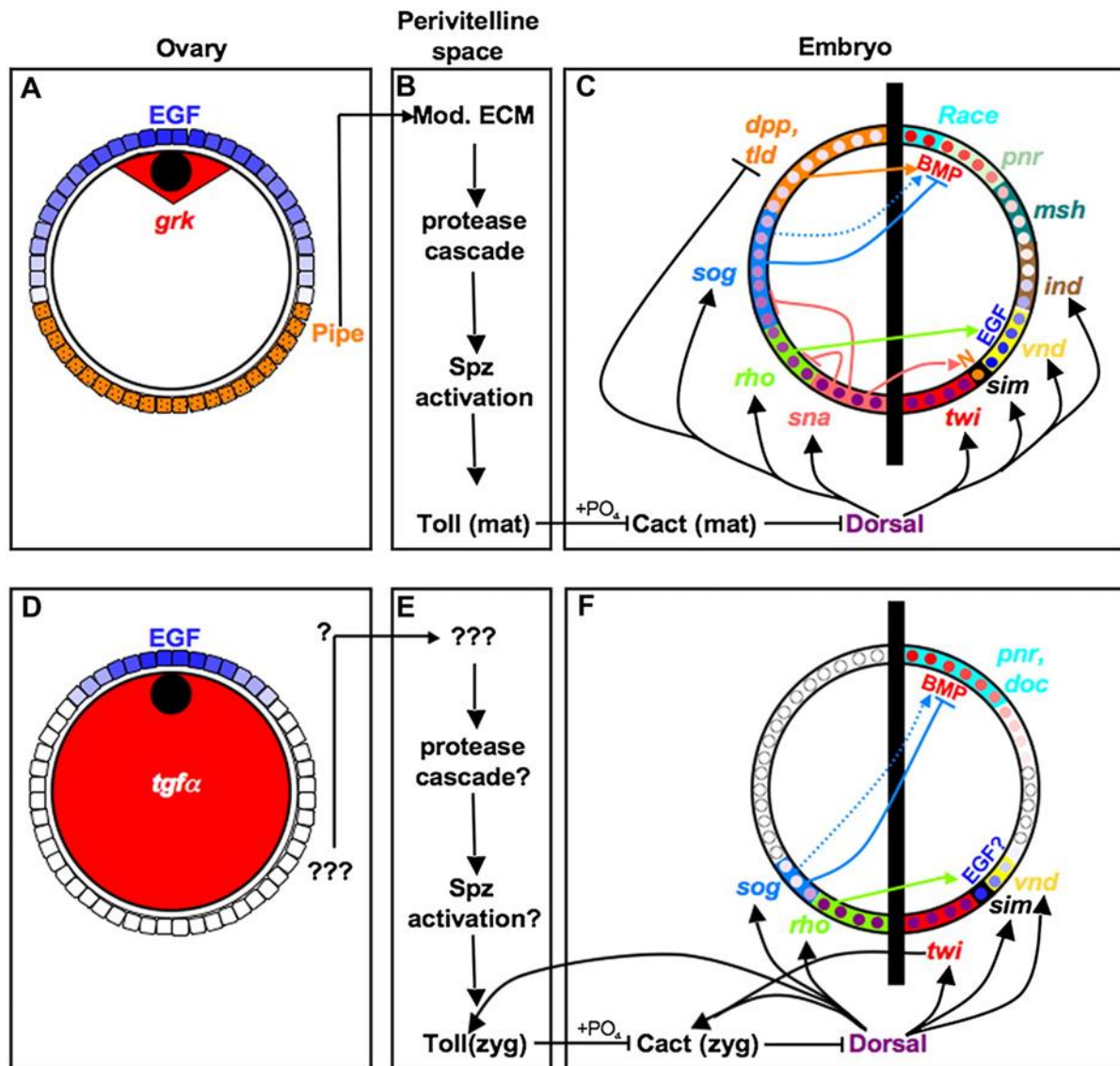


**Figure 7. Comparative analysis of dorsoventral GRNs in *Drosophila* and *Tribolium*.**

(A-C) Gene regulatory network (GRN) of DV patterning in *Drosophila*. (A) In the ovary, *gurken* mRNA accumulates adjacent to the oocyte nucleus. The localized expression of Gurken protein activates the EGFR signaling which defines the dorsal side of the follicular epithelium and restricts the expression of *pipe* to the ventral side of the follicular epithelium. (B) In the perivitelline space, the modified ECM activates the protease cascade which leads to the activation of Toll ligand Spaetzle and subsequently the activation of Toll receptor. (C) In the embryo, the activated Toll signaling degrades the Cactus inhibitor and allows the Dorsal transcription factor to enter into nuclei. The ventrally localized activation of Toll signaling forms the nuclear Dorsal concentration gradient which acts as a morphogen and differentially regulates different target genes along the dorsoventral axis based on concentration-dependent manner. (D-F) GRN of DV patterning in *Tribolium*. (D) In the ovary, like in *Drosophila*, the EGF signaling is activated and breaks the DV symmetry of the egg chamber. However, the *gurken* mRNA in *Tribolium* is present uniformly in the oocyte. Furthermore, the target components of EGF signaling have not been functionally identified in *Tribolium*. (E) Initial data suggest that the protease cascade is necessary to activate the Toll signaling in the perivitelline space however, it is not clear how the maternally established DV asymmetry signals are transmitted to the embryo (indicated by ???). (F) The ventral activation of Toll signaling establishes the nuclear Dorsal gradient but in contrast to *Drosophila* the nuclear gradient formation in *Tribolium* is highly dynamic and involves positive and negative feedback loops at the zygotic level of gene regulations. Reproduced from Lynch and Roth, 2011



However, the Toll ligand Spaetzle and the protease cascade required for its activation have not been functionally identified in *Tribolium*. Furthermore, like in *Drosophila*, the activation of Toll ligand Spaetzle requires the proteolytic processing of the protease cascade. However, after parental RNAi, only two proteases *Tc-nudel* (TC000870) and *Tc-easter* (TC002112), showed dorsalized phenotypes, indicating that these proteases are required to activate the Toll ligand Spaetzle (Dao, 2014).

Nevertheless, the ventral activation of *Toll* signaling in *T. castaneum* initiates the nuclear uptake of NF- $\kappa$ B transcription factor Dorsal. In contrast to *Drosophila*, the nuclear Dorsal gradient formation in *Tribolium* is highly dynamic over developmental time. In early embryos, nuclear Dorsal accumulation is initiated in all nuclei around the DV axis. However, the nuclear Dorsal gradient later refines to the ventral most region of the embryo and subsequently disappears before gastrulation (Figure 8). The ventral refinement of the nuclear Dorsal gradient is not associated with cell movements or nuclear division cycle (Lynch and Roth, 2011; Chen et al., 2000). It has been found that this dynamic behavior of nuclear Dorsal gradient is due to positive and negative feedbacks loops containing its zygotic target genes (Lynch and Roth, 2011; Nunes da Fonseca et al., 2008).

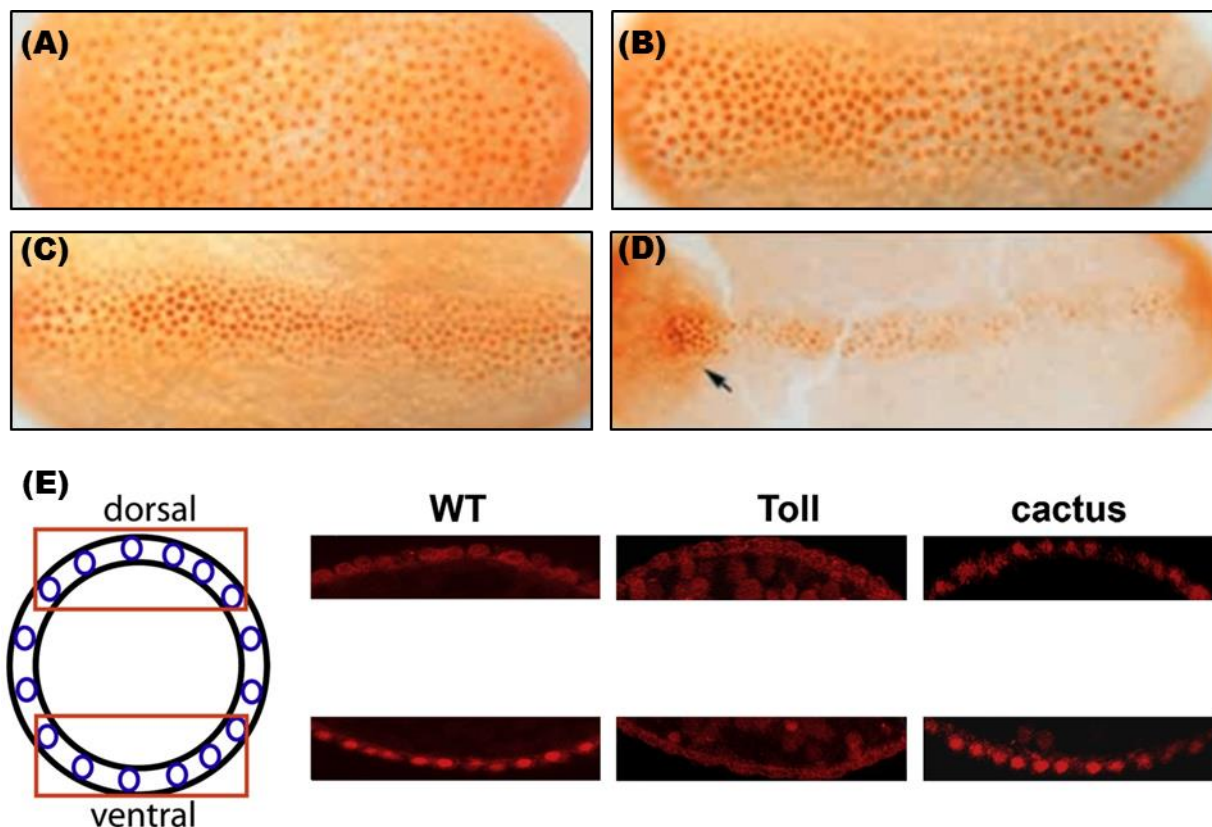


**Figure 8. Nuclear Dorsal gradient formation and refinement in *Tribolium castaneum*.**

(A-D) Whole-mount antibody staining with Dorsal antibody. Progressive gradient refinement is observed at different times of development in *Tribolium*. The arrow points to the anterior 'cap' where Dorsal expression overlaps with the presumptive serosa. Picture modified from Chen et al., 2000. (E) Nuclear Dorsal gradient in wild-type, *Tc-Toll* and *Tc-cactus* knockdown embryos. Nuclear Dorsal is present only on ventral side in wild-type and *Tc-cactus* knockdown embryos, while in *Tc-Toll* knockdown embryos, no nuclear Dorsal was observed at either of the sides. Reproduced from Nunes da Fonseca et al., 2008.

In contrast to *Drosophila*, both the receptor Toll and the inhibitor Cactus are zygotically expressed and regulated by NF- $\kappa$ B/Toll signaling (Lynch and Roth, 2011; Nunes da Fonseca et al., 2008). Knockdown experiments of *Tc-Toll* by embryonic RNAi showed strong dorsalized phenotype indicating that *Tc-Toll* is zygotically expressed in *T. castaneum*. Furthermore, the *Tc-cactus* expression is mostly absent after *Tc-Toll* RNAi indicating that *Tc-cactus* expression is regulated by NF- $\kappa$ B/Toll signaling. However, the *Tc-cactus* expression is later upregulated and maintained by *Tc-twist*. After *Tc-twist* knockdown, *Tc-cactus* expression is strongly reduced indicating that *Tc-cactus* expression depends on *Tc-twist*. Therefore, the presence of self-regulatory circuits is essential for regulating the nuclear Dorsal gradient dynamics and the ultimate extinction of Dorsal nuclear localization (Figure 9) (Nunes da Fonseca et al., 2008).

In contrast to *Drosophila*, NF- $\kappa$ B/Dorsal signaling in *Tribolium* does not function directly as a repressor of BMP signaling but only its antagonist *sog* regulates the Dpp gradient to the dorsal side (Sachs et al., 2015; Lynch and Roth, 2011). Knockdown of *Tc-sog* in *Tribolium* leads to complete loss of CNS, while narrow periodic stripes of CNS are present after *Tc-Toll* knockdown. However in *Drosophila*, the loss of *Toll* signaling produced completely dorsalized phenotype, while *sog* mutant causes minor defects in the CNS. These findings suggest that the function of Toll signaling in *Drosophila* is achieved by the Dpp/Sog system in *Tribolium*, which represents an ancestral state of the DV patterning mechanism (van der Zee et al., 2006; Nunes da Fonseca et al., 2008).

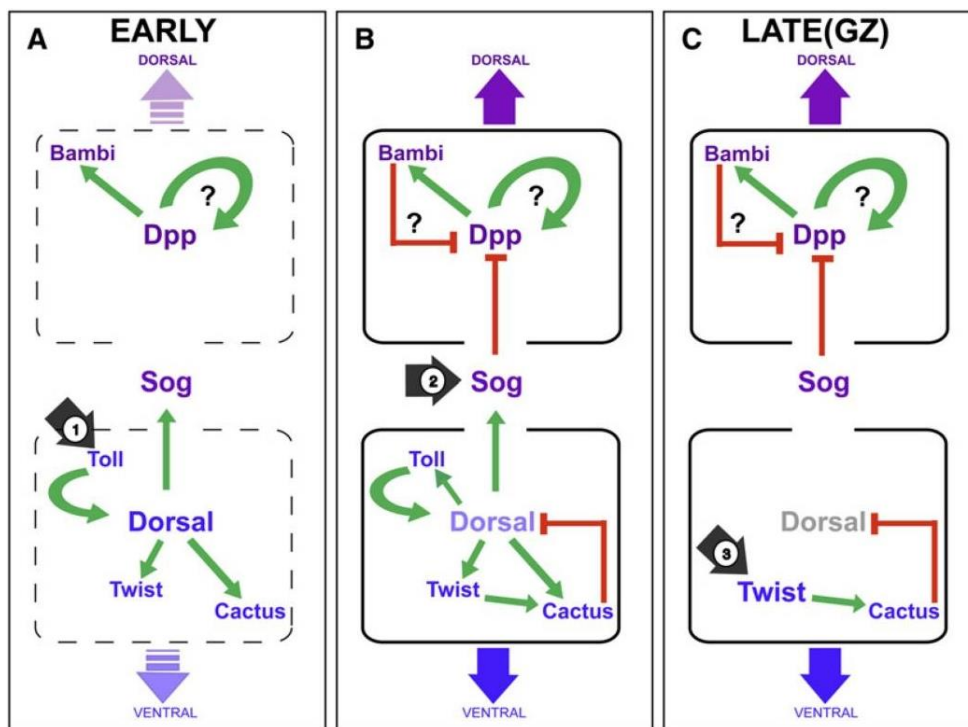


**Figure 9. Model of self-regulatory circuits of DV pattern formation in *Tribolium castaneum*.**

(A) A ventrally biased self-organized system initiates the nuclear accumulation of NF- $\kappa$ B transcription factor Dorsal and regulation of zygotic target genes (arrow 1). (B) A dorsally biased second self-organized loop. *Tc-sog* which is a direct target of NF- $\kappa$ B transcription factor Dorsal links the two systems (arrow 2). (C) After gastrulation, the ventral patterning of the posterior segments is achieved by *Tc-twist* expression in the growth zone (arrow 3). Drawing model reproduced from Rosenberg and Desplan, 2008.

## 4. Aim of the Thesis

---

The gene regulatory network (GRN), establishing dorsoventral (DV) pattern formation in *Drosophila melanogaster* is one of the best characterized GRNs. The complete understanding of DV axis formation in *D. melanogaster* provides an excellent platform for evolutionary comparisons of embryonic DV patterning within insects (Lynch and Roth, 2011; Nunes da Fonseca et al., 2008). In addition to some exciting deviations in comparison to *Drosophila*, DV axis formation in *Tribolium castaneum* represents the more ancestral state, making it an ideal model organism for comparative evolutionary analysis of DV patterning mechanisms (Stappert et al., 2016).

For a long time, the identification of DV patterning genes in *T. castaneum* was based on candidate gene approach. Through this comparative approach, only the genes which have DV function in *Drosophila* were analyzed in *T. castaneum*, leading to biased conserved genes function analyses (Lynch and Roth, 2011). Hence, novel DV patterning genes in *T. castaneum* that are not represented in *D. melanogaster* could not be identified through candidate gene approach. Here, the iBeetle large scale RNAi screen provides an excellent opportunity for unbiased identification of novel DV patterning genes in *T. castaneum* (Schmitt-Engel et al., 2015). Therefore, the aim of my research project is to overcome the candidate gene approach by participating in an unbiased large scale RNAi screen. The identification of new DV patterning genes in the iBeetle screen that lack DV function in *D. melanogaster* will contribute to understanding the evolutionary novelty of DV patterning mechanism in *T. castaneum*.

## 5. Material and Methods

**Table 1. List of buffers/media/solutions**

buffers/media/solutions	compositions
Alkaline phosphatase (AP) buffer	100 µl Tris solution (1 M, pH=9.5), 50 µl MgCl <sub>2</sub> (1 M), 20 µl NaCl (5 M), 2 µl 20% Tween-20 and up to 1 ml H <sub>2</sub> O.
Blocking solution	100 µl BSA (1 mg/ml), 30 µl NGS (60 mg/ml) and up to 1 ml PBST.
Hybridization sol. 1	25 ml 100% Formamid, 12.5 ml 20x SSC, 50 µl Heparin (50 mg/ml) and up to 50 ml H <sub>2</sub> O.
Hybridization sol. 2	25 ml 100% Formamid, 12.5 ml 20x SSC, 50 µl Heparin (50 mg/ml) 500 µl salmon sperm (ssDNA) and up to 50 ml H <sub>2</sub> O.
PBS (10x)	80 g NaCl, 2 g KCl, 26.8 g Na <sub>2</sub> HPO <sub>4</sub> ·7H <sub>2</sub> O, 2.4 g KH <sub>2</sub> PO <sub>4</sub> and up to 1 L H <sub>2</sub> O (pH=7.4).
PBST	100 ml 1x PBS and 1 ml 20% Tween-20
5% PFA	1x PBS and 10% Formaldehyde (1:1)
SSC (20x)	175.3 g NaCl, 88.2 g sodium citrate-2H <sub>2</sub> O and up to 1 L H <sub>2</sub> O (pH=7.0).
1 M MgCl <sub>2</sub>	203.31 g magnesium chloride-6H <sub>2</sub> O (MgCl <sub>2</sub> ·6H <sub>2</sub> O) and up to 1 L H <sub>2</sub> O.
5 M NaCl	292.2 g sodium chloride (NaCl) and up to 1 L H <sub>2</sub> O
100 mM Glycine-HCL	11.1 g Glycine-HCL dissolved in 1 L H <sub>2</sub> O, (pH=2.3)
1M Tris solution	121.14 g Tris (hydroxymethyl) Aminomethane, up to 1 L H <sub>2</sub> O. (pH=9.5)
Probe resuspension buffer	Formamide and 2x SSC (1:1)
Hoyers medium	200 g Chloral hydrate, 30 g Gum arabic (powder), 20 ml Glycerol and 50 ml H <sub>2</sub> O.

**Table 2. Software and databases**

Name	Source
Primer3 (v. 0.4.0)	<a href="http://bioinfo.ut.ee/primer3-0.4.0/">http://bioinfo.ut.ee/primer3-0.4.0/</a>
iBeetle-Base	<a href="http://ibeetle-base.uni-goettingen.de/">http://ibeetle-base.uni-goettingen.de/</a>
Tribolium Browser	<a href="http://bioinf.uni-greifswald.de/blast/tribolium/blast.php">http://bioinf.uni-greifswald.de/blast/tribolium/blast.php</a>
NCBI-Blast	<a href="https://blast.ncbi.nlm.nih.gov/Blast.cgi">https://blast.ncbi.nlm.nih.gov/Blast.cgi</a>
SMART	<a href="http://smart.embl-heidelberg.de/">http://smart.embl-heidelberg.de/</a>
Tm Calculator	<a href="http://tmcaculator.neb.com/">http://tmcaculator.neb.com/</a>
Sequence Massager	<a href="http://www.attottron.com/cybertory/analysis/seqMassager.htm">http://www.attottron.com/cybertory/analysis/seqMassager.htm</a>
Citavi	<a href="https://www.citavi.com/en/index.html">https://www.citavi.com/en/index.html</a>
Helicon Focus 6	<a href="http://www.heliconsoft.com/focus/help/german/HeliconFocus.html">http://www.heliconsoft.com/focus/help/german/HeliconFocus.html</a>
Multiple-seq Alignment	<a href="https://www.ebi.ac.uk/Tools/msa/clustalo/">https://www.ebi.ac.uk/Tools/msa/clustalo/</a>
Pairwise-seq Alignment	<a href="http://www.ebi.ac.uk/Tools/psa/">http://www.ebi.ac.uk/Tools/psa/</a>
Phylogeny.fr	<a href="http://www.phylogeny.fr/">http://www.phylogeny.fr/</a>
FigTree	<a href="http://tree.bio.ed.ac.uk/software/figtree/">http://tree.bio.ed.ac.uk/software/figtree/</a>
mVISTA	<a href="http://genome.lbl.gov/vista/mvista/submit.shtml">http://genome.lbl.gov/vista/mvista/submit.shtml</a>



**Table 3. List of oligonucleotides**

iB_07888_F1_5'	ggccgcggACCGCAACAATGCTTCTCTT
iB_07888_R1_3'	cccggggcTTTCTTCGACGGAATTGTCC
iB_07888_F2_5'	ggccgcggGACATCGCCATTCTGATCCT
iB_07888_R2_3'	cccggggcGGCACTTGGACCTTTTTCAA
iB_06699_F1_5'	ggccgcggTCAAAGGGAAGTGAAGCAC
iB_06699_R1_3'	cccggggcGGCTCCTTCCTCATTGACTTC
iB_06699_F2_5'	ggccgcggGCCAAAATAGCTGCAGAAGG
iB_06699_R2_3'	cccggggcGCACCTCAACCCAATCATTT
iB_06774_F1_5'	ggccgcggTGGATGATCGCAAGAGTTTG
iB_06774_R1_3'	cccggggcCAGCGTACGGTCTTCCATTT
TC031906_F1_5'	ggccgcggCATAACCAGCTGCAAGCAAA
TC031906_R1_3'	cccggggcCTTCTGTCCTTACGCCTTGC
TC031906_F2_5'	ggccgcggTGTTGCAAACAGGAAAGCTG
TC031906_R2_3'	cccggggcCCCTCAAAACACAACAGCAA
iB_05549_F1_5'	ggccgcggAGCACCAGACCCAGAACAAC
iB_05549_R1_3'	cccggggcCCGTAACCGTAACCGTTCAT
iB_09824_F1_5'	ggccgcggCAGGACCGTTTAGCCAAAAA
iB_09824_R1_3'	cccggggcGGAACACGGCCTTATTCAAA
iB_09592_F1_5'	ggccgcggCGTTGTGTGGAACAACCAAA
iB_09592_R1_3'	cccggggcGGAAACTCCCTCCAGACCTC
iB_02234_F1_5'	ggccgcggCTCATCTTGGAACACGTCGAT
iB_02234_R1_3'	cccggggcATCGTTTCCGTAGTTCGACA
iB_07888_QF3_5'	GTGACAATCAACGGACATGG
iB_07888_QR3_3'	GATTTGAAAGTGGCGGAAAA
Tc-zen1_F	ggccgcggTCCCAATTTGAAAACCAAGC
Tc-zen1_R	cccggggcCGTTCCACCCTTCCTGATAA
Tc-snail_F	ggccgcggGAACCATCATGGCCAAAAAC
Tc-snail_R	cccggggcGTCCTAATGTGCCCTTGAG
Tc-sog_F	ggccgcggTACCGAAACCTGGAGTGCGTGTT
Tc-sog_R	cccggggcCCTTCCAGTCGCCACTACAT
Tc-twist_F	ggccgcggGCTGATGGACCTGACCAACT
Tc-twist_R	cccggggcCTCCAATCACCTCCATCC
Tc-Toll_F	ggccgcggAACCCGAAGCGTTTTATGTC
Tc-Toll_R	cccggggcTACGTCCAGTTTCCGATGAG
Universal_5'	GAGAATTCTAATACGACTCACTATAGggccgcgg
Universal_3'	AGGGATCCTAATACGACTCACTATAGGGcccggggc

## 5.1 iBeetle RNAi screening

The iBeetle pupal screen was performed as mentioned in Schmitt-Engel et al., 2015. Female pupae of pBA19 strain (carrying the pig 19 enhancer trap) were used for pupal injection. Before injection, pupae at approx. 75-90% of pupal development were affixed to microscope slides using a double sided sticky tape. dsRNA solution of 1 µg/µl (Eupheria Biotech GmbH, Dresden) was injected into 10 females pupae per iB-fragment. The sequences of all iB-fragments and their corresponding primers are available in the iBeetle-Base (<http://ibeetle-base.uni-goettingen.de/>). 22 iB-fragments together with negative and positive controls were injected in one repetition. Five repetitions were performed in parallel to make one experimental bundle (Figure 10).

Lethality of injected females was recorded after injections during day-3, day-9, day-11 and day-13. At day-3, four males of black strain with black cuticle color were mated with ten injected females in order to facilitate easy assessment of injected females for lethality analysis. First egg collection (day-9) was used for cuticle preparation (day-13) while second egg collection (day-11) was used for muscles analysis (day-14).

**Cuticle preparation (day-13):** The embryos were gently washed with water before and after being treated twice with 50% Klorix/bleach for dechoriation (each washing and dechoriation step was performed for 3 min). After dechoriation, the embryos were embedded in Hoyers medium-lactic acid on a microscope slide and incubated at 65 °C overnight.

**Ovary analysis (day-13):** In case of low egg productivity at day-9 and day-11, four females were dissected to analyze the ovarian phenotype. The freshly dissected ovaries were incubated in 4% Formaldehyde in PBS on ice until all four females were dissected and the ovaries were cleared from the fat body and trachea. Ovaries were mounted in PBS on a microscope slide without disturbing the ovary morphology and were subsequently analyzed under the microscope.

**Muscle preparation and analysis (day-14):** For muscle preparation, the embryos were washed and dechorionated as described for cuticle preparation. After dechoriation, the embryos were embedded on a microscope slide in Halocarbon oil (Votalef 10S) and were analyzed under the fluorescence microscope.

**Stink gland analysis (day-21):** To analyze the abdominal stink gland content, the injected females were dissected. The darkness or the absence of the stink gland content of the dissected females was observed under the stereomicroscope.

**Cuticle analysis (day 15-32):** Cuticle analysis was performed using the fluorescence microscope with GFP filter-set or dark field setup. The slide was first scanned with 10x objective using fluorescence or dark field setup in order to get the first impression of the phenotype. Later the detailed assessment of the phenotype was performed using high magnification objectives (20x or 40x filters). The number of empty eggs with or without cuticle remnants and larvae with morphological defects were documented along with the


corresponding pictures of the phenotype. Phenotype annotations were performed electronically using an online iBeetle-interface (Figure 11).

**Re-screening of the iBeetle candidates:** Re-screening of the selected iBeetle candidates with potential dorsoventral (DV) phenotypes was performed by injecting two dsRNA fragments (iB-fragments and non-overlapping fragments, concentration of 1 µg/µl) of the same gene into two different genetic backgrounds (pBA19 and San Bernadino wild-type strains). Only egg productivity, lethality and cuticle analyses were performed during the re-screen.

	Monday	Tuesday	Wednesday	Thursday	Friday	Saturday	Sunday
week 1		d0 Injection (10h)		d0 Injection (10h)	d3 Transfer (1,5h)		d3 Transfer (1,5h)
		<b>Repetition (1)</b>		<b>Repetition (2)</b>	Cuticle anal. (2h)		
week 2	d0 Injection (10h)	Cuticle analysis (8h)	d0 Injection (10h)	d3 Transfer (1,5h)	d0 Injection (10h)	d3 Transfer (1,5h)	
	<b>Repetition (3)</b>		<b>Repetition (4)</b>	d9 Sieving (0,75h)		d9 Sieving (0,75h)	
						d11 Sieving (0,75h)	
week 3	d13 Sieving Ovaries (4h)	d14 Fresh Prep Muscle analysis (8h)	d9 Sieving (0,75h)	d14 Fresh Prep Muscle analysis (8h)	d9 Sieving (0,75h)		d13 Sieving Ovaries (4h)
	d13 Cuticle Prep (3h)		d13 Sieving Ovaries (4h)		d11 Sieving (0,75h)		d13 Cuticle Prep (3h)
	d3 Transfer (1,5h)		d13 Cuticle Prep (3h)		Cuticle analysis (6h)		
	d11 Sieving (0,75h)						d9 Sieving (0,75h)
week 4	d14 Fresh Prep Muscle analysis (8h)	d21 Stinkgld.(1,5h)	d14 Fresh Prep Muscle analysis (8h)	d13 Sieving Ovaries (4h)	d14 Fresh Prep Muscle analysis (8h)		
		d13 Sieving Ovaries (4h)		d13 Cuticle Prep (3h)			
		d13 Cuticle Prep (3h)					
		d11 Sieving (0,75h)		d21 Stinkgld.(1,5h)			
week 5	Cuticle analysis (8h)		Cuticle analysis (8h)	d21 Stinkgld.(1,5h)	Cuticle analysis (8h)		
				d21 Stinkgld.(1,5h)			
				d21 Stinkgld.(1,5h)			

**Figure 10. Workflow and schedule for the iBeetle pupal RNAi screen:**

Each color represents one repetition. Parental RNAi of 22 iBeetle genes were performed in one repetition including positive and negative controls. Five repetitions were performed in parallel in one experimental bundle. Each experimental step along with their corresponding required time and day is shown in the schedule. After concluding the first bundle, the same schedule was repeated for another round of experiments.



**iBeetle-Base**  
 A database of  
*Tribolium* RNAi phenotypes

Search ▾ Query pipeline Ontology ▾ Gene search ?  Go Genome browser ▾ Resources Help ▾ Login

**Search for morphological defects** ? Search strategy

Developmental stage ?  
 larva ▾

Morphological structure ?  
 ...

Penetrance ?  
 >50 % ▾

Annotations  
 max data sets

**Optional further specifications** !
 

Temporal, local or logical specifications  
 not selected ▾

Altered aspect  
 not selected ▾

Nature of change  
 not selected ▾

**Gene information** —

**General information**

Tc number TC012650

Gene ? NC\_007424.3:12508074..12522708

**Sequence information**

Transcripts / Proteins (1)
 

[Get mRNA sequence](#)  
[Get CDS sequence](#)  
[Get protein sequence](#)

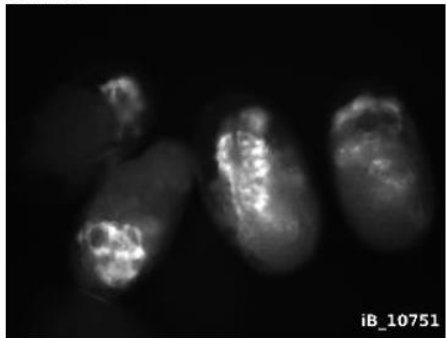
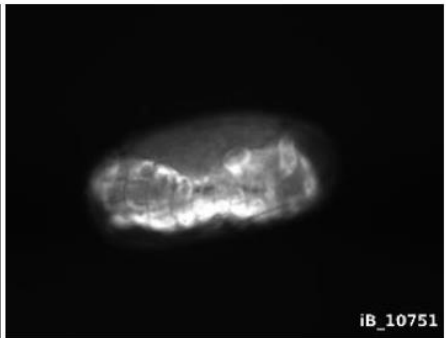
**Ortholog information (from OrthoDB)** ?
 

Closest fly homologs [sog - short gastrulation \(CG9224\)](#)

View orthologs at OrthoDB for: [TC012650](#)

**Analysis of embryonic musculature and early development**

number of eggs/embryos/larvae on slide: > 50 [larval musculature pattern irregular](#) - Penetrance (percentage of animals/eggs on slide): more than 80%

affected eggs/embryos/larvae - Penetrance (percentage of animals/eggs on slide): more than 80%

remarks: muscle pattern potentially obscured by segmentation defect,

**Figure 11. Screenshot of the iBeetle-Base website showing the annotated RNAi phenotypic data.**

The start page of the iBeetle-Base. After each gene knockdown during the iBeetle RNAi screen, the resulting phenotypic data was documented in an online electronic database. Phenotypic data for several thousands of knocked down genes are available online at iBeetle-Base (<http://ibeetle-base.uni-goettingen.de/>). Furthermore, the database also provides sequence information and additional links for all *Tribolium castaneum* genes (Dönitz et al., 2014; Schmitt-Engel et al., 2015).

## 5.2 Embryonic RNA isolation

The *Tribolium castaneum* San Bernadino wild-type strain (SB strain) was used for all experiments with the exception of iBeetle screen (pBA19 strain was used for pupal injection). Beetles were kept at 30 °C in boxes, which contained a mixture of 75% wheat flour “Extra” type 405 and 25% dark wheat flour type 1050 (Diamant) together with 25 g/kg dry yeast and 0.3 g/kg fungicide (Fumagilin). For egg collection, the beetles were transferred to “Instant” wheat flour (type 405 Diamant).

RNA isolation was performed as described by Stappert et al., 2016. The embryos were washed with water to remove all the adherent flour. After washing, the embryos were dechorionated with 50% Klorix/bleach for 2 min and were washed again with clean water to remove the remaining bleach. Eggs were transferred to a 1.5 ml Eppendorf tube and were homogenized in 500 µl Trizol reagents (Sigma) using a sterile pestle. The samples were centrifuged for 10 min (12,000xg) at 4 °C and the supernatant was transferred into a new Eppendorf tube. 500 µl of the Trizol reagents were added and the samples were incubated for 5 min at room temperature. After incubation, 200 µl of the chloroform (stored at -20 °C) were added to the samples and were mixed gently followed by incubation for 2-3 min at room temperature. The samples were centrifuged for 15 min (12,000xg) at 4 °C and the upper aqueous phase was transferred to a new 1.5 ml Eppendorf tube. The RNA was precipitated by adding 50 µl 3M NaAc (pH 5.2) and 800 µl 100% ethanol (EtOH) and was incubated overnight at -80 °C. After overnight incubation, the samples were centrifuged for 20 min (full speed) at 4 °C and the supernatant was discarded. The RNA pellet was washed by adding 500 µl 3M NaAc (pH 5.2) and the samples were centrifuged for 20 min (full speed) at 4 °C. The supernatant was discarded, the pellet was washed again by adding 800 µl of the 70% EtOH and the samples were centrifuged for 20 min (full speed) at 4 °C. After the washing steps, the pellet was dried for 5 min and afterwards resuspended in RNase-free water (21µl). The concentration of RNA was measured by spectrophotometer (NanoDrop, 2000c, Thermo Scientific) and the samples were stored until further use at -80 °C.

## 5.3 cDNA synthesis

For cDNA synthesis, the SuperScript™ VILO™ cDNA Synthesis Kit was used according to manufacturer's instructions. Master-Mix of 6 µl (4 µl of 5x VILO reaction mix and 2 µl of 10x SuperScript enzyme mix) was used together with RNA template (up to 2.5 µg). The final volume of 20 µl was adjusted with nuclease free water. The samples were first incubated for 10 min at 25 °C and then for one h at 42 °C. The reaction was stopped by increasing the temperature to 85 °C followed by 5 min long incubation. The samples were stored until further use at -20 °C.

## 5.4 Polymerase chain reaction (PCR)

The first PCR for digoxigenin (DIG) labeled probes synthesis and dsRNA synthesis was performed with gene specific primers which were tagged with partial sequence of T7 promoter. The second PCR was performed with gene specific forward primer and 3' T7

universal primer or with 5' and 3' T7 universal primers for DIG labeled probes and dsRNA synthesis, respectively. The following reaction mix and thermal cycling setup were used for PCR. 5 µl of the final reactions were analyzed on 1% agarose gel.

**Table 4. Reaction setup for standard PCR**

Components	20 µl PCR reaction
REDTaq® ReadyMix™ PCR Reaction Mix	10 µl
H <sub>2</sub> O	7 µl
cDNA	1 µl
5' Primer (10 µM)	1 µl
3' Primer (10 µM)	1 µl

**Table 5. Thermal cycling setup for standard PCR**

No.	Step	Time	Temperature
1	Initial denaturation	5 min	94 °C
2	Denaturation	30 s	94 °C
3	Primer annealing	30 s	55 °C
4	Elongation	1 min	72 °C
Repeat steps 2-4 for 35 times			
5	Final elongation	5 min	72 °C

## 5.5 Double stranded RNA synthesis

Double stranded RNA synthesis was performed according to the manufacturer instructions of MEGAscript™ T7 Transcription Kit. For *in vitro* transcription, 12 µl of master mix (2 µl of each NTPs (UTP, ATP, CTP, GTP), 2 µl T7 transcription buffer and 2 µl T7 polymerase mix) were mixed with 8 µl of dsRNA PCR template. The reaction was incubated for 6-8 h at 37 °C. After incubation, the reaction was stopped by adding 115 µl RNase-free water and 15 µl ammonium-acetate stop solution. The reaction was purified by adding 150 µl phenol-chlorophorm and the samples were mixed shortly before centrifugation at 5000 rpm for 5 min. The upper aqueous layer was transferred to a new Eppendorf tube and the RNA in the samples was precipitated by adding 150 µl isopropanol. The samples were incubated overnight at -20 °C followed by a centrifugation step for 15 min at 4 °C (full speed). Supernatant was discarded and the pellet was washed with 300 µl of 70% EtOH. The samples were centrifuged again for 5 min at 4 °C (full speed) and the supernatant was discarded. The pellet was dried for 5 min and then re-suspended in 50 µl RNase free water. The concentrations of dsRNA in the samples were measured by spectrophotometer. The samples were incubated for 5 min at 75 °C and were allowed to cool down slowly at room temperature. The dsRNA samples were stored at -20 °C.

## 5.6 DIG labeled probes synthesis

DIG labeled probe synthesis was performed as described by Stappert et al., 2016. The following master mix was used for DIG labeled probes synthesis (reagents from Roche).

7.5 µl RNase-free water

0.5 µl RNase-inhibitor

2 µl 10x transcription buffer

2 µl DIG labeling mix

2 µl T7 RNA polymerase

For *in vitro* transcription, 14 µl of master mix was mixed with 6 µl of the second PCR template for probes synthesis. The reaction was incubated for 4 h at 37 °C. After incubation, the reaction was stopped by adding 30 µl RNase-free water and 50 µl 2x stop solution. Precipitation was performed by adding 5 µl tRNA, 10 µl lithium chloride and 300 µl 100% EtOH and the samples were incubated overnight at -20 °C followed by a centrifugation step for 15 min at 4 °C (full speed). Supernatant was discarded and 300 µl of 70% ethanol was added to the samples. The samples were centrifuged again for 5 min at 4 °C (full speed) and the supernatant was discarded. The pellet was dried for about 5 min followed by resuspension in 50 µl 50% Formamide, 2x SSC solution and the samples were stored at -20 °C.

## 5.7 Fixation of embryos

First the eggs were washed with water to remove all the adherent flour. After washing, the eggs were dechorionated in 50% Klorix/bleach for 3 min and were washed again with clean water to remove the remaining bleach. After dechorionation, the eggs were transferred to a glass vial, which contained fixation solution (2 ml 10% Formaldehyde, 3 ml 1x PBS and 5 ml Heptane). After incubation of embryos in fixation solution for at least one h at room temperature on a plate shaker at 100 rpm, the lower phase was removed gently and was replaced by 5 ml methanol. The embryos were devitellinized by shaking and were transferred to Eppendorf tubes. The devitellinated embryos were washed several times with methanol and were stored until further use at -20 °C.

## 5.8 *In situ* hybridization (ISH)

The fixed embryos were gradually transferred from 100% methanol to PBST solution (first 2:1 and then 1:2 100% Methanol:PBST) followed by 2 washes in PBST for 5 min each. The embryos were fixed in 5% PFA solution (equal amount of 1xPBS and 10% Formaldehyde) for 30 min on rotating wheel. The embryos were washed with PBST (four times, 5 min each) and were transferred to hybridization solution. First 1:1 PBST/hybridization solution-1 and then 100% hybridization solution-1 for 10 min each at room temperature followed by pre-hybridization in 100% hybridization solution-2 for 1 h at 60 °C. 2 µl of ISH probes diluted in 100 µl hybridization solution-2 were added to the embryos and the samples were incubated

overnight at 60 °C on the rotating wheel. Next day, the probes were washed away by washing the embryos with pre-warmed hybridization solution-1 three times, 5 min each followed by four times washing for 30 min at 60 °C on the rotating wheel. The embryos were transferred gradually from hybridization solution-1 to PBST (2:1 hybridization solution-1/PBST and then 1:2 hybridization solution-1/PBST) followed by 100% PBST washing for 10 min each at room temperature. The embryos were incubated two times in blocking solution for 30 min at room temperature followed by incubation of embryos in Anti-Digoxigenin-AP (Alkaline Phosphatase) antibody (1:4000 in blocking solution) overnight at 4 °C. Next day, the embryos were rinsed twice followed by three washes with 100% PBST for 15 min at room temperature. Before the color reaction, the embryos were rinsed three times with AP-buffer. The color reaction was started by adding the staining solution (20 µl NBT/BCIP in 1 ml AP-buffer) to the embryos and the samples were kept in dark. The staining was observed under the stereomicroscope. The reaction was stopped by rinsing the embryos twice followed by three times washing with 100% PBST for 5 min each. Background staining was removed by incubating the embryos in 100% ethanol for about 30 min followed by three washing steps with 100% PBST for 5 min each. The embryos were embedded in the mounting medium containing 4',6-diamidin-2-phenylindol (DAPI) (Vectashield, Vector laboratories) and the samples were kept at 4 °C.

## 5.9 Double *in situ* hybridization (D-ISH)

Double *in situ* hybridization was performed in the same way as described in single *in situ* hybridization but with the following changes.

- During probe hybridization, 2 µl of each probe (“gene X” DIG labeled and “gene Y” fluorescein labeled probes) diluted in 100 µl hybridization solution were added together to the samples.
- Next day, the first antibody incubation was done with anti-fluorescein-AP (1:4000 in blocking solution) overnight at 4 °C.
- First staining was performed with NBT/BCIP (20 µl NBT/BCIP in 1 ml AP-buffer) as described in single *in situ* hybridization. Background staining was removed by incubating the embryos in 100% EtOH for about 30 min followed by three washing steps with 100% PBST for 5 min each.
- The first antibody was inactivated by washing the embryos with 100mM glycine-HCL (pH 2.3) three times for 20 min followed by two times of washing with 100% PBST for 20 min at room temperature. The embryos were washed twice with blocking solution for 30 min followed by incubation in second antibody (Anti-Digoxigenin-AP, 1:4000 in blocking solution) overnight at 4 °C.
- Next day, the embryos were rinsed twice followed by three washes with 100% PBST for 15 min at room temperature. Before the color reaction, the embryos were washed three times with 0.1M Tris-HCL buffer (pH 8.0) for 10 min at room temperature.
- Second staining was performed with FastRed (1 Fast Red tablet in 1 ml 0.1M Tris-HCL buffer, pH 8.0). Staining was observed under the stereomicroscope. The reaction



was stopped by rinsing the embryos twice followed by three times washing in 100% PBST for 5 min each.

- The embryos were embedded in the mounting medium containing DAPI and the samples were kept at 4 °C.
- Note: Ethanol treatment is not recommended for FastRed staining. NBT/BCIP and DIG labeled probes yield strong staining while FastRed and fluorescein labeled probes staining is usually weaker, therefore we used the combination of weaker probes with strong color reaction and vice versa.

## 5.10 Antibody staining

The dechoriation and fixation of the embryos was performed as described for *in situ* hybridization. For antibody staining, longer fixation time (more than one hour) and embryos preservation in methanol is not recommended. The freshly devitellinated embryos were rinsed twice with 100% methanol followed by gradual rehydration from methanol to PBST (first 2:1 and then 1:2 100% methanol/PBST). The embryos were washed once with 100% PBST for 10 min before incubation in blocking solution (100 µl BSA, 250 µl NGS and upto 5ml volume with PBST) for 30 min at room temperature. Samples were incubated in the first antibody diluted in fresh blocking solution (for both Dorsal and Phospho-Smad Rabbit mAb 1:50 dilution was used, 100 µl per sample) over night at 4 °C. Next day, the embryos were rinsed twice followed by two washes with PBST for 20 min at room temperature. The embryos were incubated in blocking solution for one h and then incubated with the second antibody (Goat-Anti-Rabbit IgG, Alexa Fluor 488) diluted in fresh blocking solution (1:1000) over night at 4 °C. Next day, the embryos were washed twice with PBST for 15 min. The embryos were embedded in the mounting medium containing DAPI and the samples were kept at 4 °C.

## 5.11 Microscopy and photos processing

Embedded embryos were mounted on a microscope slide with double spacers on both sides of the slide. Confocal microscope with Z-stack option of 3 intervals (30-40 slices) with their corresponding DAPI and Alexa-Fluor-488 channels were used to take photos of fluorescence antibody stained embryos. For *in situ* staining, Axioplan-2 microscope (Zeiss) was used to take photos with Z-stack option (10 Z-stacks for each embryo) and later Helicon-Focus-6 software was used to merge these Z-stacks into a single photo.

## 5.12 Phylogenetic analysis

Multiple sequence alignments of the corresponding protein sequences were performed with Clustal Omega (<https://www.ebi.ac.uk/Tools/msa/clustalo/>). Evolutionary analyses were conducted in Phylogeny.fr (<http://www.phylogeny.fr/index.cgi>) using the alignment curation with Gblocks and Maximum Likelihood method with 100 bootstraps value. Tree visualization and adjustments were performed with FigTree software.

### 5.13 Quantitative reverse transcription PCR (qRT-PCR)

Primers for the gene of interest were designed in a way that the length of the amplicon was about 100-150 bp and the primers span an intron as well. Validated RPS3 primers were used as a reference gene. Applied biosystems (ABI 7500) software was used to plan an experimental setup. Three biological replicates were used for wild-type samples and controls (pool of all the samples and a non-template control) while for iB-07888 knock down, only one biological replicate was used. GoTaq® qPCR Master Mix-Promega was used with the following thermal cycling setup:

Holding stage: 95 °C for 02:00 min

Cycling stage: 95 °C for 00:03 min (40 cycles)

Melt-curve stage: 95 °C for 00:15 min, 60 °C for 01:00 min, 95 °C for 00:15 min, 60 °C for 00:15 min.

RNA extraction and cDNA synthesis was performed as described earlier. The cDNA product was diluted to 10 ng/μl and the aliquots were stored at -80 °C. The aliquots were diluted to final concentration of 4ng/μl immediately before setting up the plates and 5 μl from the final concentration was used for RT-qPCR reaction. 5 μl of template were added to 15 μl of the master mix (primer1 (10 μM) 0.80 μl, primer2 (10 μM) 0.80 μl, GoTaq® qPCR Master Mix 10 μl, H<sub>2</sub>O 3.40 μl) with multichannel pipette into MicroAmp 96-well plate. The plate was sealed and the experiment was performed with the above mentioned program setup.

LinRegPCR version 12.16 was used to calculate the baseline correlation and Cp values (Tuomi et al., 2010; Ruijter et al., 2009). The expression ratio was calculated by the following formula:

$$R = \frac{(E_{\text{target}})^{\Delta C p_{\text{target}}} (C p_{\text{sample}} - C p_{\text{target}})}{(E_{\text{reference}})^{\Delta C p_{\text{reference}}} (C p_{\text{sample}} - C p_{\text{reference}})}$$

Where R = expression ratio, E = mean PCR efficiency and ΔCP = number of cycle where amplicon reaches the threshold of florescence.

## 6. Results

### 6.1 The iBeetle large scale RNA interference screen

The aim of the iBeetle large scale RNA interference (RNAi) screen was to overcome the candidate gene approach and to identify the missing and novel components of dorsoventral (DV) axis formation in *Tribolium castaneum* in an unbiased way. During the first part of my PhD project, I participated in the iBeetle large scale RNAi screening (Phase-II). The iBeetle RNAi screening and re-screening of the selected candidate genes took 19 months. In total, I have screened  $\approx 850$  genes in the second phase of the iBeetle RNAi screen (Total  $\approx 3400$  genes in Phase-II by four screeners).

In the iBeetle RNAi screen, a fixed schedule of five repetitions was performed in parallel in one experimental bundle (Figure 10). After concluding each bundle, the same schedule was repeated for another round of experiments. 22 iB-fragments together with one negative control and two positive controls were injected in one repetition. dsRNA solution of  $1 \mu\text{g}/\mu\text{l}$  was injected into 10 females pupae per iB-fragment. Different phenotypic analyses were performed in parallel for a single gene knockdown (Figure 12).

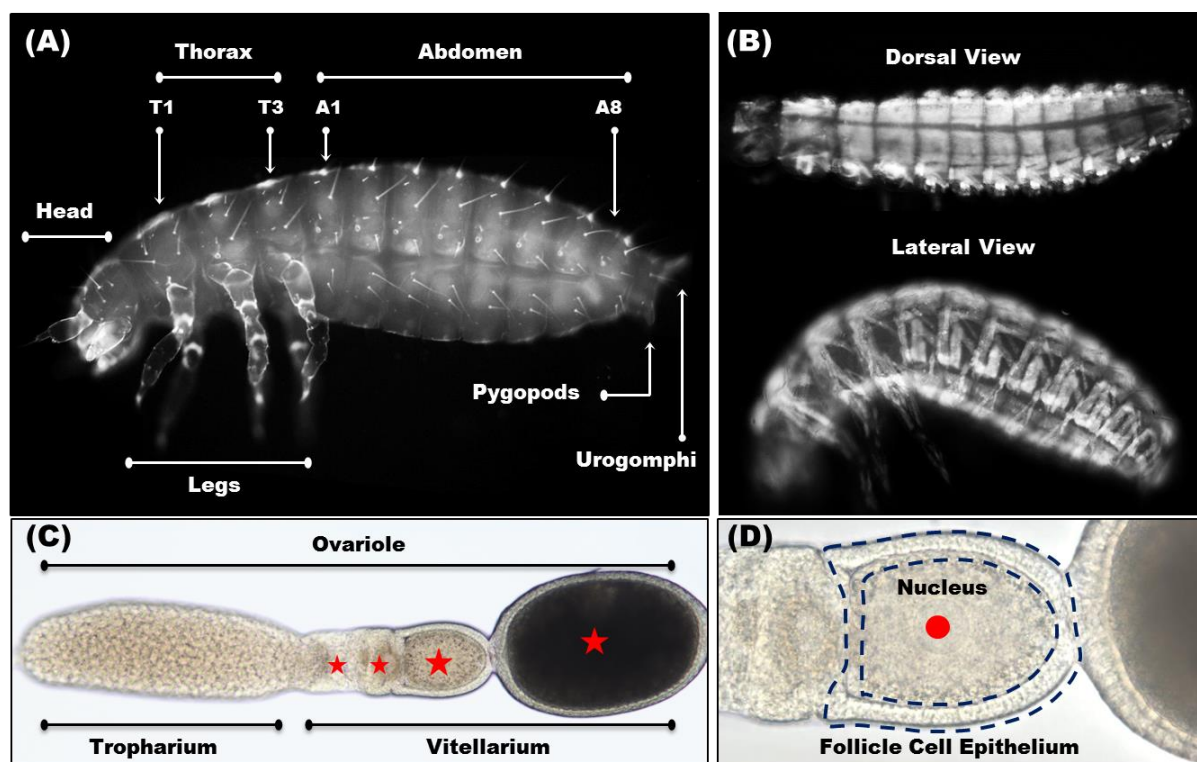


**Figure 12. Phenotype analyses in the iBeetle large scale RNAi screen.**

In the screen, different analyses were performed for each gene knockdown. (A) Cuticle analysis of the knockdown embryos was performed for any abnormal cuticle phenotypes. (B) Muscle analysis was performed by observing the larval muscle patterns (dorsal and lateral view). (C-D) Ovary analysis was performed for oogenesis defects. (C) Single ovariole of *T. castaneum* ovary (the red stars represent the egg chambers). (D) Close-up view of a single egg chamber (red dot depicts the oocyte nucleus and the dashed blue lines show the follicle cell epithelium).

For instance, cuticle analysis was performed by analyzing their offspring embryos for any abnormal cuticle phenotypes (addition, deletion or transformation of larval segments or appendages). Somatic muscle analysis was performed under the fluorescence microscope by observing the larval specific muscle patterns (Figure 12B). In case of low egg productivity, the ovary analysis was performed for oogenesis defects.

After knockdown of each gene, the phenotypes were documented along with their corresponding pictures of the phenotypes (Figure 13). Phenotype annotations were performed electronically using an online interface based on EQM (entity, quality and modifier) system and using of controlled vocabularies (Dönitz et al., 2014; Dönitz et al., 2013). For example, a larva with leg phenotypes was annotated with larva leg/segments (entity, E) size/number (quality of the change, Q) increased/decreased/shortened (nature of the change, M). The complete data of the iBeetle RNAi screening of both Phase-I and Phase-II are available online at the iBeetle-Base (<http://ibeetle-base.uni-goettingen.de/>).

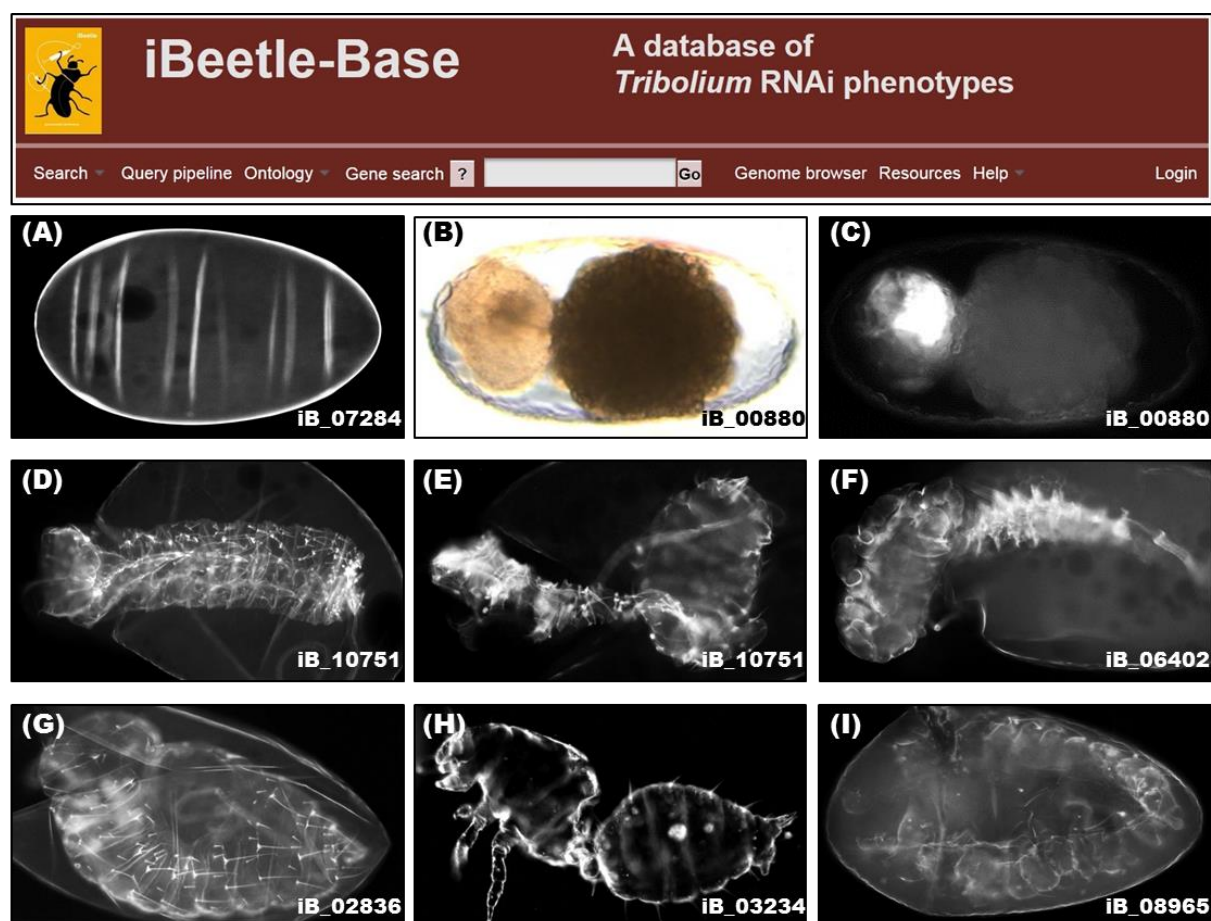


**Figure 13. Potential dorsoventral cuticle phenotypes from the iBeetle large scale RNAi screen.**

The iBeetle data set of the Phase-II was screened for these potential DV phenotypes for re-screening and in-depth analysis. (A) Empty egg phenotype during cuticle analysis. (B-C) Embryos with undefinable tissue development (without and with fluorescence, respectively). (D) Complete everted (inside-out) phenotype, (E) partially anterior everted phenotype, (F) partially posterior everted phenotype and (G) dorsal not closed phenotype. (H) Larval DV orientation irregular phenotype and (I) larval ventral not closed phenotype.

Based on signaling pathways involved in DV axis formation (EGF, Toll and BMP signaling), a range of cuticle phenotypes from the iBeetle screen was relevant to our project. For instance, if the knockdown genes belong to EGF signaling, potentially it will lead to sterility or empty eggs phenotypes (Figure 13A). Genes involved in Toll signaling will potentially lead to empty eggs phenotypes (with or without cuticle crumbs/remnants) and everted phenotypes (both partially and completely everted) (Figure 13D-F). Knockdown of *short gastrulation (sog)* like genes will potentially lead to everted phenotypes. Knockdown of targets of BMP signaling will potentially lead to empty eggs and dorsal or ventral not closed phenotypes (Figure 13G and 13I, respectively). Keeping in view the nature of these DV phenotypes, the iBeetle data set of the Phase-II was screened for the respective annotated phenotypes. In total, 218 empty eggs phenotypes (with and without fluorescence) and 81 abnormal cuticle phenotypes (59 everted, 19 dorsal/ventral not closed and 3 DV orientation irregular phenotypes) were annotated in the iBeetle-Base (Figure 14). For re-screening, the list was reduced to only 30 genes based on phenotype penetrance, gene annotation and exclusion of the large data set of the empty eggs phenotypes.

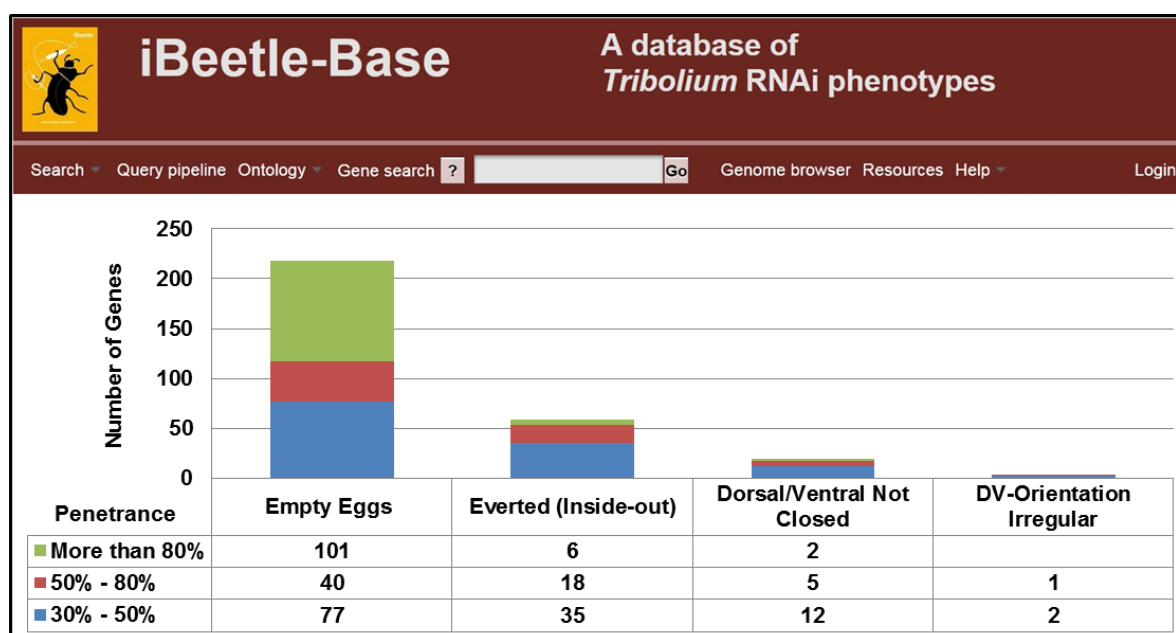


**Figure 14. Genes with potential function in DV patterning from the iBeetle large scale RNAi screen.**

The iBeetle annotated phenotypes of the knockdown genes from the second phase were screened for potential DV phenotypes. In total 218 empty eggs and 81 abnormal cuticle phenotypes (everted (inside-out), dorsal/ventral not closed and DV orientation irregular) were identified with different penetrance.

Furthermore, previously known components and targets of DV patterning pathways (EGF signaling, protease cascade, Toll signaling and BMP signaling) were searched in the iBeetle data set. 38 out of 50 genes showed the respective DV phenotypes while 5 genes caused no phenotype and 7 were not present in the iBeetle RNAi screen (Supp. Figure 1).

## 6.2 Re-screening and selection of the iBeetle candidates

As the iBeetle screen was the first pass screen, which means that each gene knockdown was performed only once (Schmitt-Engel et al., 2015), the re-screening was important to confirm the annotated phenotypes. In total, 30 genes were selected for the re-screening from abnormal cuticle phenotypes based on gene function, phenotype annotation and phenotype penetrance (only genes with more than 50% phenotype penetrance were selected for the re-screening). The re-screening of the selected iBeetle candidates with potential DV phenotypes was performed by injecting two dsRNA fragments (iB-fragments and non-overlapping fragments (NOFs), concentration of 1 µg/µl) of the same gene into two different genetic backgrounds (pBA19 and San Bernadino (SB) strains). Only egg productivity, lethality and cuticle analyses were performed during the re-screen. The re-screening results were classified in three categories e.g. reproduced (the iBeetle annotated phenotype was completely reproduced with almost the same penetrance level), partially reproduced (the iBeetle annotated phenotype was reproduced with low penetrance) and not reproduced (the iBeetle annotated phenotype was not reproduced in the re-screening e.g. hatched as a wild-type or showed different phenotypes like lethality or pantagmatic defects) (Figure 15).

Altogether, the annotated phenotypes of 26 genes were reproduced with iB-fragment after injection in the pBA19 strain. Out of which 18 genes showed complete phenotype reproducibility and 8 genes showed partial phenotype reproducibility, while the phenotypes of the remaining 4 genes were not reproduced during the re-screen (Figure 15). However, the percentage of phenotype reproducibility was reduced, when gene knockdowns were performed by using non-overlapping dsRNA fragments (NOFs) and a different genetic background (SB strain). In addition, two iBeetle candidates (iB-09824 and iB-02326) showed potential strain specific effect by giving stronger phenotype in pBA19 strain and weaker or no phenotype in SB strain (Supp. Table 2-6).

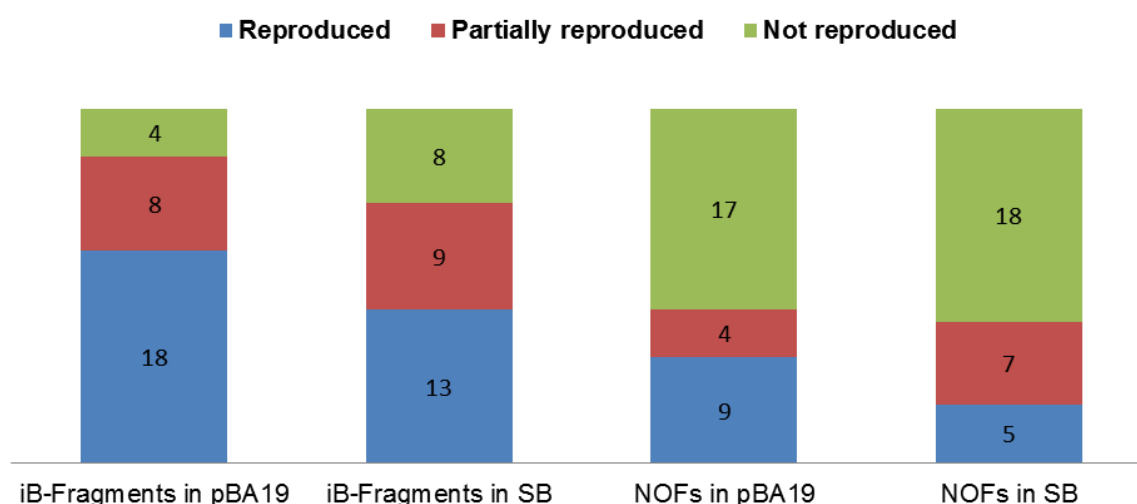


**Figure 15. Reproducibility of the selected iBeetle candidates in the re-screen.**

In total, 30 genes of abnormal cuticle phenotypes were re-screened. The complete, partial and no phenotype reproducibility are shown in blue, red and green colors, respectively. NOFs-non-overlapping dsRNA fragments, SB-San Bernadino.



Five iBeetle candidates which lacked off-target and strain specific effect (which phenotypes were reproduced with both fragments and both strains) were selected for in-depth analysis. The knockdown of two of these fully reproducible genes iB-09592 (*exostosin*) and iB-02234 (*sulfateless*), showed partially everted (abdomen not present) cuticle phenotypes (Figure 16B and 16C). However, they didn't show any early embryonic DV phenotypes (data not shown), but initial analysis of both genes knockdown embryos showed reduced serosa phenotype, which was confirmed by *in-situ* hybridization which show reduced expression of *Tc-zen1* during blastoderm stage (Supp. Figure 2B and 2C). Furthermore, *Tc-twist* expression domain was also reduced in iB-09592 knockdown embryos (Figure 2E). Further experiments are necessary to confirm the phenotypes of iB-09592 and iB-02234 and their potential new role in DV pattern formation. Moreover, two other reproduced iBeetle candidates (iB-07888 and iB-09824), which belongs to trypsin superfamily showed everted (inside-out) and strongly fragmented (potentially everted) cuticle phenotypes during the iBeetle screen (Figure 16D and 16E). Further analyses of these genes showed an important role in DV axis formation which will be described in the next sections. Finally, iB-06402 (*uninflatable*), knockdown of which causes partially everted cuticle phenotypes (Figure 16F), was also fully reproduced during the re-screen. However, this gene was recently identified with RNA-seq approach by Stappert et al., 2016.

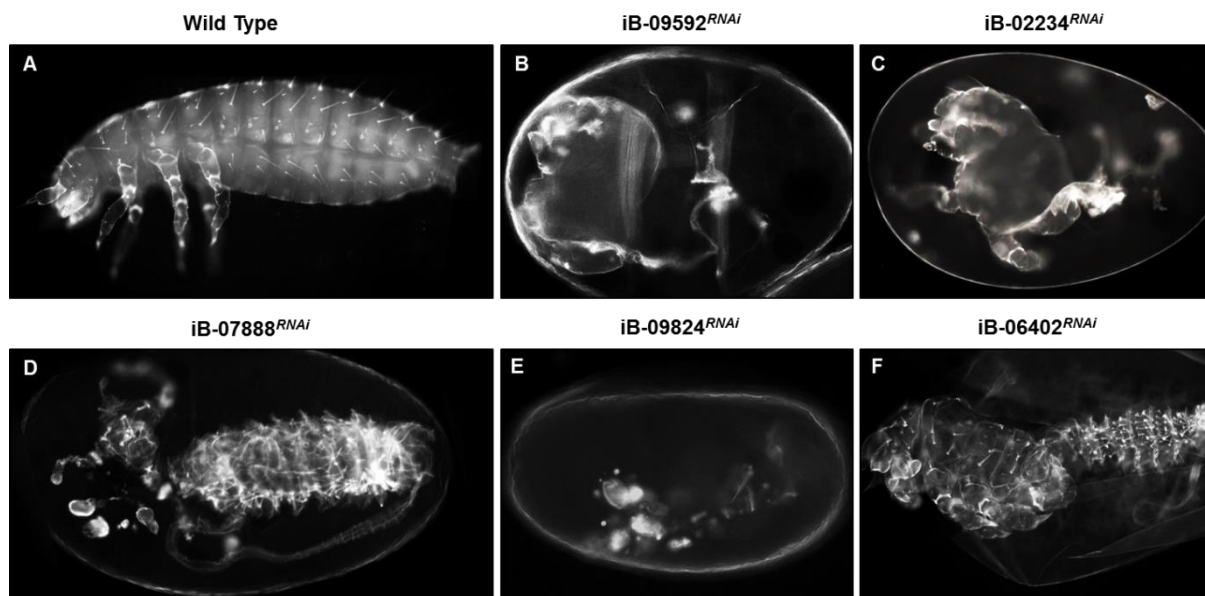


**Figure 16. Cuticle phenotypes of the completely-reproduced iBeetle candidates in the re-screen.**

In total, five iBeetle candidates which reproduced completely were selected for in-depth analysis. (B-F) Cuticle phenotypes of the completely-reproduced iBeetle candidates, iB-09595, iB-02234, iB-07888, iB-09824 and iB-06402, respectively. (A) Wild-type cuticle, (B-C) partially everted (abdomen not present), (D) complete everted (inside-out), (E) strongly fragmented (potentially everted) and (F) partially everted cuticle phenotypes.

### 6.3 iB-09824 (TC032710) anionic trypsin-2-like serine protease

One of the iBeetle candidate iB-09824 (TC032710), which belongs to trypsin superfamily, showed potentially everted and strongly fragmented cuticle phenotypes during the iBeetle screen (Figure 16E). The annotated cuticle phenotypes of iB-09824 were also reproduced with NOF during the re-screen. To investigate the potential DV function of iB-09824 in *T. castaneum*, we performed whole-mount *in-situ* hybridization in iB-09824 knockdown embryos using DV marker genes. Expression of *Tc-zen1*, *Tc-twist* and *Tc-sog* in iB-09824 knockdown embryos revealed completely dorsalized phenotypes (Figure 17). In wild-type embryos, *Tc-zen1* is expressed in the serosa during the differentiated blastoderm stage (Figure 17A). However, the expression of *Tc-zen1* in iB-09824 knockdown embryos was expanded towards posterior and the oblique serosa-embryo border was rotationally symmetric (Figure 17D), similarly like in *Tc-Toll* and *Tc-sog* knockdown embryos (Figure 17B and 17C, respectively). Moreover, *Tc-twist* and *Tc-sog*, which are ventrally expressed during early blastoderm stage in wild-type embryos (Figure 17E and 17I, respectively), were not present in iB-09824 knockdown embryos (Figure 17H and 17L, respectively). The same was observed in *Tc-Toll* and *Tc-easter* (iB-07073) knockdown embryos. The expression analysis of DV marker genes in iB-09824 knockdown embryos indicate that the knockdown of iB-09824 is causing completely dorsalized phenotypes.

Phylogenetic evolutionary analysis was performed to identify the potential orthologs of iB-09824 (TC032710) in *Drosophila melanogaster*. Multiple sequence alignment of 21 protein sequences of *D. melanogaster* and *T. castaneum* (best blast hits of iB-09824) was performed with Clustal Omega and evolutionary analysis were conducted in Phylogeny.fr. No obvious *D. melanogaster* ortholog of iB-09824 (TC032710) was identified in the analysis (Figure 18A). It is important to note that the phylogenetic analysis of iB-09824 resulted with low bootstrap support. Therefore, further analysis with alternative sequence trimming methods will be necessary to achieve the final conclusive results of the phylogenetic analysis. For the detection of conserved domains, sequence analysis of iB-09824 (327 amino-acid) was performed by SMART (Simple-Modular-Architecture-Research-Tool). One domain of Tryp-SPc (trypsin-like serine protease, position 77 to 311) along with signal peptide (position 1 to 18) was predicted by SMART (Figure 18B).

Furthermore, no specific expression pattern of iB-09824 was observed by *in-situ* hybridization (data not shown), however, the RNA-seq data from official gene set version 3 (OGS3) showed very weak read coverage during the differentiated blastoderm stage, suggesting the presence of the transcript. No read coverage was present for pre-blastoderm, ovarian and unfertilized egg stages.



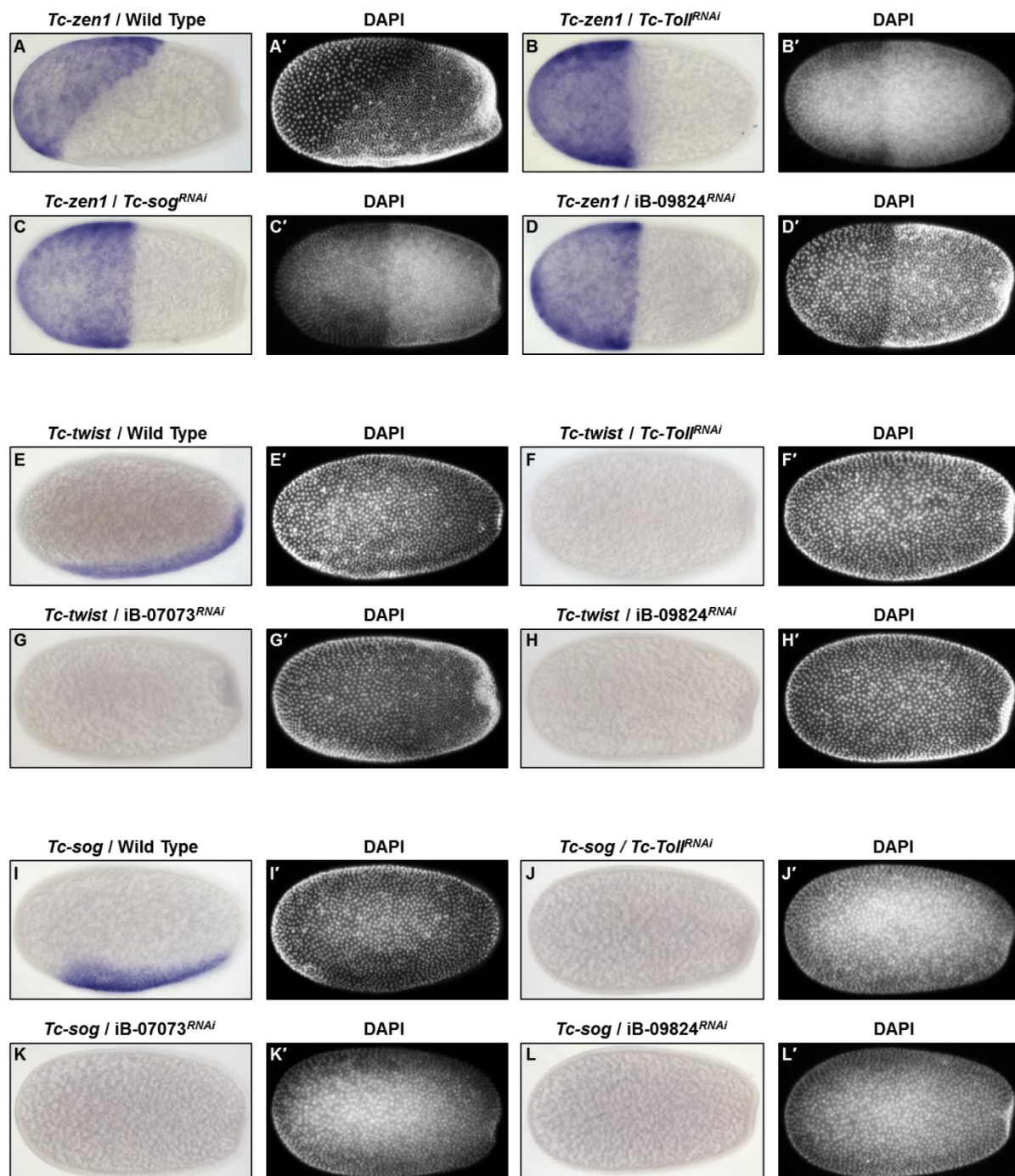


**Figure 17. Expression pattern of *Tc-zen1*, *Tc-twist* and *Tc-sog* after iB-09824 knockdown.**

(A-L) Whole-mount *in-situ* hybridization of blastoderm stage embryos. (A-D) *Tc-zen1* expression pattern, (E-H) *Tc-twist* expression pattern and (I-L) *Tc-sog* expression pattern. The anterior of the embryos points to the left and the dorsal side of the embryos points upwards. (A'-L') Nuclear staining (DAPI) of the respective embryos. Knockdown of iB-09824 (TC032710) produced complete dorsalized phenotype. (A) *Tc-zen1* is expressed in the serosa in wild-type embryos. (B-D) The expression of *Tc-zen1* is expanded and the serosa-embryo border is straight in *Tc-Toll*, *Tc-sog* and iB-09824 knockdown embryos, respectively. (E) *Tc-twist* and (I) *Tc-sog* expression in wild-type embryos. (H and L) *Tc-twist* and *Tc-sog* are not expressed in iB-09824 knockdown embryos, (F, G, J and K) likewise *Tc-Toll* and iB-07073 knockdown embryos, respectively.

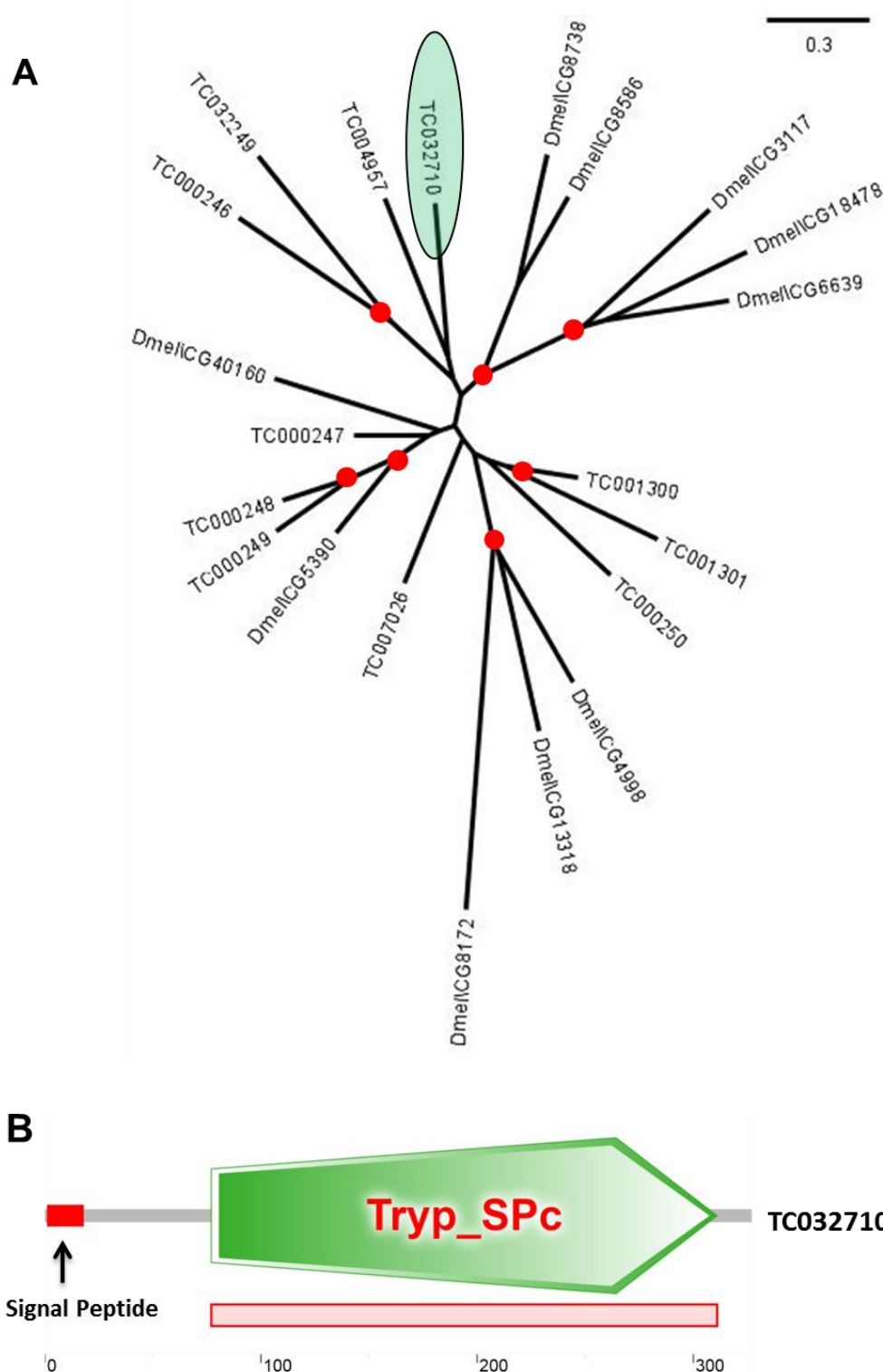


**Figure 18. Phylogenetic and sequence analysis of iB-09824 (TC032710).**

(A) Phylogenetic tree of iB-09824 (TC032710). The phylogenetic evolutionary analyses were conducted in Phylogeny.fr. Clades marked with filled red circles have the bootstrap value of more than 50%. iB-09824 (TC032710) is highlighted with green circle in the phylogenetic tree. The branch length measured the number of substitutions per site. In the phylogenetic tree, iB-09824 (TC032710) clustered separately from *D. melanogaster* genes. (B) Conserved domains identification of iB-09824 (TC032710). A Tryp-SPc domain (position 77 to 311) and a signal peptide (position 1 to 18 indicated by an arrow) were predicted by SMART. Grey line indicates the region without having any conserved domain while the red bar predicts that Tryp-SPc domain is catalytically inactive.

## 6.4 iB-07888 (TC011067) serine protease P125

Another iBeetle candidate (iB-07888) known as serine protease P125, which belongs to trypsin superfamily has an important role in DV pattern formation in *T. castaneum*. Knockdown of iB-07888 by parental RNAi resulted in larvae with everted (inside-out) and head-deleted cuticle phenotypes in the iBeetle screen. For in-depth analysis, the expression pattern of iB-07888 was determined by whole-mount *in-situ* hybridization. In wild-type embryos, iB-07888 is initially expressed during early blastoderm stage in a narrow ventral domain along the entire AP axis (Figure 19A and 19B), while later at differentiated blastoderm stage, the strong ventral expression of iB-07888 was confined to the ventral domain of the presumptive head region (Figure 19C). As the development proceeds, the weak ventral expression was still present during gastrulation and serosal window stage, however, iB-07888 is also expressed in the head lobes during serosal window stage (Figure 19F).

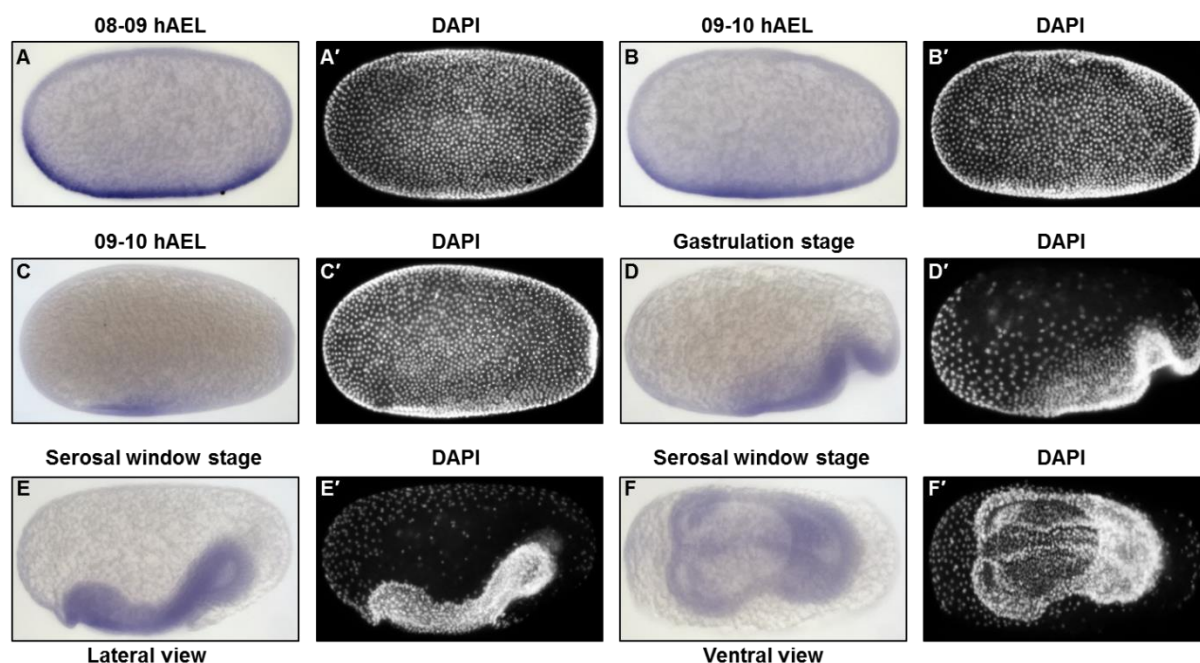


**Figure 19. Expression pattern of iB-07888 (TC011067) by whole-mount *in-situ* hybridization.**

(A-C) Whole-mount *in-situ* hybridization of blastoderm stage embryos, (D) gastrulating embryo and (E-F) serosal window stage embryos. The anterior of the embryo points to the left and the dorsal side of the embryos points upwards, except for (F) which shows the ventral surface view of the embryo. (A'-F') Nuclear staining (DAPI) of the respective embryos. (A-B) Ventral expression of iB-07888 during blastoderm stage along the AP axis. (C) Confined ventral expression of iB-07888 in the presumptive head region. (D-E) During gastrulation, iB-07888 is weakly expressed ventrally and (F) later it is expressed in the head lobes during serosal window stage.

Furthermore, the RNA-seq data of iB-07888 available in *Tribolium* official gene set version 3 (OGS3), showed strong read coverage at blastoderm stage, while very weak read coverage was present for ovarian and unfertilized egg stages. Moreover, high expression levels of iB-07888 in differentiated blastoderm stage were observed by quantitative reverse transcription PCR (qRT-PCR) (Supp. Figure 3). This result corresponds to the *in-situ* hybridization results, which shows strong expression of iB-07888 in wild-type embryos at 06-10 hAEL



I performed parental RNAi knockdown experiment of Toll signaling to determine, whether the narrow ventral expression of iB-07888 during early blastoderm stage is established by Toll signaling. The early ventral expression of iB-07888 was absent in iB-09824 (anionic trypsin-2-like serine protease), iB-07073 (*easter* like) and *Tc-Toll* knockdown embryos (Figure 20). The absence of iB-07888 expression in iB-09824, iB-07073 and *Tc-Toll* knockdown embryos suggest that the early ventral expression of iB-07888 is established by Toll signaling. However, iB-07888 itself is essential for normal Toll signaling and nuclear dorsal gradient formation. iB-07888 knockdown embryos showed typical dorsalized embryonic phenotype with extended symmetric serosa-embryo border along the DV axis and short germ rudiment formation (Figure 21).

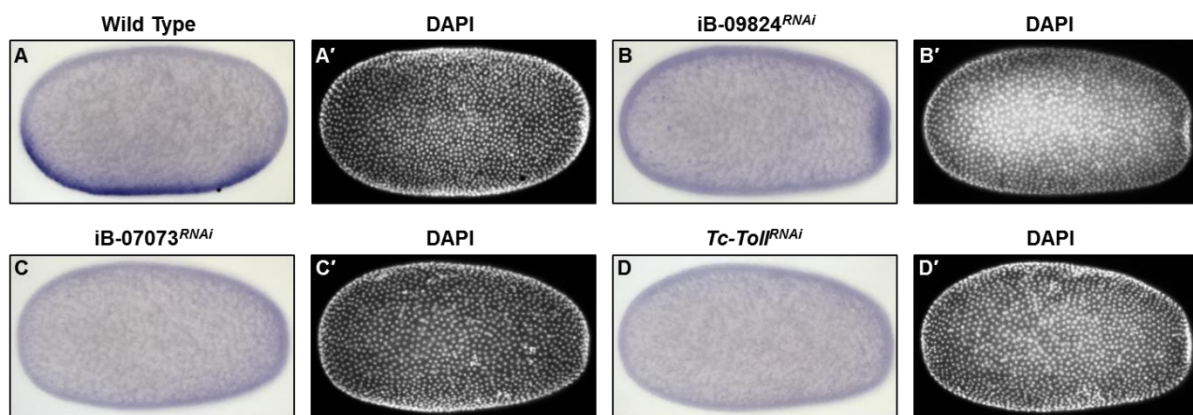


**Figure 20. Expression pattern of iB-07888 after iB-09824, iB-07073 and *Tc-Toll* knockdown.**

(A-D) Whole-mount *in-situ* hybridization of blastoderm stage embryos. The anterior of the embryo points to the left and the dorsal side points upwards. (A'-D') Nuclear staining (DAPI) of the respective embryos. (A) Ventral expression of iB-07888 in wild-type embryo. (B-D) iB-07888 is not expressed in iB-09824, iB-07073 and *Tc-Toll* knockdown embryos, respectively.

To further investigate the function of iB-07888 in DV patterning, I carried out *in-situ* hybridization of different DV marker genes in iB-07888 knockdown embryos. In wild-type embryos, *Tc-zen1* is expressed in the serosa (Figure 22A), however, the expression of *Tc-zen1* in iB-07888 knockdown embryos was expanded towards posterior and the oblique serosa-embryo border was rotationally symmetric (Figure 22D) similarly like in *Tc-Toll* and *Tc-sog* knockdown embryos (Figure 22B and 22C, respectively). In wild-type embryos, *Tc-twist* is expressed ventrally during the early blastoderm stage (expression starts at 7 hAEL). However, upon iB-07888 knockdown, the expression of *Tc-twist* was delayed till the primitive pit stage (10 hAEL) and later the expression starts in a broad ventral domain (Figure 22H). Interestingly, *Tc-sog* expression was completely absent in iB-07888 knockdown embryos (Figure 22K) with the exception of a few knockdown embryos, which showed weak lateral expression of *Tc-sog* at the primitive pit stage (Figure 22L). Expression patterns of *Tc-twist* and *Tc-sog* in iB-07888 knockdown embryos at different developmental stages are shown in Supp. Figure 4 and Supp. Figure 5, respectively.

The above mentioned *in-situ* hybridization results of iB-07888 were also reproduced with NOF (dsRNA concentration of 1 µg/µl) and with low concentration of dsRNA (0.5 µg/µl) while, strong knockdown (3 µg/µl) leads to sterility (data not shown).

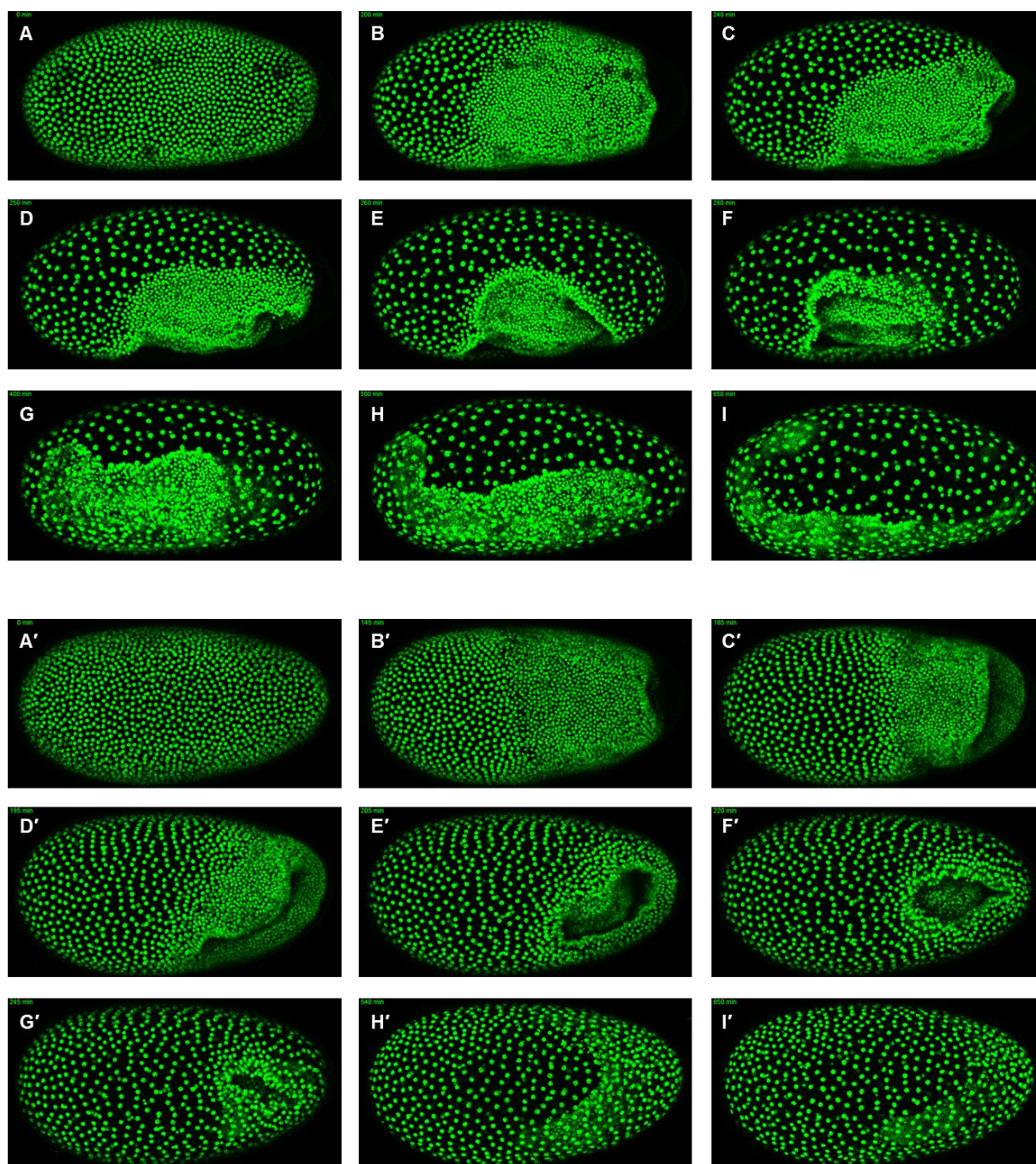


**Figure 21. Embryonic development of *T. castaneum* wild-type and iB-07888 knockdown embryos.**

(A-I) Wild-type embryo, (A'-I') iB-07888 knockdown embryo. The anterior of the embryos points to the left. (A) Uniform blastoderm stage, (B) differentiated blastoderm stage, (C) early gastrulation, (D) late gastrulation (E) horseshoe amniotic fold stage (F) serosa window closure stage (G) germband stage (H) extended germband stage and (I) fully extended germband stage. (A') Uniform blastoderm stage, (B') differentiated blastoderm stage with extended serosa, (C') early gastrulation, (D') late gastrulation and (E'-I') potential germband formation with DV phenotype. Live imaging of iB-07888 knockdown embryos showed dorsalized embryonic phenotype with extended serosa and rotationally symmetric serosa-embryo border. Produced by Matt Benton.



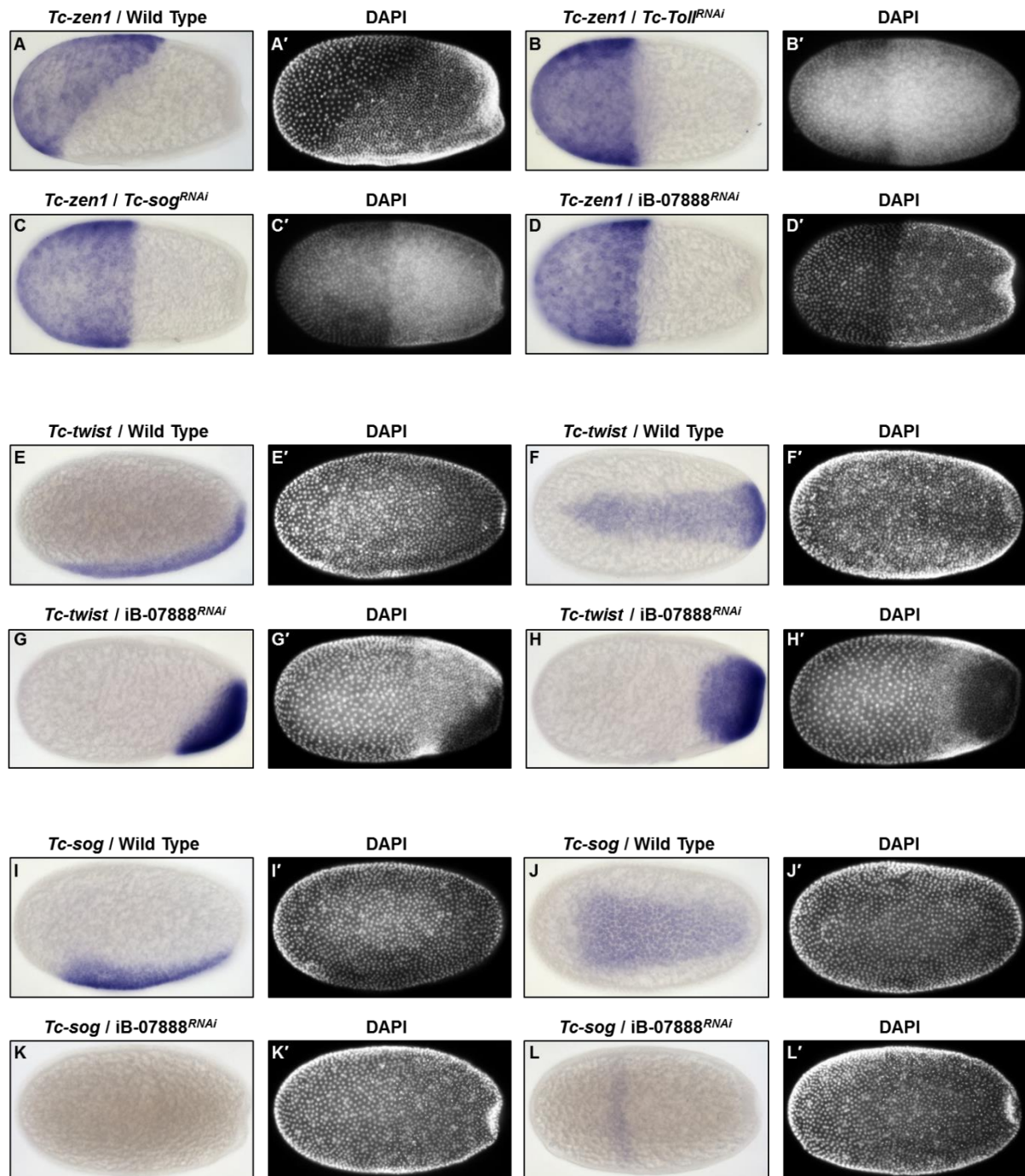


**Figure 22. Expression pattern of *Tc-zen1*, *Tc-twist* and *Tc-sog* after iB-07888 knockdown.**

(A-L) Whole-mount *in-situ* hybridization of blastoderm stage embryos. (A-D) Expression of *Tc-zen1*, (E-H) expression of *Tc-twist* and (I-L) expression of *Tc-sog*. The anterior of the embryo points to the left and the dorsal side of the embryos points upwards, except for (F, H, J and L) which show the ventral surface view of the embryos. (A'-L') Nuclear staining (DAPI) of the respective embryos. Knockdown of iB-07888 (TC011067) produced dorsalized phenotype. (A) *Tc-zen1* is expressed in the serosa in wild-type embryos. (B-D) The expression of *Tc-zen1* is expanded and the serosa-embryo border is straight in *Tc-Toll*, *Tc-sog* and iB-07888 knockdown embryos, respectively. (E-F) *Tc-twist* expression in wild-type embryos. (G-H) *Tc-twist* expression pattern in iB-07888 knockdown embryos in a broad ventral domain. (G lateral view and H ventral view of the same embryo). (I-J) *Tc-sog* expression in wild-type embryos. (K) Absence of *Tc-sog* expression in iB-07888 knockdown embryos. (L) Weak lateral expression of *Tc-sog* in iB-07888 knockdown embryos (ventral view).

Furthermore, *Tc-snail* and *Tc-sim* which are expressed ventrally during blastoderm stage in wild-type embryos, showed a delayed expression in a broad posteriorly restricted ventral domain in the iB-07888 knockdown embryos (Figure 23A-D). In wild-type embryos, *Tc-doc* is expressed in the serosa and in addition at the dorsal side of the embryo during differentiated blastoderm stage, however, after iB-07888 knockdown, the expression of *Tc-doc* was rotationally symmetric within the serosa (Figure 23E-F).

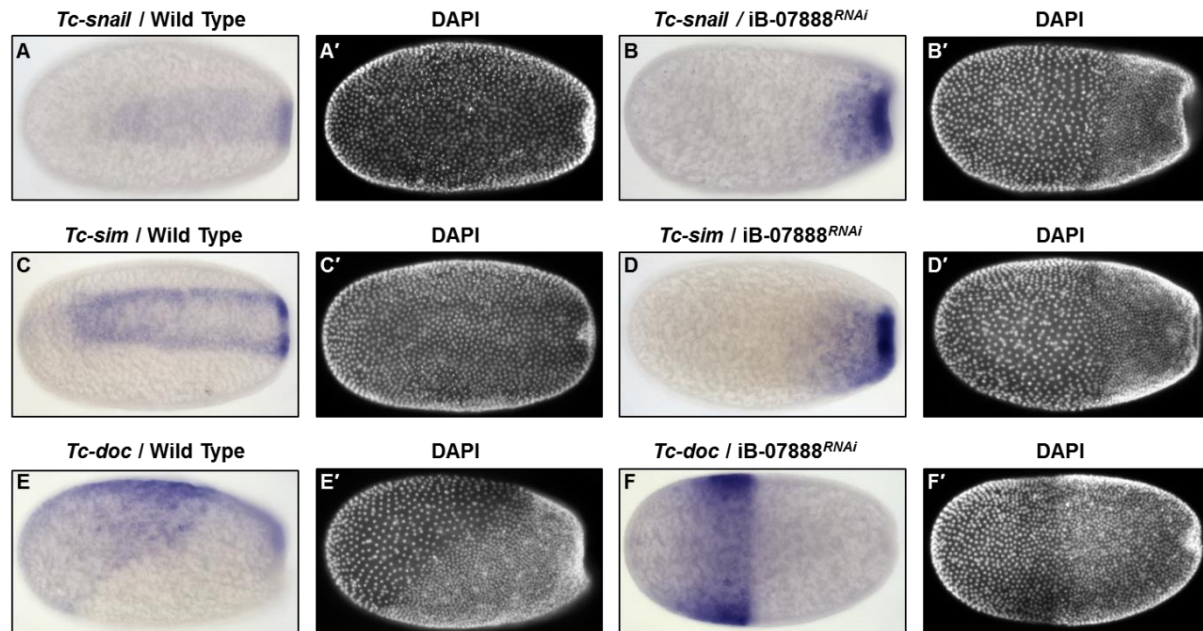


**Figure 23. Expression pattern of *Tc-snail*, *Tc-sim* and *Tc-doc* after iB-07888 knockdown.**

(A-F) Whole-mount *in-situ* hybridization of differentiated blastoderm stage embryos. The anterior of the embryo points to the left. (A-D) Ventral surface view of the embryos and (E-F) lateral view of the embryos. (A'-F') Nuclear staining (DAPI) of the respective embryos. (A) *Tc-snail* expression in wild-type embryo, (B) *Tc-snail* expression in iB-07888 knockdown embryo, (C) *Tc-sim* expression in wild-type embryo, (D) *Tc-sim* expression in iB-07888 knockdown embryo, (E) *Tc-doc* expression in wild-type embryo and (F) *Tc-doc* expression in iB-07888 knockdown embryo. After iB-07888 knockdown, both *Tc-snail* and *Tc-sim* are expressed in a broad ventral domain (B and D, respectively) while the expression of *Tc-doc* is rotationally symmetric within the serosa (F).

To investigate, whether the broad posteriorly restricted ventral expression of *Tc-twist*, *Tc-snail* and *Tc-sim* after iB-07888 knockdown is due to the expansion of the serosa, I performed double knockdown of iB-07888 with *Tc-zen1* and *Tc-dpp*. Control *in-situ* hybridization experiments confirmed the absence of *Tc-zen1* expression after iB-07888+*Tc-zen1* knockdown and reduced *Tc-zen1* expression domain with straight serosa-embryo border after iB-07888+*Tc-dpp* knockdown (Figure 24C-D). The expression of *Tc-twist* was delayed in both double knockdown embryos, however, later it express in a broad ventral domain but in contrast to single knockdown of iB-07888, the expression domain of *Tc-twist* was expanded towards the anterior in double knockdown embryos (Figure 24G-H). Unexpectedly, the expression domain of *Tc-sog* was broader and expanded in iB-07888+*Tc-dpp* knockdown embryos in contrast to iB-07888+*Tc-zen1* knockdown embryos, where the expression of *Tc-sog* was either completely absent or with weak lateral expression, like in single knockdown embryos of iB-07888 (Figure 24J-L). These results suggest that the posteriorly restricted ventral expression of *Tc-twist*, *Tc-snail* and *Tc-sim* after iB-07888 knockdown is due to the



serosa expansion. In the absence of serosa, the phenotype can be observed in more anterior regions of the embryo, implying that it is a DV and not an AP phenotype.

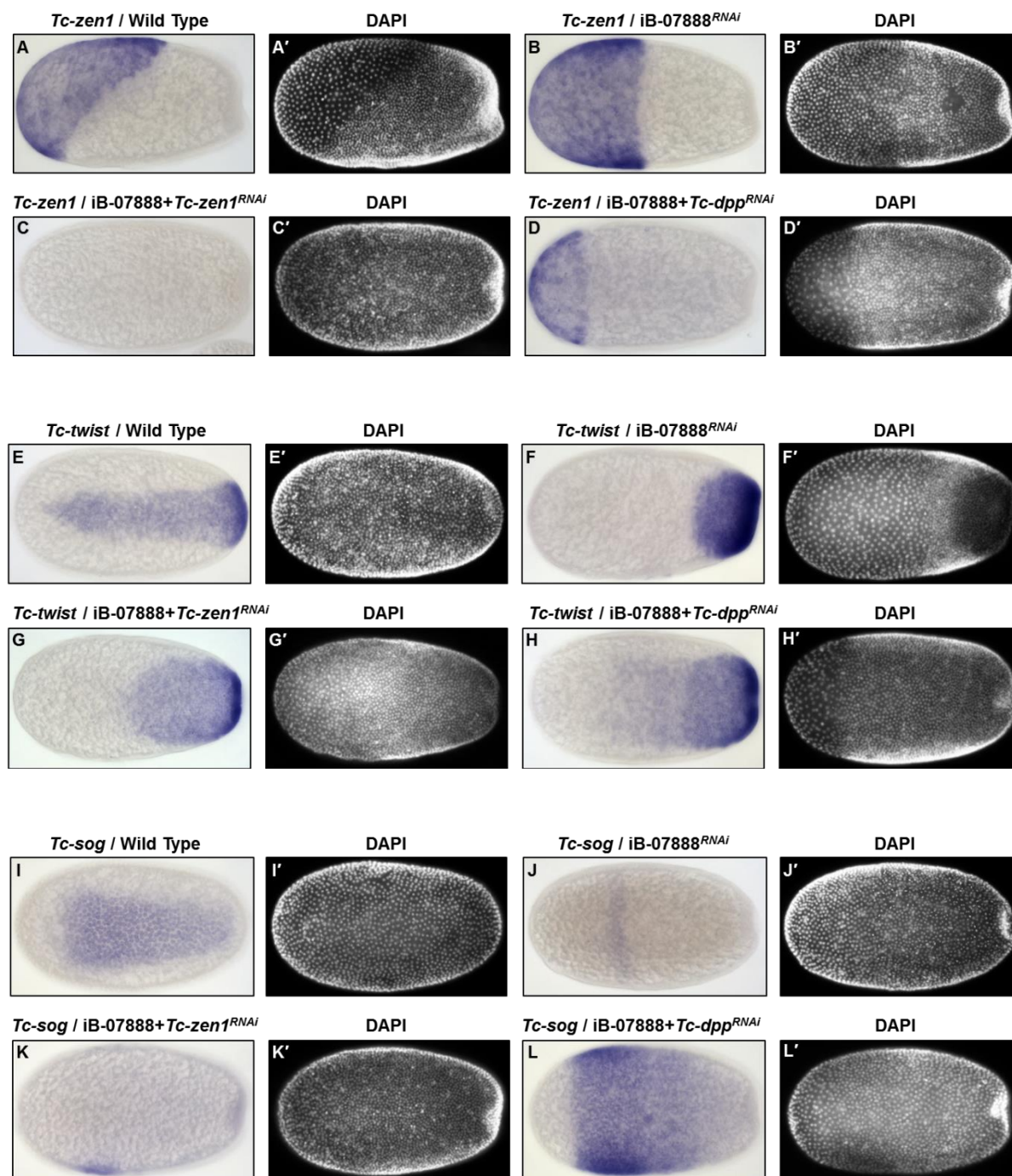


**Figure 24. Expression pattern of *Tc-zen1*, *Tc-twist* and *Tc-sog* after iB-07888+*Tc-zen1* and iB-07888+*Tc-dpp* double knockdown.**

(A-D) expression of *Tc-zen1*, (E-H) expression of *Tc-twist* and (I-L) expression of *Tc-sog*. The anterior of the embryo points to the left. (A-D and K) lateral view of the embryos and (E-L) ventral surface view of the embryo. (A'-L') nuclear staining (DAPI) of the respective embryos. (C) After iB-07888+*Tc-zen1* knockdown, the expression of *Tc-zen1* is not present, (D) while it is reduced in iB-07888+*Tc-dpp* knockdown embryos. (G-H) *Tc-twist* is expressed in a broad ventral domain and it is expanded towards the anterior of the embryos in both double knockdown embryos. (K) After iB-07888+*Tc-zen1* knockdown, *Tc-sog* is not expressed except for some knockdown embryos, which showed weak lateral expression, (L) while it is expressed in a broad ventral domain in iB-07888+*Tc-dpp* knockdown embryos.



Whole-mount dorsal antibody staining was performed in wild-type and iB-07888 knockdown embryos. In wild-type embryos, the nuclear Dorsal uptake is initiated uniformly, however, later in the blastoderm stage, the nuclear Dorsal gradient gradually refines to the ventral most domain (Figure 26A). After iB-07888 knockdown, similar to wild-type, the early uniform nuclear Dorsal accumulation was present during early nuclear division stage (Figure 25). However, during uniform blastoderm stage, the nuclear Dorsal/NF- $\kappa$ B localization was delayed and the Dorsal gradient refinement was absent (Figure 26B), while later, in the primitive pit stage embryos, weak nuclear Dorsal accumulation was observed in a broad ventral domain (Figure 26C and 26D). Upon iB-07888 knockdown with 1  $\mu$ g/ $\mu$ l dsRNA concentration, a series of nuclear Dorsal accumulation in a broad ventral domain were observed. Few knockdown embryos showed uniform weak nuclear Dorsal accumulation in a broad ventral domain (Figure 26C), while several other embryos showed stochastic nuclear Dorsal staining in a broad ventral domain (Figure 26D). I assume that the strength of iB-07888 knockdown influenced the nuclear Dorsal accumulation. For instance, stochastic nuclear Dorsal staining was observed only in 1  $\mu$ g/ $\mu$ l knockdown embryos, while knockdown embryos with 0.5  $\mu$ g/ $\mu$ l dsRNA concentration showed only uniform weak nuclear Dorsal uptake in a broad ventral domain (Figure 27B). Furthermore, in contrast to single iB-07888 knockdown embryos, Dorsal staining of iB-07888+*Tc-zen1* and iB-07888+*Tc-dpp* knockdown embryos showed broader weak nuclear Dorsal accumulation along the AP axis (Figure 27C and 27D respectively).

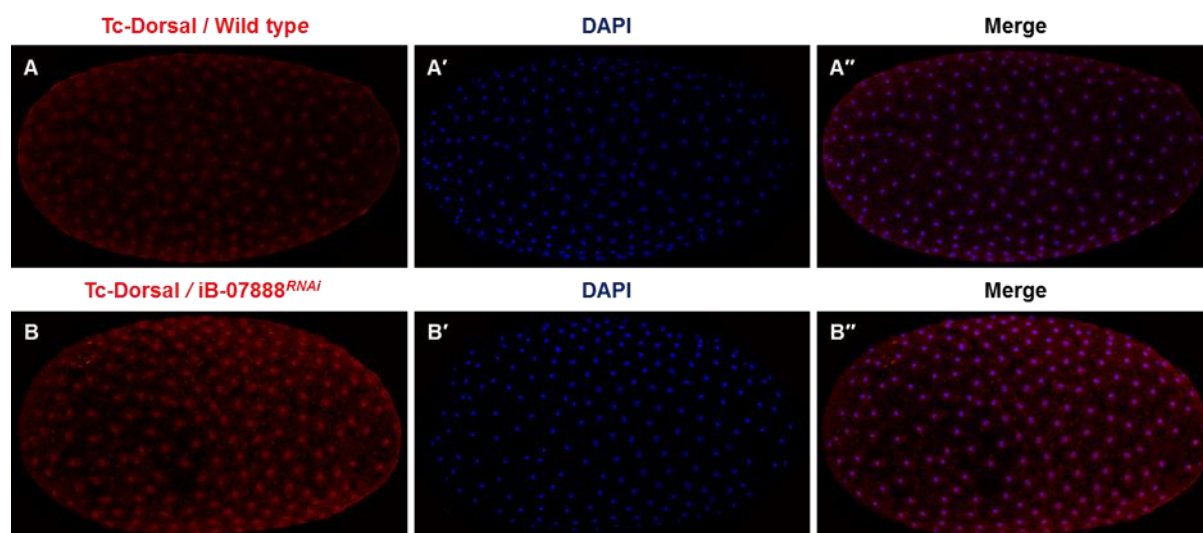


**Figure 25: Early nuclear Dorsal localization in wild-type and iB-07888 knockdown embryos.**

(A-B) Whole-mount Dorsal antibody staining, (A'-B') nuclear staining (DAPI) of the respective embryos and (A''-B'') represent merged images of the respective Dorsal staining and nuclear staining (DAPI). The anterior of the embryos points to the left. (B) Early uniform nuclear Dorsal accumulation is present in iB-07888 knockdown embryos, (A) likewise in wild-type embryos.

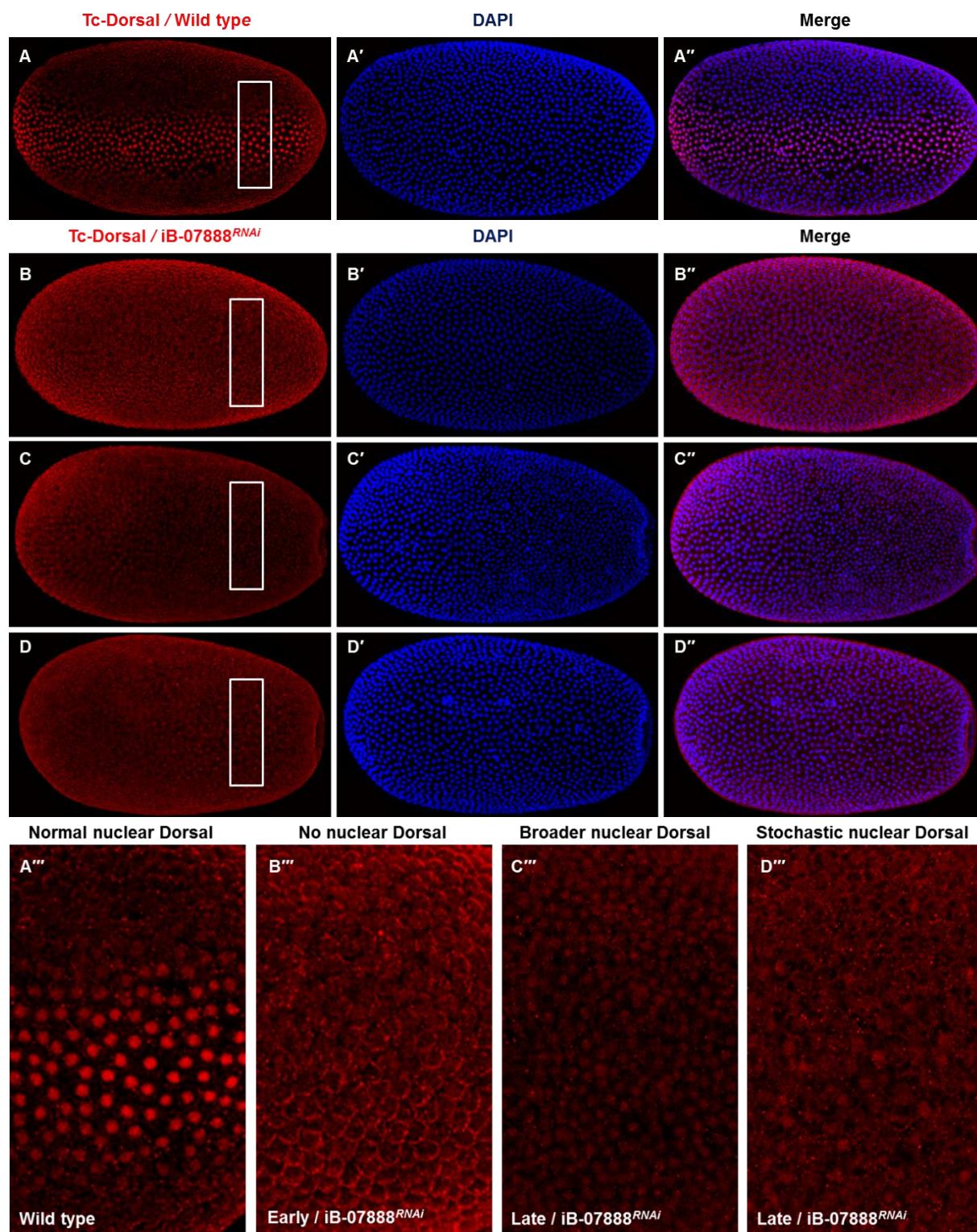


**Figure 26. Nuclear Dorsal/NF-κB gradient formation in wild-type and iB-07888 knockdown embryos.**

(A-D) Whole-mount Dorsal antibody staining and (A'-D') nuclear staining (DAPI) of the respective embryos. (A''-D'') represents merged images of the respective Dorsal staining and nuclear staining (DAPI), while (A'''-D''') show magnified view (A-D, white rectangle) of the respective Dorsal stained embryos. All embryos show the ventral surface view while the anterior of the embryo points to the left. (A) Ventral nuclear Dorsal gradient formation along the AP axis in wild-type embryo, (B) no detectable nuclear Dorsal in iB-07888 knockdown embryo at blastoderm stage, (C) uniform nuclear Dorsal and (D) stochastic nuclear Dorsal accumulation in a broad ventral domain restricted only to the posterior half of iB-07888 knockdown embryos at primitive pit stages. (B''') iB-07888 knockdown delays the nuclear Dorsal gradient formation and (C'''-D''') later the nuclear Dorsal gradient forms in a broad ventral domain.



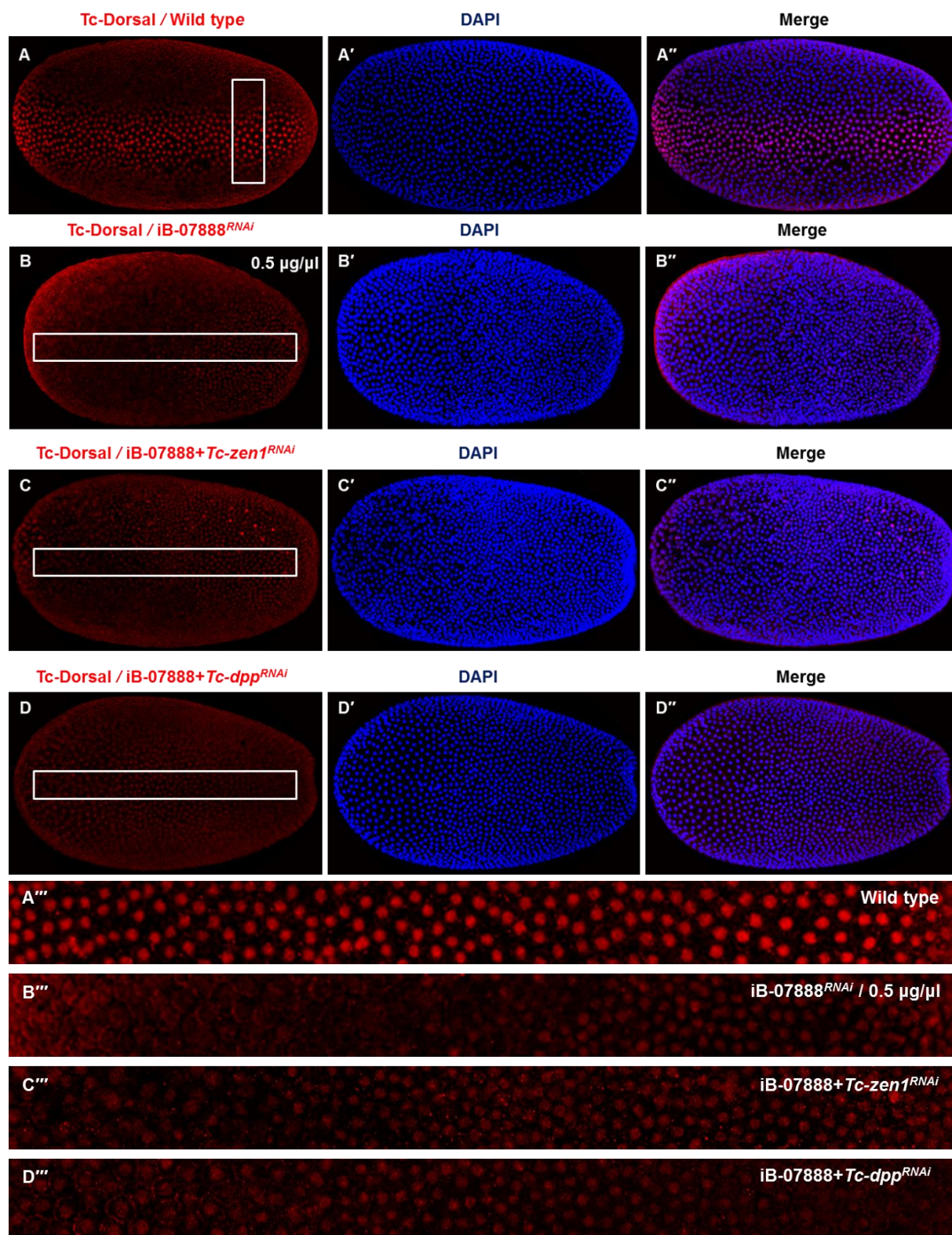


**Figure 27. Nuclear Dorsal/NF-κB gradient in wild-type and iB-07888 double knockdown embryos.**

(A-D) Whole-mount Dorsal antibody staining, (A'-D') nuclear staining (DAPI) of the respective embryos, (A''-D'') represent merged images of the respective Dorsal staining and DAPI and (A'''-D''') show magnified view (A-D, white rectangle) of the respective Dorsal stained embryos. All embryos show the ventral surface view while the anterior of the embryo points to the left. (A''') Nuclear Dorsal gradient formation along the AP axis in wild-type embryo, (B''') broad uniform nuclear Dorsal accumulation in weak knockdown embryos (0.5 μg/μl) and (C'''-D''') extended broad nuclear Dorsal accumulation along the AP axis in iB-07888+*Tc-zen1*<sup>RNAi</sup> and iB-07888+*Tc-dpp*<sup>RNAi</sup> knockdown embryos, respectively.

In addition, pMAD staining was performed in iB-07888 knockdown embryos. In wild-type blastoderm stage embryos, pMAD expression was present on the dorsal side along the AP axis. The anterior and posterior-most dorsal side of the embryo showed broader pMAD expression, while it was narrowed towards posterior in the middle of the embryo (Figure 28A). However, after iB-07888 knockdown, the pMAD expression was broader and expanded towards the ventral side but with strong lateral expression at the anterior of the embryo (Figure 28B), like in *Tc-sog* knockdown embryo (Figure 28C).

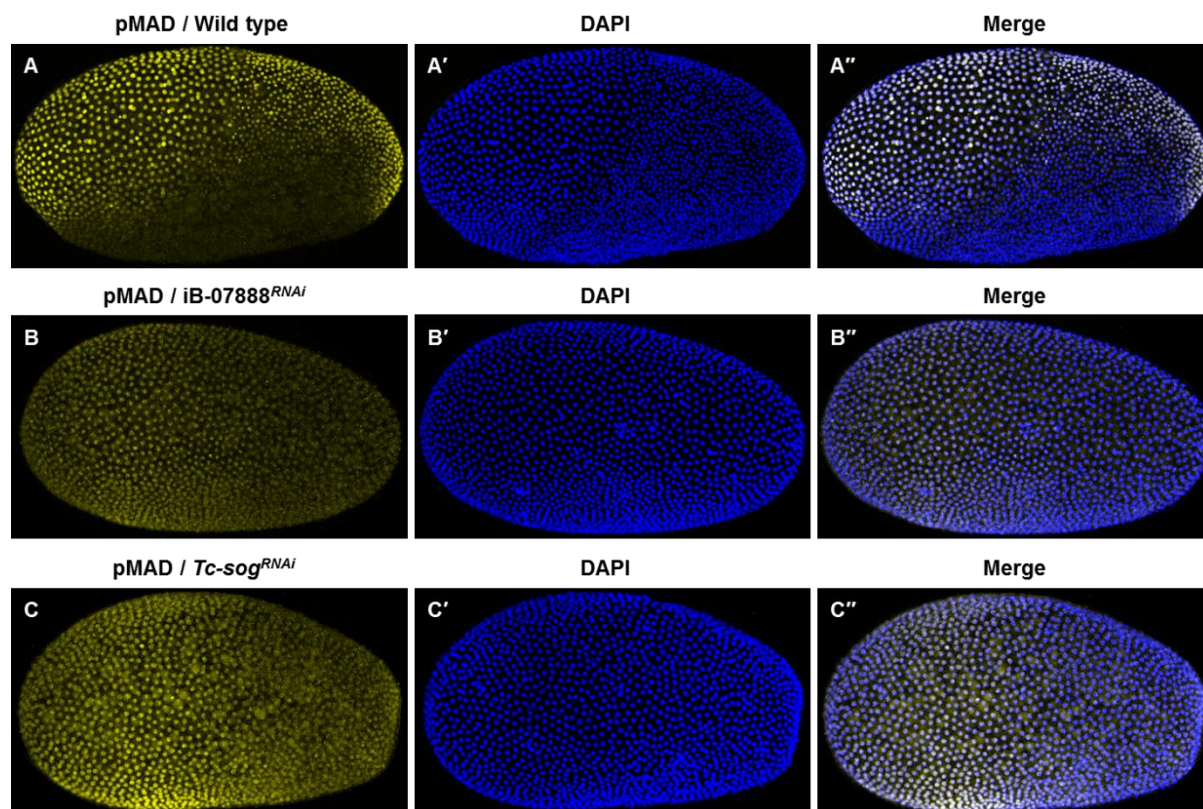


**Figure 28. pMAD antibody staining in wild-type, iB-07888 and *Tc-sog* knockdown embryos.**

(A-C) Whole-mount pMAD antibody staining, (A'-C') nuclear staining (DAPI) of the respective embryos, (A''-C'') represent merged images of the respective pMAD staining and DAPI. The anterior of the embryo points to the left. (A) pMAD expression in wild-type embryo, (B) pMAD expression in iB-07888 knockdown embryo and (C) pMAD expression in *Tc-sog* knockdown embryo. In contrast to wild-type, pMAD staining in iB-07888 and *Tc-sog* knockdown embryos is expanded towards the ventral side of the embryo.

Phylogenetic evolutionary analysis was performed to identify the potential orthologs of iB-07888 (TC011067) in *D. melanogaster*. Multiple sequence alignment of the 21 protein sequences of *D. melanogaster* and *T. castaneum* (best blast hits of iB-07888) was used for molecular phylogenetic analysis. No obvious *D. melanogaster* ortholog of iB-07888 (TC011067) was identified in the analysis (Figure 29A). Nevertheless, only TC004957 clustered together with iB-07888 (TC011067) in the same clade with bootstrap support higher than 50%. However, it is important to note that the overall phylogenetic analysis of iB-07888 resulted with low bootstrap support. Further analysis with alternative sequence trimming methods will be necessary to identify the potential *D. melanogaster* orthologs. Furthermore,



sequence analysis of iB-07888 by SMART detected one domain of Tryp-SPc (position 91 to 282) and a signal peptide (position 1 to 16) (Figure 29B).

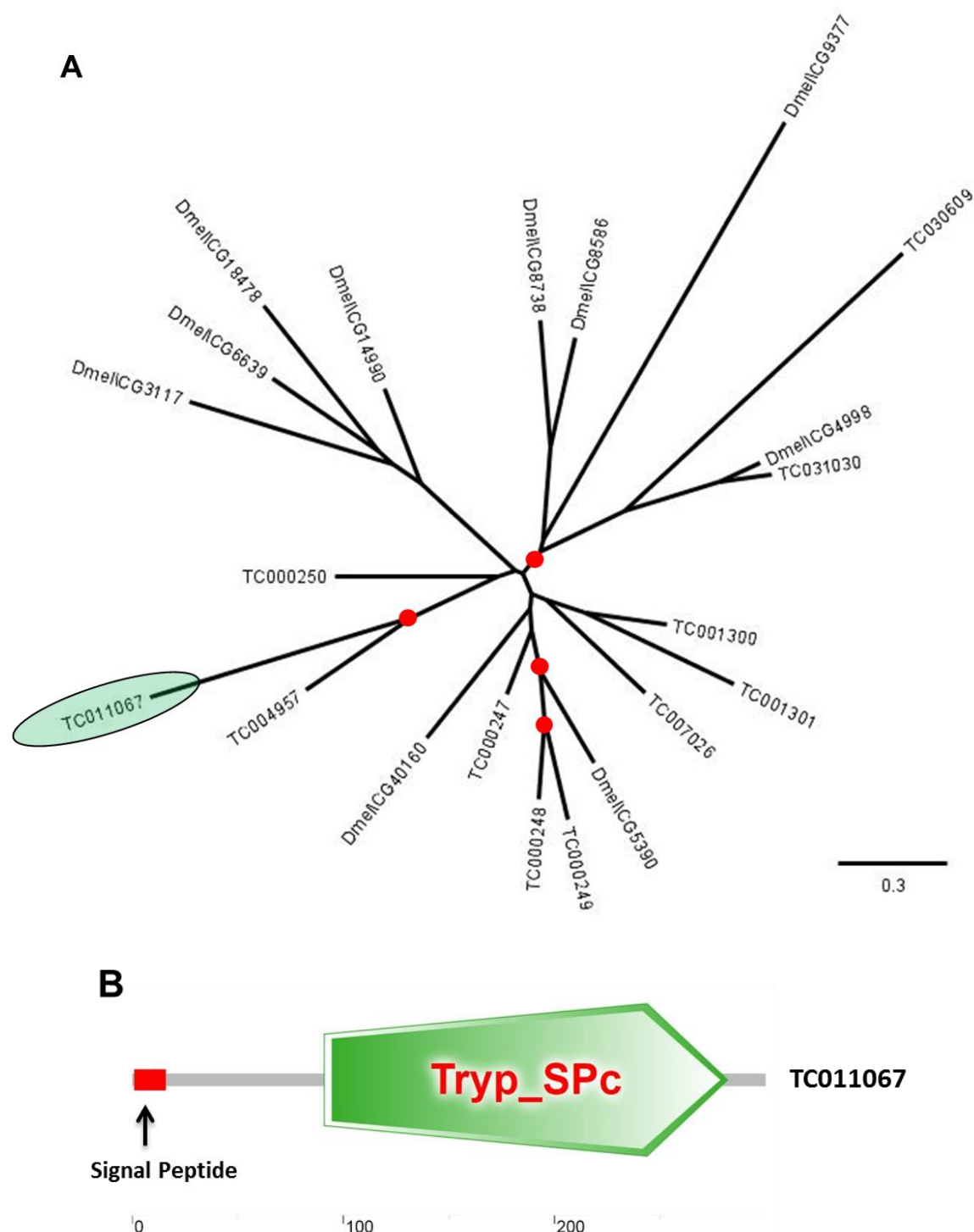


**Figure 29. Phylogenetic and sequence analysis of iB-07888 (TC011067).**

(A) Evolutionary phylogenetic tree of iB-07888 (TC011067). Clades marked with filled red circles have the bootstrap value of more than 50%. iB-07888 (TC011067) is highlighted with green circle in the phylogenetic tree. The branch length measured the number of substitutions per site. In the phylogenetic tree, iB-07888 (TC011067) clustered separately from *D. melanogaster* genes. (B) Conserved domains identification of iB-07888 (TC011067). A conserved Tryp-SPc domain (position 91 to 282) and a signal peptide (position 1 to 16 indicated by an arrow) were predicted by SMART after iB-07888 sequence analysis.

## 6.5 iB-06699 (TC034678) Leukocyte elastase inhibitor

iB-06699 (TC034678) known as leukocyte elastase inhibitor-like protein which belongs to serpin superfamily has a novel role in DV pattern formation in *T. castaneum*. In the iBeetle screen, knockdown of iB-06699 resulted in larvae with everted (inside-out) cuticle phenotype, however, the annotated cuticle phenotype was not fully reproduced during the re-screen (Supp. Table 2-6). Importantly, iB-06699 knockdown embryos showed severe embryonic DV phenotype at the gastrulation stage. However, later, the embryonic development continued and the embryo formed a germband, but in contrast to wild-type embryos, the anterior head lobes of the germband developed at the posterior side of the egg in most iB-06699 knockdown embryo (Figure 31).

The expression pattern of iB-06699 (TC034678) was analyzed by whole-mount *in-situ* hybridization. In wild-type embryos, strong nuclear expression of iB-06699 was detected at early nuclear division stage embryos (Figure 30A). However, later the nuclear expression is confined only to the serosal nuclei during blastoderm stage, while the cytoplasmic expression still remains uniform in the whole embryo (Figure 30B). Moreover, iB-06699 is also expressed in the primitive pit region during early gastrulation stage (Figure 30C) and later it is expressed uniformly in the germ rudiment (Figure 30D).

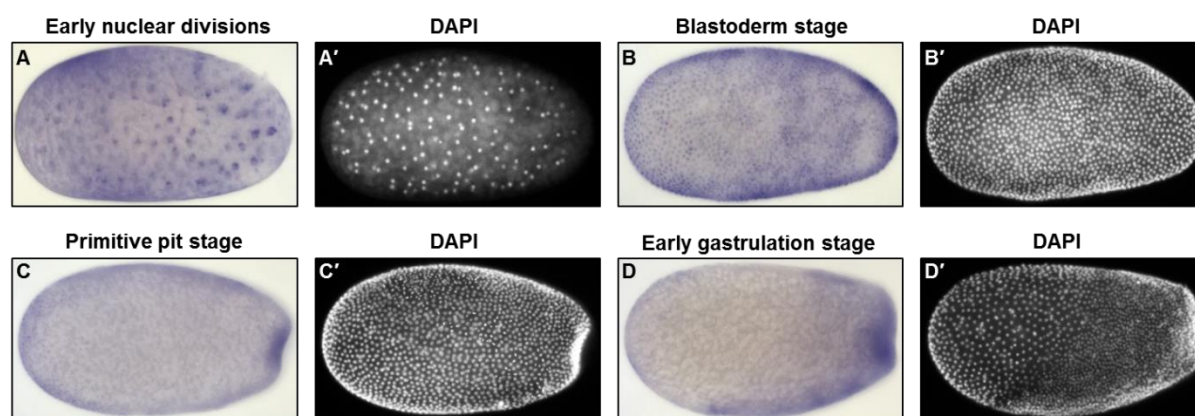


**Figure 30. Expression pattern of iB-06699 (TC034678) by whole-mount *in-situ* hybridization.**

(A-D) Whole-mount *in-situ* hybridization of iB-06699 in wild-type embryos. The anterior of the embryo points to the left and the dorsal side of the embryos points upwards. (A'-D') nuclear staining (DAPI) of the respective embryos. (A) Strong nuclear expression of iB-06699 is present during early nuclear division stage embryo. (B) Confined serosal nuclear expression during blastoderm stage. (C) Expression of iB-06699 in the primitive pit region and (D) uniform expression in the germ rudiment during early gastrulation.

Phylogenetic evolutionary analysis was performed to identify the potential orthologs of iB- iB-06699 (TC034678) in *D. melanogaster*. Multiple sequence alignment of the 21 protein sequences of *D. melanogaster* and *T. castaneum* (best blast hits of iB-06699) was used for phylogenetic analysis. Four *D. melanogaster* genes and one *T. castaneum* gene grouped together with iB-06699 (TC034678) in the same branch, suggesting that these genes are closely related to iB-06699 and are the potential *D. melanogaster* orthologs (Figure 32A). Furthermore, the protein sequences of iB-06699 were analyzed by SMART. A conserved

SERPIN domain (position 36 to 398), a signal peptide (position 1 to 19) and a low complexity region (position 473 to 484) were predicted after iB-06699 sequence analysis (Figure 32B).

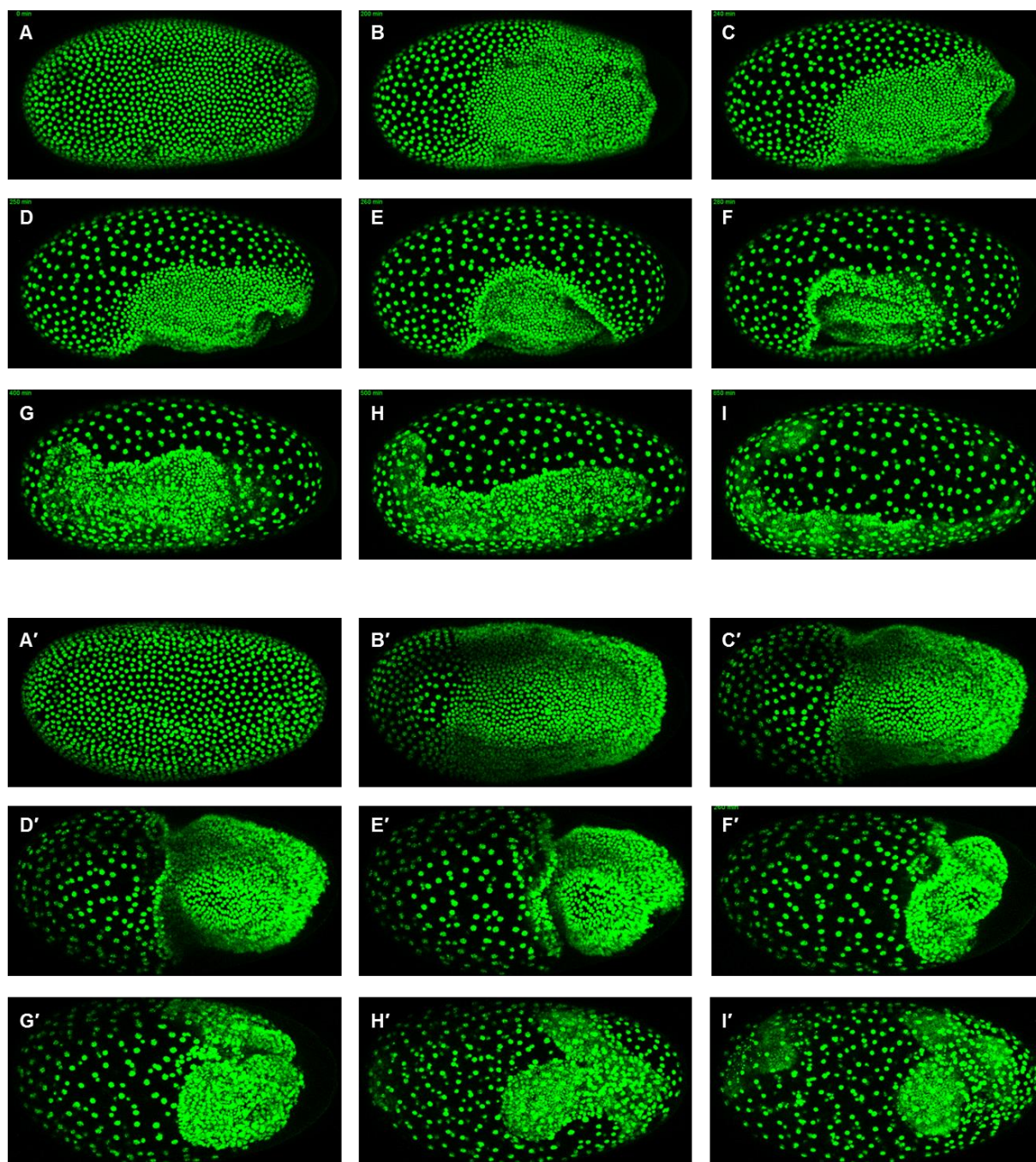


**Figure 31. Embryonic development of *T. castaneum* wild-type and iB-06699 knockdown embryos.**

(A-I) Wild-type embryo, (A'-I') iB-06699 knockdown embryo. The anterior of the embryos points to the left. (A) Uniform blastoderm stage, (B) differentiated blastoderm stage, (C) early gastrulation, (D) late gastrulation (E) horseshoe amniotic fold stage (F) serosa window closure stage (G) germband stage (H) extended germband stage and (I) fully extended germband stage. (A') Uniform blastoderm stage, (B') differentiated blastoderm stage, (C'-E') gastrulation and tissue invaginations with severe DV phenotype, (F') potential germband formation and (G'-I') germband formation in reverse AP orientation. Live imaging of iB-06699 knockdown embryos showed strong DV phenotype at the gastrulation stage, however later it forms germband and enable normal development of the embryo. Produced by Matt Benton.



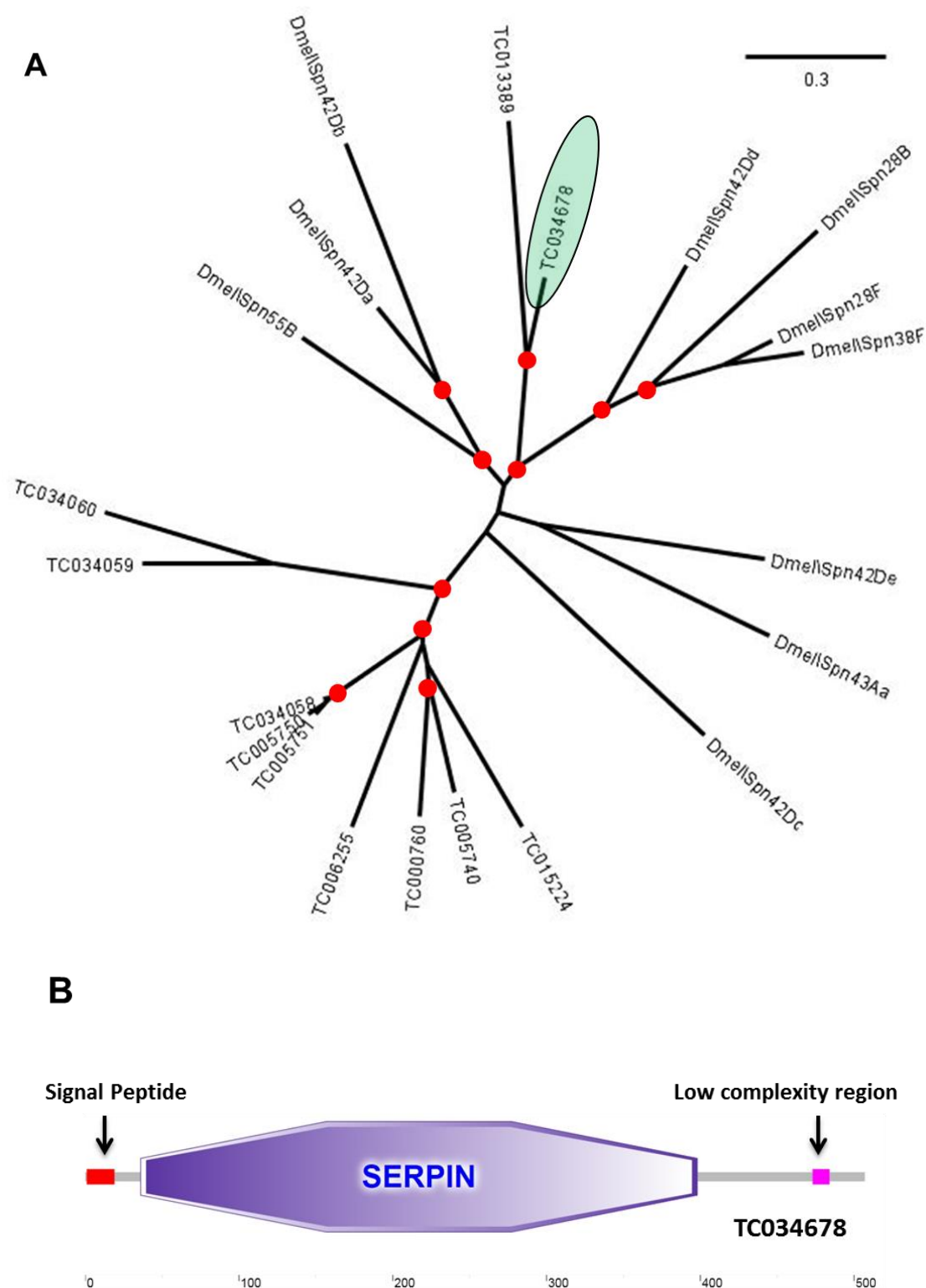


**Figure 32. Phylogenetic and sequence analysis of iB-06699 (TC034678).**

(A) Evolutionary phylogenetic tree of iB-06699 (TC034678). Clades marked with filled red circles have the bootstrap value of more than 50%. iB-06699 (TC034678) is highlighted with green circle in the phylogenetic tree. The branch length measured the number of substitutions per site. Four *D. melanogaster* genes and one *T. castaneum* gene grouped together with iB-06699 (TC034678) in the same branch. (B) Conserved domains identification of iB-06699 (TC034678). A conserved SERPIN domain (position 36 to 398), a signal peptide (position 1 to 19) and a low complexity region (position 473 to 484) were predicted after iB-06699 sequence analysis. Grey lines indicate the region without having any conserved domain.



To further investigate the potential function of iB-06699 in DV patterning in *T. castaneum*, I performed the whole-mount *in-situ* hybridization in iB-06699 knockdown embryos (3 µg/µl of dsRNA concentration) using DV marker genes. In wild-type embryos, *Tc-zen1* is expressed in the serosa during differentiated blastoderm stage (Figure 33A-B). However, compared to wild-type, the expression domain of *Tc-zen1* was reduced (Figure 33C-D) in iB-06699 knockdown embryos. *Tc-dorsal* is also expressed in the serosa, but after iB-06699 knockdown, *Tc-dorsal* expression was completely absent, like in *Tc-zen1* knockdown embryos (Supp. Figure 6). Moreover, the ventral expression pattern of *Tc-twist* resembled the wild-type expression pattern in most of the cases (Figure 33G) except for a few knockdown embryos, in which the anterior-most expression domain was slightly broader (Figure 33H). Interestingly, *Tc-sog* ventral expression was expanded laterally along the DV axis in iB-06699 knockdown embryos. The lateral expansion was more robust at the anterior domain of *Tc-sog* expression in iB-06699 knockdown embryos (Figure 33K-L). The expression pattern of DV marker genes in iB-06699 knockdown embryos suggest that the knockdown of iB-06699 is causing ventralized phenotype.

Furthermore, the strength of the gene knockdown influenced the robustness of the phenotype. *Tc-sog* expression was weakly expanded after parental RNAi with dsRNA concentration of 1 µg/µl (data not shown), while the phenotype was much stronger after iB-06699 knockdown with dsRNA concentration of 3 µg/µl. Interestingly, no obvious cuticle phenotype was secreted after iB-06699 knockdown, even with 3 µg/µl of dsRNA concentration. The respective knockdown phenotypes of iB-06699 (reduced serosa and expanded *Tc-sog* expression) were also reproduced after iB-06699 knockdown with NOF (3 µg/µl) (data not shown).

Whole-mount Dorsal antibody staining was performed in wild-type and iB-06699 knockdown embryos. In wild-type embryos, the nuclear Dorsal uptake was initiated uniformly during early nuclear divisions, however, later in the blastoderm stage, the nuclear Dorsal concentration refined to the ventral most domain along the AP axis of the embryo (Figure 34A). No obvious nuclear Dorsal expansion was detected in iB-06699 knockdown embryos during blastoderm stage (Figure 34B). However, few embryos showed very weak nuclear Dorsal expansion to the dorsal side of the embryo (Figure 34C). Furthermore, pMAD staining was performed in iB-06699 knockdown embryos. In wild-type embryos, pMAD expression was detected along the AP axis with anterior and posterior-most dorsal side of the embryo showing broader pMAD expression, while narrowing towards posterior in the middle of the embryo. After iB-06699 knockdown, pMAD expression at posterior of the embryo was reduced during blastoderm stage compared to wild-type expression domain (Figure 35B).

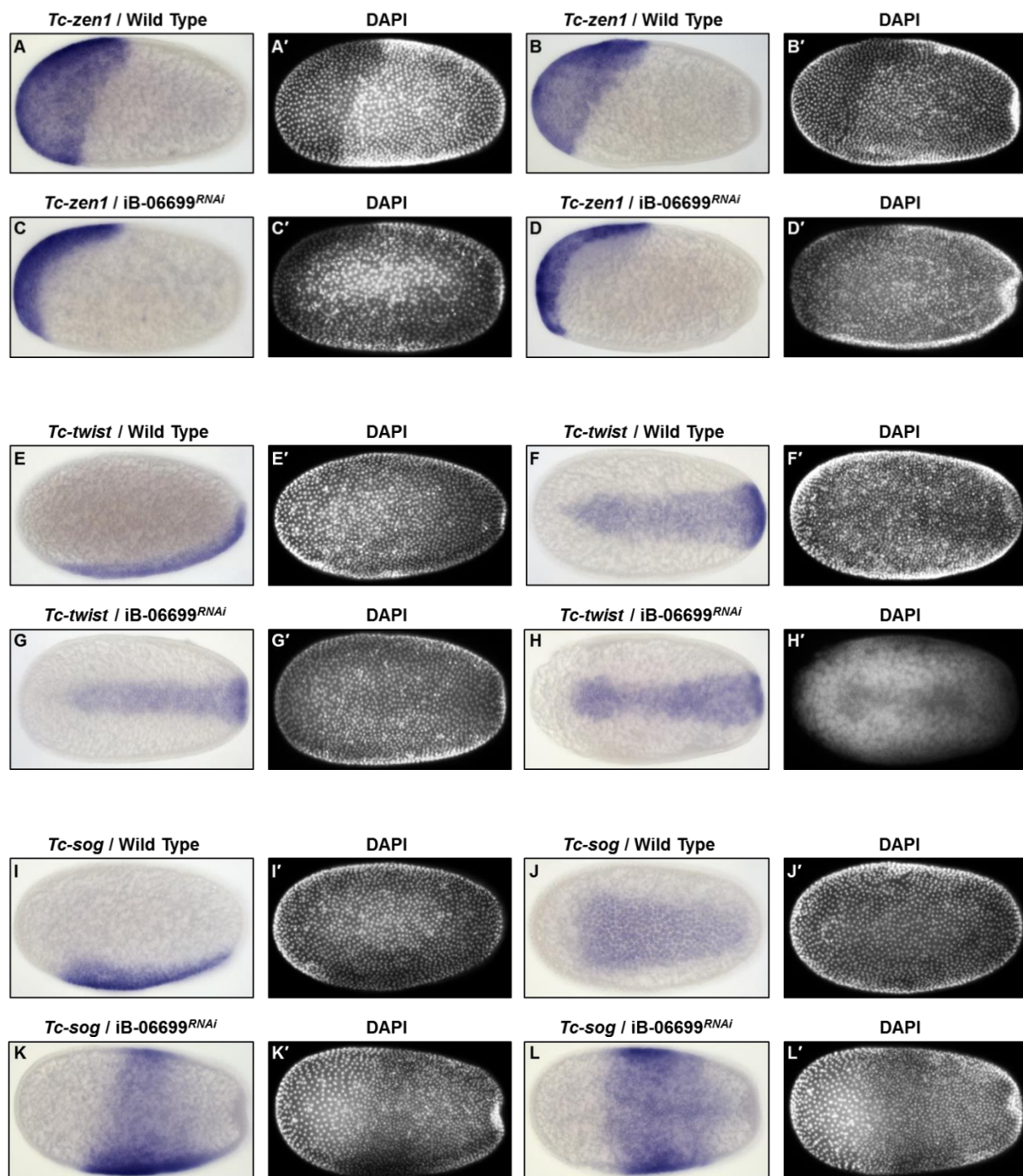


**Figure 33. Expression pattern of *Tc-zen1*, *Tc-twist* and *Tc-sog* after iB-06699 knockdown.**

(A-L) Whole-mount *in-situ* hybridization of blastoderm stage embryos. (A-D) Expression of *Tc-zen1*, (E-H) expression of *Tc-twist* and (I-L) expression of *Tc-sog*. The anterior of the embryo points to the left and the dorsal side of the embryos points upwards, except for F, G, H, J and L which show the ventral surface view of the embryos. (A'-L') Nuclear staining (DAPI) of the respective embryos. (A-B) *Tc-zen1* is expressed in the serosa (early blastoderm stage (A) and primitive pit stage (B)). (C-D) The expression of *Tc-zen1* in iB-06699 knockdown embryos is reduced (early blastoderm stage (C) and primitive pit stage (D)). (G) Wild-type like expression pattern of *Tc-twist* in iB-06699 knockdown embryo. (H) Slightly broader anterior expression domain of *Tc-twist* in iB-06699 knockdown embryo. (K-L) Expanded expression domain of *Tc-sog* in iB-06699 knockdown embryos (K lateral view and L ventral view of the same embryo).

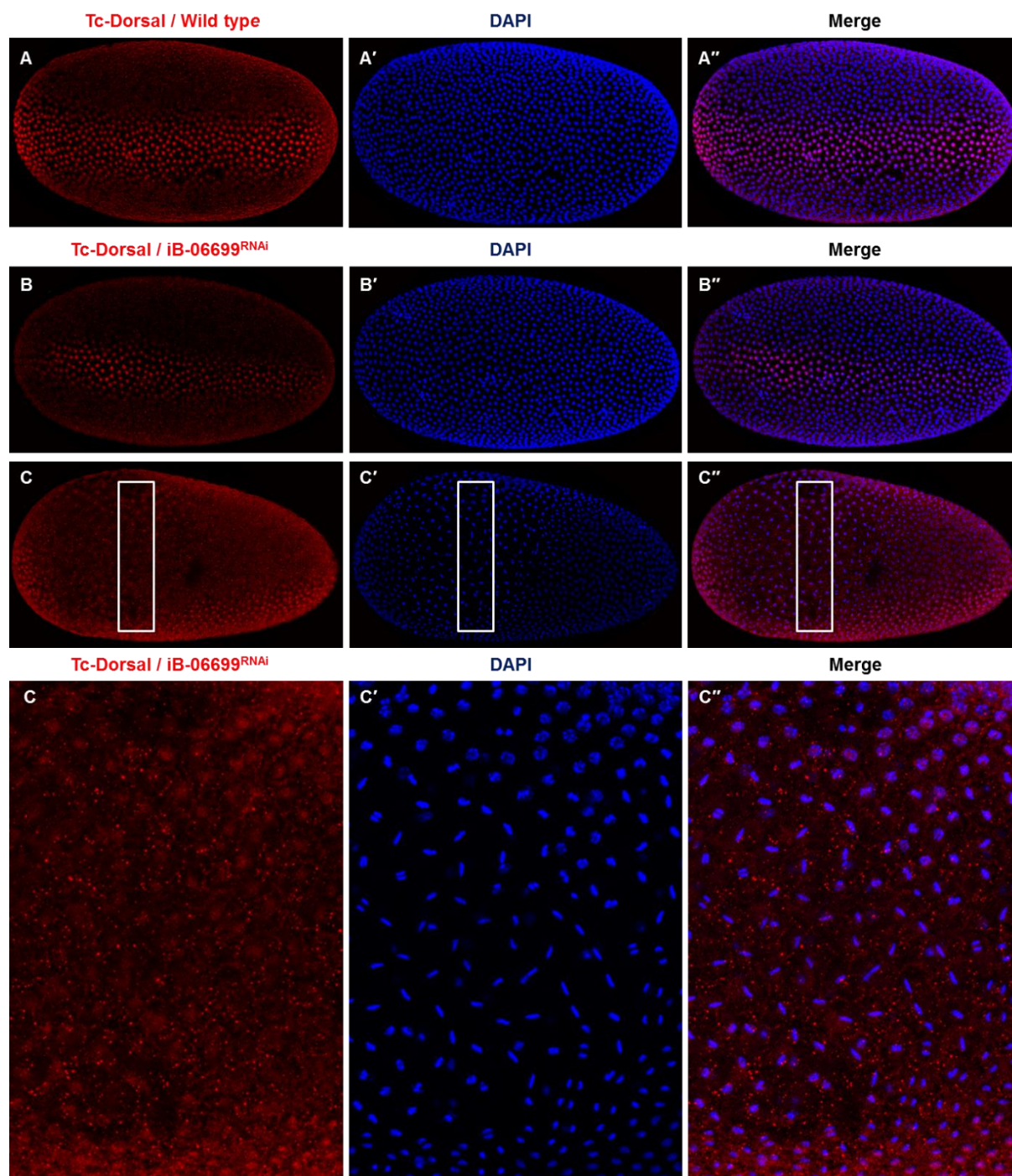


**Figure 34. Nuclear Dorsal/NF- $\kappa$ B gradient in wild-type and iB-06699 knockdown embryos.**

(A-C) Whole-mount Dorsal antibody staining, (A'-C') nuclear staining (DAPI) of the respective embryos, (A''-D'') represent merged images of the respective Dorsal staining and nuclear staining (DAPI). (C, C', C'') Magnified view (white rectangle) of the respective Dorsal stained embryo. (A-B) Ventral surface view and (C) lateral view. The anterior of the embryo points to the left. (A) Nuclear Dorsal gradient along the AP axis in wild-type embryo, (B-C) Nuclear Dorsal gradient in iB-06699 knockdown embryos. Nuclear Dorsal gradient expansion is not detectable in most knockdown embryos except (C) which shows weak nuclear Dorsal expansion at the lateral side of the embryo.



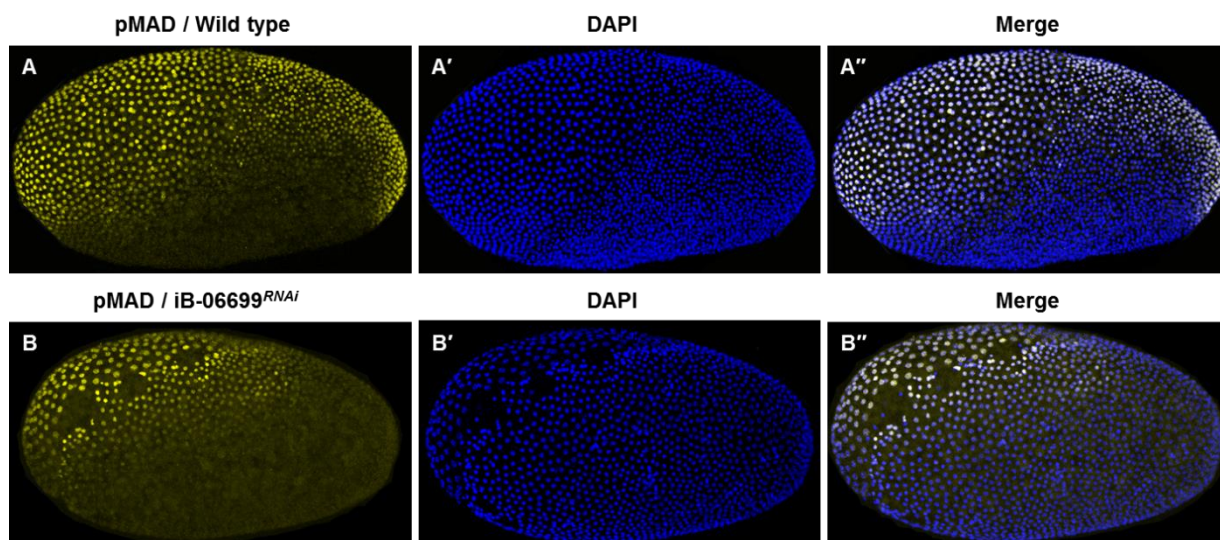


**Figure 35. pMAD antibody staining in wild-type and iB-06699 knockdown embryos.**

(A-B) Whole-mount pMAD antibody staining, (A'-B') nuclear staining (DAPI) of the respective embryos, (A''-B'') represent merged images of the respective pMAD staining and DAPI. The anterior of the embryos points to the left and dorsal of the embryos points upwards. (A) Wild type pMAD expression along the AP axis on the dorsal side of the embryo. (B) Reduced pMAD expression at the posterior of the embryo in iB-06699 knockdown embryo.

## 6.6 iB-06774 *spaetzle* (ligand of the Toll receptor)

A mini-screen was performed to identify the *spaetzle* candidate in *T. castaneum*, which acts as a ligand of the Toll receptor. Candidate gene approach together with iBeetle data-set was used to identify the potential *spaetzle* candidate in *T. castaneum*. For instance, the *D. melanogaster spaetzle* orthologs (CG6134) along with other *D. melanogaster spaetzle* related genes (homologs) sequences were used as query with blast against the *T. castaneum* OGS. In total, 14 genes with *spaetzle* domains were identified in *T. castaneum* and then these genes were looked up in the iBeetle-Base for potential DV phenotypes. Only genes, whose knockdown resulted in potential DV phenotypes (empty eggs, cuticle crumbs etc.) were selected for a mini-screen (Supp. Figure 7). The selected candidate genes with potential DV phenotypes were knocked down by parental RNAi using the original iBeetle dsRNA fragments. In additions, *in-situ* hybridization of the potential *spaetzle* candidates was performed during the mini-screen.

In the mini-screen, only knockdown of iB-06774 resulted in complete dorsalized phenotype and DV asymmetric expression pattern. The expression pattern of iB-06774 was analyzed by whole-mount *in-situ* hybridization. In wild-type embryos, iB-06774 is expressed uniformly during early blastoderm stage (Figure 36A). However, later the expression of iB-06774 is confined to the presumptive head region with a DV asymmetric expression pattern (Figure 36B-E). During serosal window stage, iB-06774 is expressed in two lateral stripes in the thoracic region (Figure 36F).

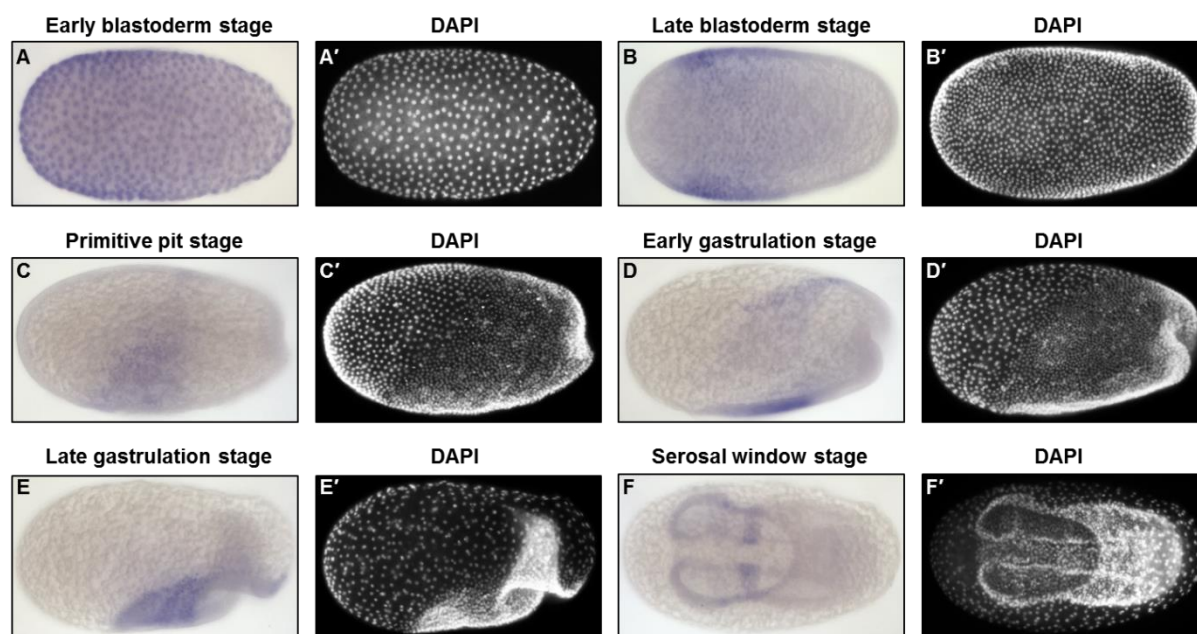


**Figure 36. Expression pattern of iB-06774 by whole-mount *in-situ* hybridization.**

(A-B) Whole-mount *in-situ* hybridization of blastoderm stage embryos, (C) primitive pit stage embryo, (D-E) gastrulating embryos and (F) serosal window stage embryo. The anterior of the embryo points to the left and the dorsal side of the embryos points upwards, except for F, which shows the ventral surface view of the embryo. (A'-F') Nuclear staining (DAPI) of the respective embryos. (A) Uniform expression of iB-06774 during early blastoderm stage. (B-E) DV asymmetric expression pattern in the presumptive head region. (F) Expression of iB-06774 in the thoracic region during serosal window stage.

The expression pattern of iB-06774 was investigated in the embryos after knockdown of different DV marker genes. A narrow lateral stripe was present, while the anterior expression domain (head region) was absent in *Tc-Toll*, iB-09824 and *Tc-sog* knockdown embryos (Figure 37B-D).

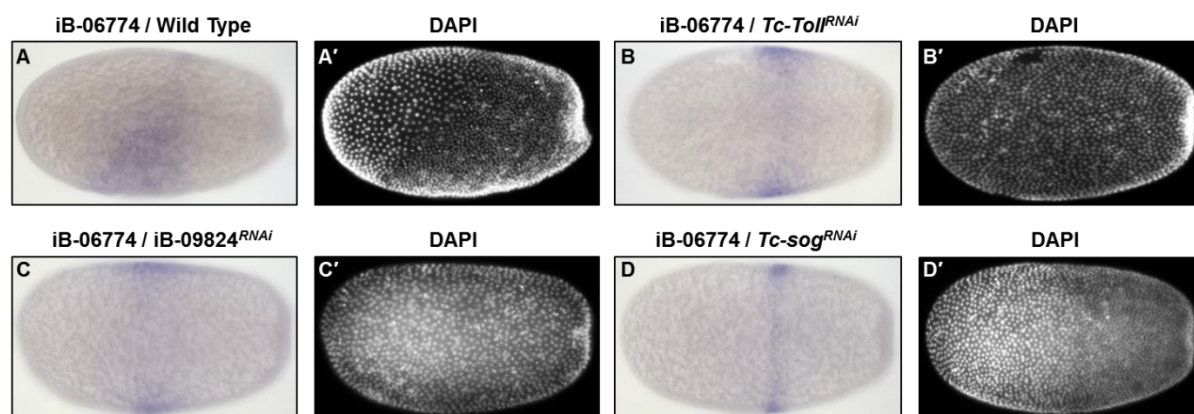


**Figure 37. Expression pattern of iB-06774 in *Tc-Toll*, iB-09824 and *Tc-sog* knockdown embryos.**

(A) Whole-mount *in-situ* hybridization of iB-06774 in wild-type and (B-D) knockdown embryos. The anterior of the embryo points to the left and the dorsal side of the embryos points upwards. (A'-D') nuclear staining (DAPI) of the respective embryos. (A) In wild-type embryo, iB-06774 is expressed in the presumptive head region. (B-D) The anterior expression domain of iB-06774 is absent in *Tc-Toll*, iB-09824 and *Tc-sog* knockdown embryos.

Knockdown of iB-06774 resulted in empty eggs and strongly fragmented cuticle crumbs phenotypes during the iBeetle screen. Whole-mount *in-situ* hybridization in iB-06774 knockdown embryos was performed to investigate the potential DV role of iB-06774 in *T. castaneum* (Figure 38). In wild-type embryos, *Tc-zen1* is expressed in the serosa during differentiated blastoderm stage (Figure 38A). However, the expression of *Tc-zen1* in iB-06774 knockdown embryos was expanded towards posterior and the oblique serosa-embryo border was rotationally symmetric (Figure 38D), like in *Tc-Toll* and *Tc-sog* knockdown embryos (Figure 38B and 38C, respectively). Moreover, *Tc-twist* and *Tc-sog* expression which is observed ventrally during early blastoderm stage in wild-type embryos (Figure 38E and 38I, respectively), is lacking in iB-06774 knockdown embryos (Figure 38H and 38L, respectively) like in *Tc-Toll* and easter like (iB-07073) knockdown embryos. The expression pattern of DV marker genes in iB-06774 knockdown embryos suggest that the knockdown of iB-06774 is inducing completely dorsalized phenotypes.



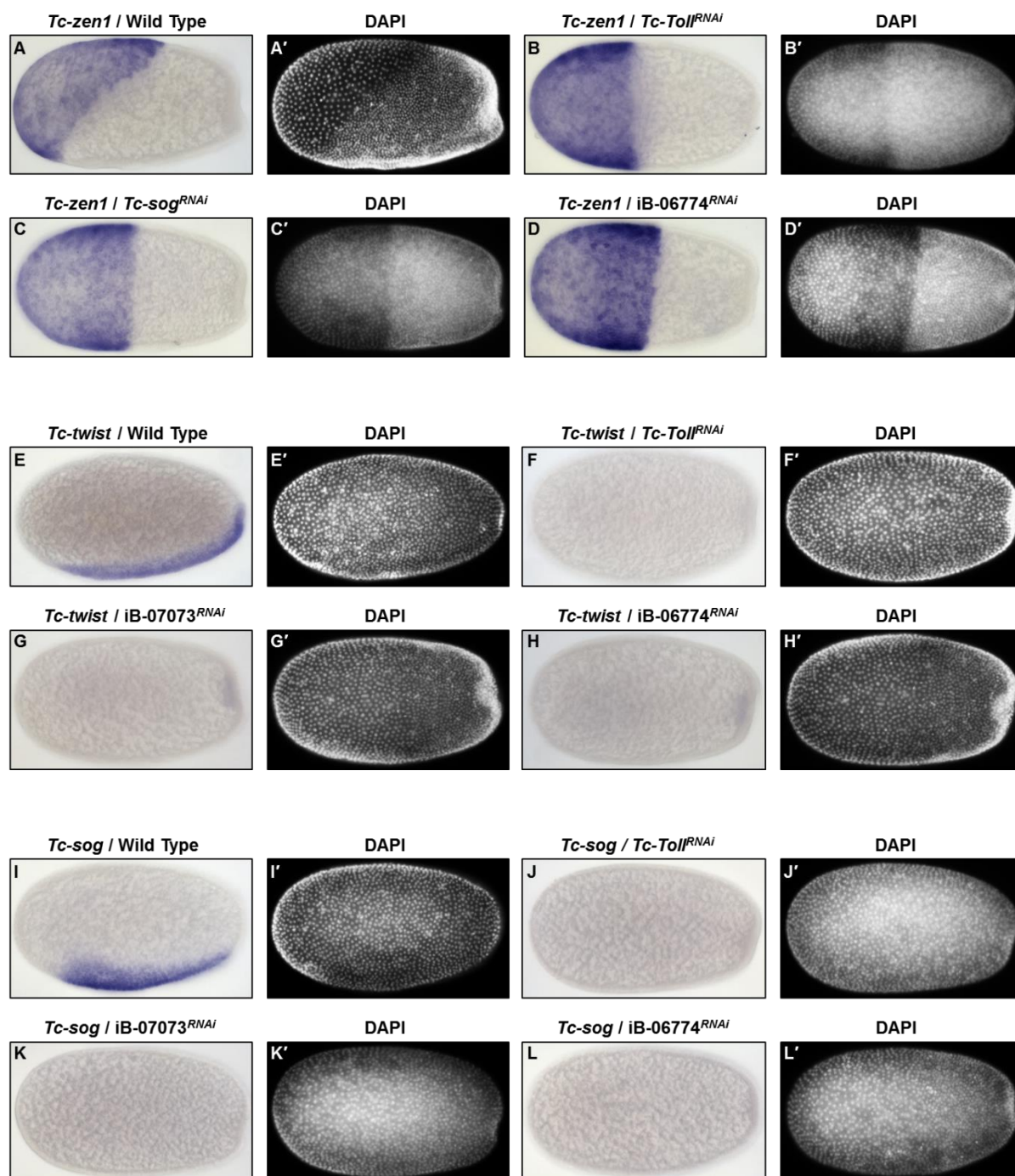


**Figure 38. Expression pattern of *Tc-zen1*, *Tc-twist* and *Tc-sog* after iB-06774 knockdown.**

(A-L) Whole-mount *in-situ* hybridization of blastoderm stage embryos. (A-D) *Tc-zen1* expression pattern, (E-H) *Tc-twist* expression pattern and (I-L) *Tc-sog* expression pattern. The anterior of the embryos points to the left and the dorsal side of the embryos points upwards. (A'-L') Nuclear staining (DAPI) of the respective embryos. Knockdown of iB-06774 produced complete dorsalized phenotype. (A) *Tc-zen1* is expressed in the serosa in wild-type embryos. (B-D) The expression of *Tc-zen1* is expanded and the serosa-embryo border is straight in *Tc-Toll*, *Tc-sog* and iB-06774 knockdown embryos, respectively. (H and L) *Tc-twist* and *Tc-sog* are not expressed in iB-06774 knockdown embryos, (F, G, J and K) likewise *Tc-Toll* and iB-07073 knockdown embryos, respectively.

Knockdown of iB-06774 caused complete dorsalized phenotype, however, it is possible that iB-06774 dsRNA fragment potentially targets three *T. castaneum* genes: TC031905, TC031906 and TC032151 (Figure 39A). Sequence homology analysis of dsRNA fragments with these three *T. castaneum* genes (TC031905, TC031906 and TC032151) was performed using mVISTA (Figure 39) (Frazer et al., 2004). Non-overlapping dsRNA fragments of TC031906 were designed to minimize the off-target effects. Knockdown of TC031906\_NOF1 resulted in a completely dorsalized phenotype like after knockdown of iB-06774, while no DV phenotype was observed after knockdown of TC031906\_NOF2 (data not shown). Moreover, multiple sequence alignment of TC031905, TC031906 and TC032151 showed strong protein sequence similarity (Supp. Figure 8) indicating that these three Tc-identifiers might represent one gene and it is a sequence annotation problem. Further knockdowns experiments with different dsRNA fragments are necessary to confirm the off-target effects and to identify the correct *spaetzle* Tc-identifier.

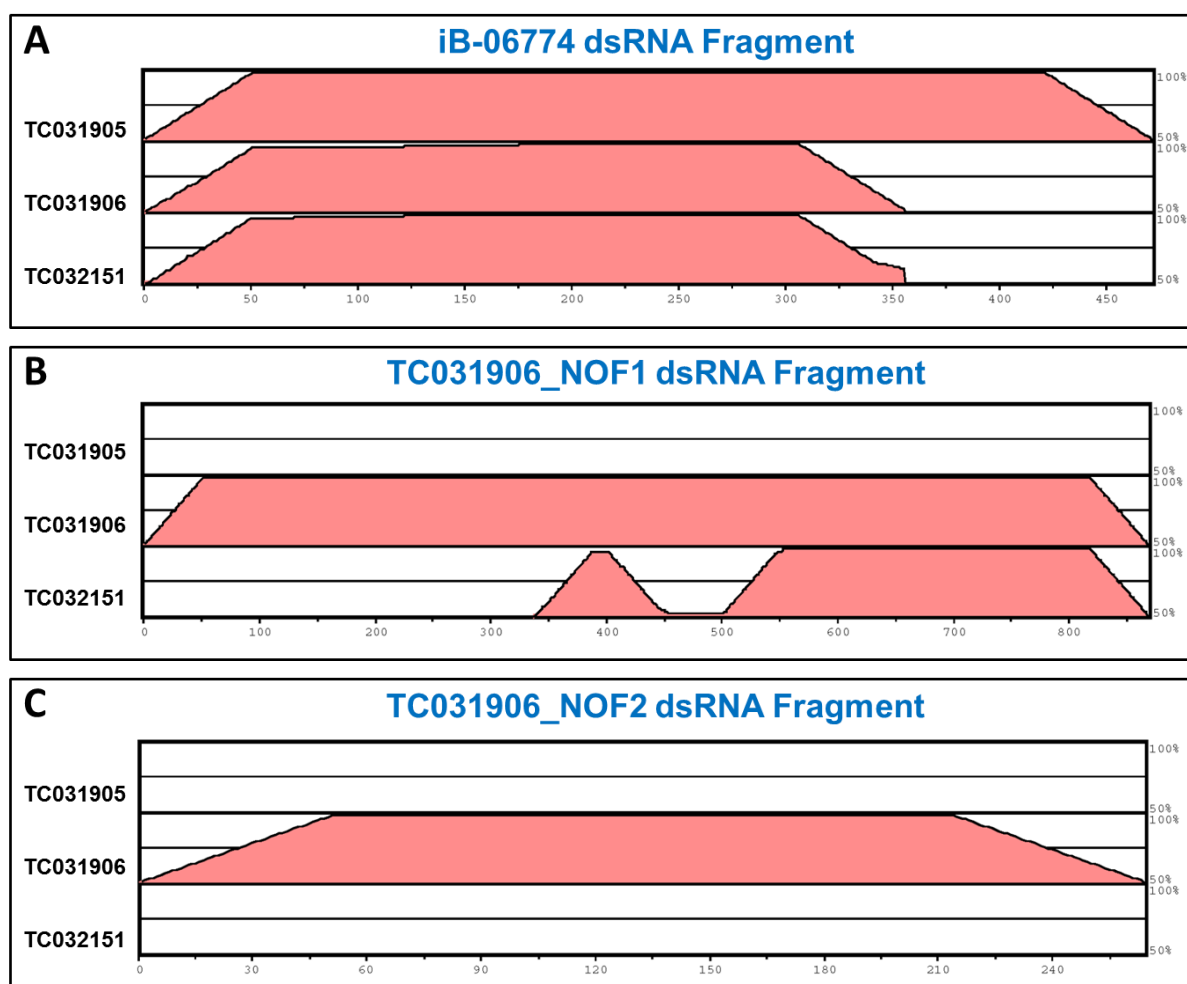


**Figure 39. Sequence similarity between dsRNA fragments and multiple *T. castaneum* genes.**

(A-C) Sequence similarity between dsRNA fragments and three *T. castaneum* genes (TC031905, TC031906 and TC032151) was investigated by mVISTA. (A) iB-06774 dsRNA fragment, (B) TC031906\_NOF1 dsRNA fragment and (C) TC031906\_NOF2 dsRNA fragment. Levels of sequence similarities of TC031905, TC031906 and TC032151 to reference sequences (dsRNA fragments) are represented in pink color. iB-06774 dsRNA fragment potentially targets three genes (TC031905, TC031906 and TC032151), TC031906\_NOF1 potentially targets two genes (TC031906 and TC032151), while TC031906\_NOF2 dsRNA fragment is specific to TC031906.



Phylogenetic evolutionary analysis was performed to identify the closest *D. melanogaster spaetzle* ortholog of iB-06774 target genes (TC031905, TC031906 and TC032151). Multiple sequence alignment of the 18 protein sequences (best blast hits of iB-06774) was used for molecular phylogenetic analysis. All three respective target genes of iB-06774 (TC031905, TC031906 and TC032151) grouped together in the same clade with bootstrap support higher than 50%. Two of the *D. melanogaster spaetzle* orthologs (*Dmel\spz* and *Dmel\spz2*) are closely clustered with iB-06774 target genes (Figure 40).

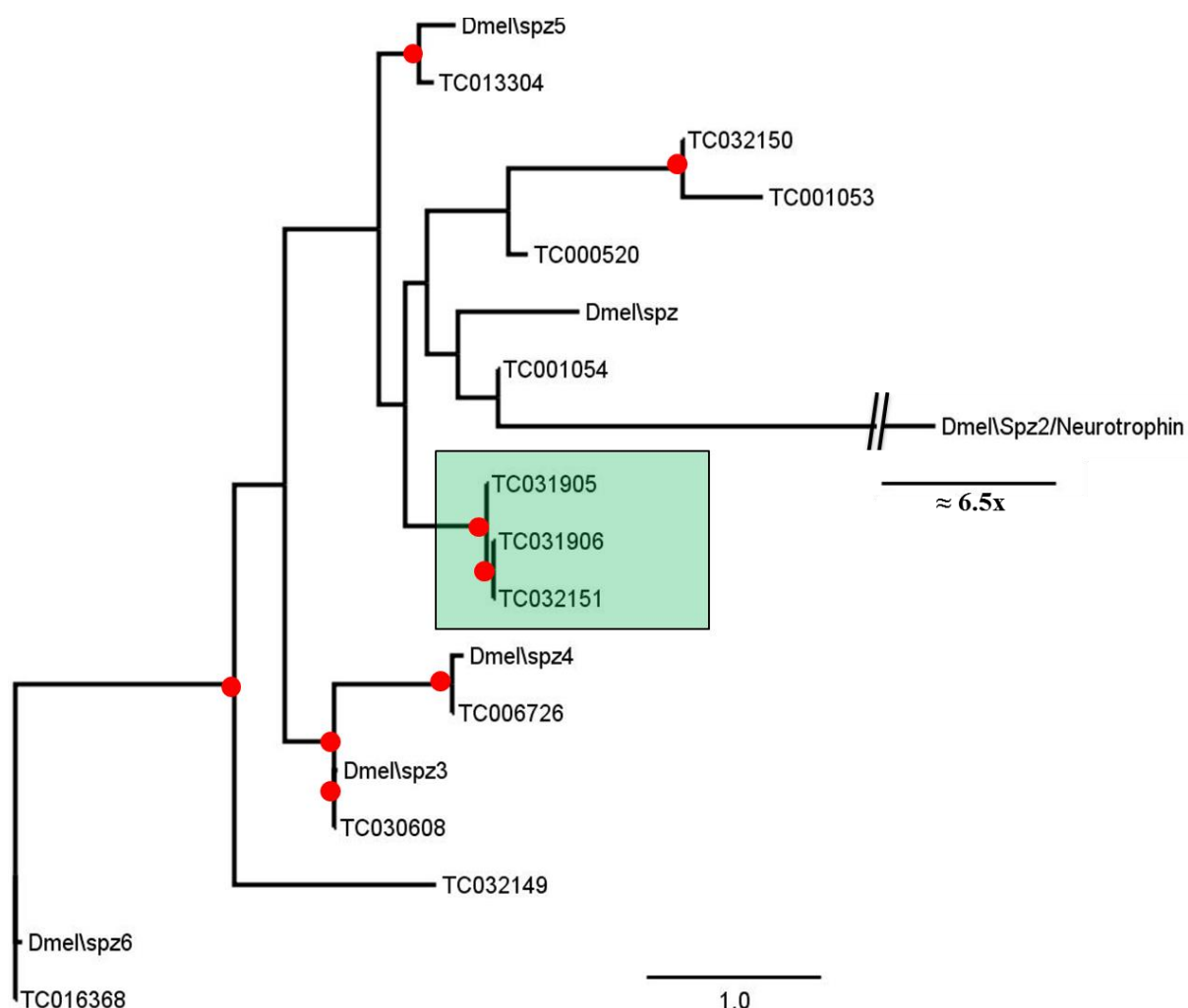


**Figure 40. Molecular phylogenetic analysis of iB-06774.**

Multiple sequence alignment of the 18 protein sequences (Spaetzle-like proteins) was used for phylogenetic evolutionary analysis. Phylogenetic analysis was performed by maximum likelihood method with 100 bootstrap values. The branch length measured the number of substitutions per site. Clades marked with filled red circles have the bootstrap value of more than 50%. Targets of iB-06774 (TC031905, TC031906 and TC032151) are highlighted with green rectangle in the phylogenetic tree.

## 7. Discussion

---

### 7.1 Novel DV patterning genes identified in the iBeetle screen

Comprehensive unbiased genetic screens provide an excellent platform to identify gene functions in particular biological processes (Schmitt-Engel et al., 2015). For a long time, the investigation of DV patterning genes in *Tribolium* was based on candidate gene approaches, which leads to biased conserved gene function analysis (Lynch and Roth, 2011). Furthermore, genes which are required for particular processes that are not represented in *Drosophila* couldn't be identified in *Tribolium* through candidate gene approach. Here, the unbiased iBeetle large scale RNAi screen provided an excellent platform to overcome the candidate gene approach and revealed new genes in several biological processes including novel DV patterning genes in *Tribolium castaneum* (Schmitt-Engel et al., 2015).

The iBeetle large scale RNAi screen was a first pass screen where each gene knockdown was performed only one time (Schmitt-Engel et al., 2015). Therefore, the re-screening of the selected potential DV candidates was necessary to investigate the potential off-targets as well as dsRNA fragment specific and strain specific effects (Supp. Table 2). Most of the iBeetle annotated phenotypes were reproduced after gene knockdown with original iBeetle dsRNA fragment in the pBA19 strain. However, the percentage of reproducibility was reduced when gene knockdowns were performed using non-overlapping fragments (NOFs) and a different genetic background (SB strain) (Figure 15). It has been found that the RNAi phenotypes in *Tribolium* are strain specific and are influenced by the genotype of the injected strain. Therefore, a proper documentation and analysis of the divergent phenotypes is necessary for further investigations (Kitzmann et al., 2013). Moreover, the lack of reproducibility of the iBeetle annotated phenotypes with NOFs possibly indicates off-target effects. But in a few cases such as *Tc-sog* (iB-10751), it may also reflect the isoform/sequence specific effects of RNAi knockdown which leads to qualitatively different phenotypes in *Tribolium* (Schmitt-Engel et al., 2015; Arakane et al., 2005). Therefore, the sequence specific strength of RNAi knockdowns has to be considered for phenotype analysis during the re-screen.

A large number of known DV patterning genes acting in different signaling pathways showed their respective knockdown phenotypes within the iBeetle screen (Supp. Table 1). Furthermore, newly investigated genes like *uninflatable* (iB\_06402) which was identified in a recent RNA-seq approach (Stappert et al., 2016) were also discovered in the iBeetle screen. Collectively, these results confirm the power and sensitivity of the iBeetle RNAi screen. Moreover, novel DV patterning genes such as two serine proteases (iB-09824 and iB-07888), a serpin inhibitor (iB-06699) and a *Toll* ligand *spaetzle* (iB-06774) were identified within the second phase of the iBeetle screen. Interestingly, no DV patterning function in *Drosophila* has been described for these genes (except *spaetzle*). Therefore, without an unbiased RNAi screen, it would have been difficult to identify these genes by a candidate gene approach. Taken together, the iBeetle RNAi screening helped to overcome the limitations of a candidate gene approach and revealed novel DV patterning genes in *T. castaneum*.

## 7.2 iB-06774 *Spaetzle* functions as a ligand for the *Toll* receptor

In *Drosophila melanogaster*, the ventrally confined activation of Toll signaling leads to the translocation of the NF- $\kappa$ B transcription factor Dorsal into the nuclei where it regulates different zygotic target genes in a concentration-dependent manner (Lynch and Roth, 2011; Moussian and Roth, 2005). The proteolytic processing of the Toll ligand Spaetzle by Easter is required for initiation of the Toll signaling pathway on the ventral side of the embryo (DeLotto and DeLotto, 1998; Morisato and Anderson, 1994). In *Drosophila*, the extracellular Spaetzle pro-protein is cleaved and processed into an active fragment (also known as C-terminal fragment of 106 amino acids) by the protease Easter. The processed Spaetzle protein subsequently binds to the Toll receptor and leads to the activation of the Toll signaling pathway (Weber et al., 2003).

One of the prerequisites to complete the upstream components of the Toll signaling pathway was the identification of the *spaetzle* ortholog in *Tribolium castaneum*. In total, 14 genes coding for Spaetzle-like proteins including seven homologs from innate immunity analysis (Zou et al., 2007) were screened in the iBeetle data set (Supp. Figure 7). This mini-screen of the selected candidates revealed that only the knockdown of iB-06774 resulted in a complete dorsalized phenotype (Figure 38 and Figure 42). Similarly like *Tc-Toll* knockdown, the ventral and ventrolateral cell fates are lost, dorsal ectoderm is expanded and the border between serosa and the germ rudiment becomes rotationally symmetric in iB-06774 knockdown embryos (Figure 41) (Nunes da Fonseca et al., 2008). Furthermore, iB-06774 is zygotically expressed in the presumptive head region in a DV asymmetric pattern during blastoderm stage. The zygotic expression of iB-06774 suggests the presence of a self-enhancing positive feedback mechanism of the Toll ligand Spaetzle in *T. castaneum*. Taken together, these results indicate that iB-06774 acts as a *spaetzle* ligand for Toll receptor in *T. castaneum* and thus defines the dorsoventral polarity of the embryo.

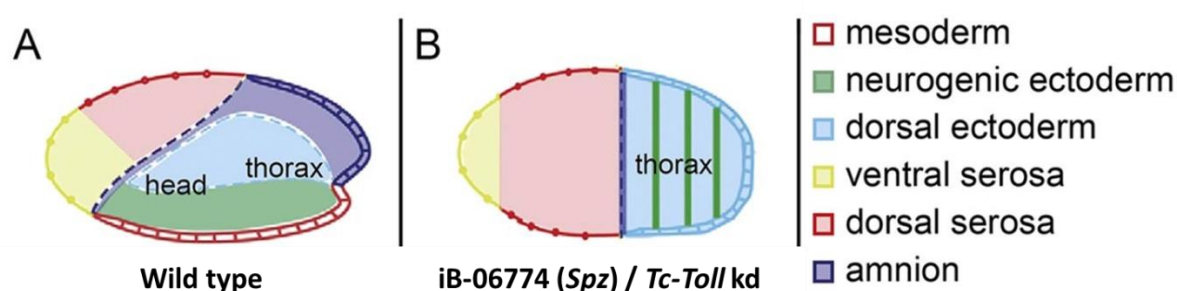


**Figure 41. Schematic drawings of wild-type and iB-06774 knockdown embryos fate maps.**

(A) Fate map of wild-type embryo (B) Fate map of iB-06774 knockdown embryo. iB-06774 knockdown produces a complete dorsalized phenotype similarly like *Tc-Toll* knockdown. After iB-06774 knockdown, the border between serosa and germ rudiment becomes straight. In contrast to wild-type, mesoderm and neurogenic ectoderm is absent while dorsal ectoderm is expanded in iB-06774 knockdown embryos. Modified from Stappert et al., 2016.

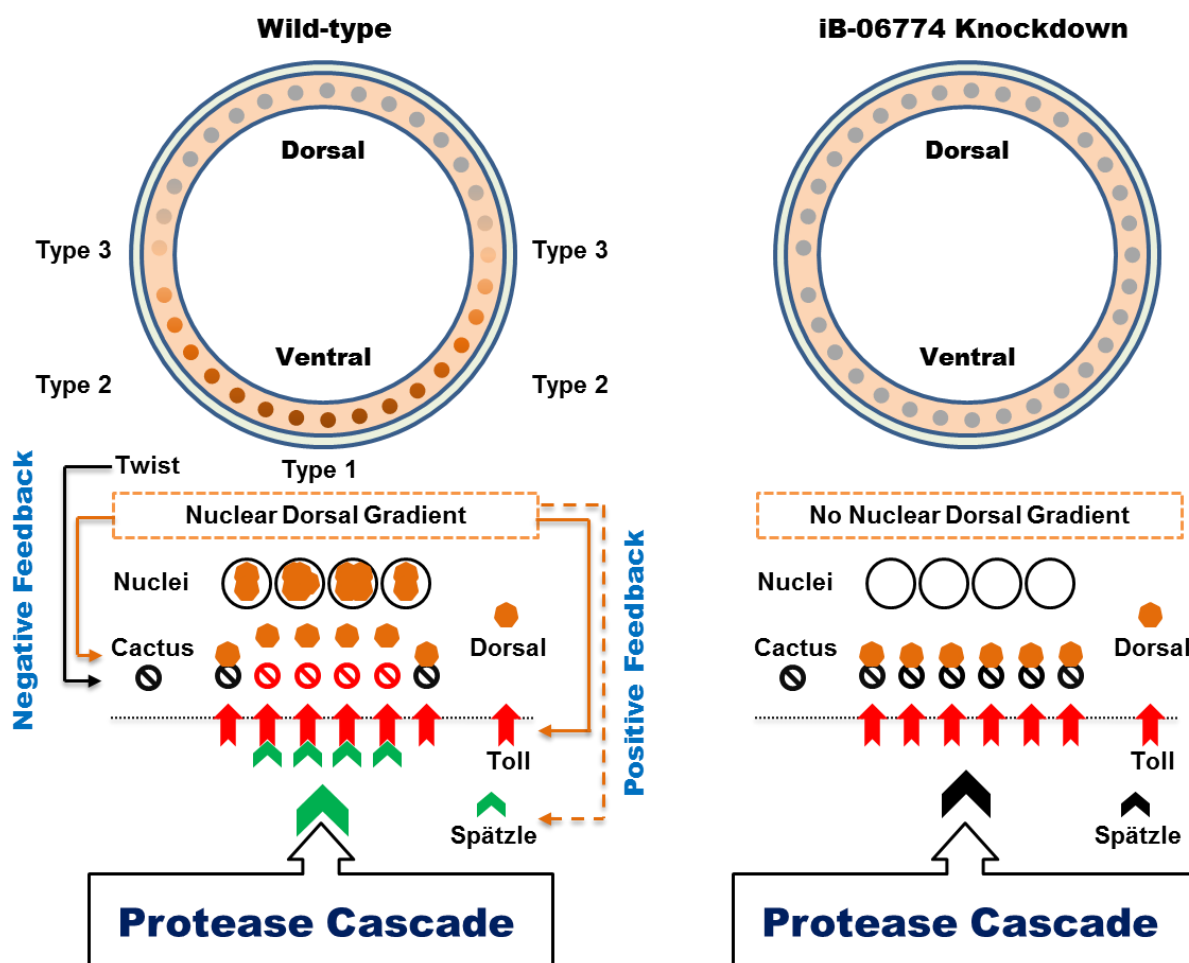


**Figure 42. *iB-06774 spaetzle* functions as a ligand for Toll receptor and produces a dorsalized phenotype.**

Schematic drawing of Toll signaling in wild-type and *iB-06774* knockdown embryos. In wild-type embryos, a protease cascade processes the Toll ligand Spätzle (*iB-06774*) and subsequently activates the Toll signaling on the ventral side of the embryo. The activation of Toll signaling leads to degradation of the Dorsal inhibitor Cactus which allows the NF-κB transcription factor Dorsal to enter the nuclei. The ventral-to-dorsal nuclear Dorsal gradient is formed and regulates the activation of zygotic target genes (Type-1, Type-2 and Type-3). Several positive and negative feedback loops are present in *Tribolium*. The Toll ligand Spätzle (*iB-06774*) is expressed zygotically which might also function as a positive feedback loop in *Tribolium* (brown dotted arrow). After *iB-06774* knockdown, Toll signaling is not activated. In the absence of Toll signaling Cactus binds to NF-κB transcription factor Dorsal and thus restricts its activity and translocation into the nuclei. Therefore, *iB-06774* knockdown embryos lack nuclear Dorsal gradient formation and the expression of its zygotic target genes.

### 7.3 iB-09824 and iB-07888 act upstream of Toll signaling

The ventrally restricted processing and activation of the Toll ligand Spaetzle to its active form (C-terminal fragment of 106 amino acids) requires the localized activity of a proteolytic cascade in the perivitelline space. In *Drosophila melanogaster*, three serine proteases (*gastrulation defective*, *snake* and *easter*) are involved in the upstream protease cascade to activate the Toll ligand Spaetzle. The autocatalytically serine protease Nudel activates the protease cascade through processing of Gastrulation defective (GD). GD cleaves and activates Snake which in turns leads to the processing and activation of Easter. The activated Easter processes the Toll ligand Spaetzle and ultimately leads to the localized activation of Toll signaling on the ventral side of the embryo (Stein and Stevens, 2014; Stein et al., 2013).

Despite the presence of potential orthologues in *Tribolium*, only two proteases (*Tc-nudel* and *Tc-easter like*) were recently identified by a candidate gene approach and functionally investigated (Dao, 2014). The absence of other essential proteases such as *snake* and *gastrulation defective* suggest that *Tribolium* uses different genes than *Drosophila* to activate the Toll ligand Spaetzle. In the course of the iBeetle large scale RNAi screen, we have identified two new serine proteases (iB-09824 and iB-07888) which belong to the trypsin superfamily and have novel functions in DV patterning in *Tribolium*. Knockdown of iB-09824 (TC032710) produced a *Toll*-like dorsalized phenotype. Like upon *Tc-Toll* knockdown, the expression of *Tc-sog* and *Tc-twist* was completely abolished and the border between serosa and germ rudiment was straight in iB-09824 knockdown embryos (Figure 17) (Nunes da Fonseca et al., 2008). Knockdown of iB-07888 (TC011067) produced a *sog*-like dorsalized phenotype (van der Zee et al., 2006) (Figure 43). After iB-07888 knockdown, the formation of the nuclear Dorsal gradient was delayed (1<sup>st</sup> stage). However, later at the primitive pit stage (2<sup>nd</sup> stage), weak nuclear Dorsal accumulation was observed in a broad ventral domain (Figure 26 and Figure 45). The *Tc-twist* expression corresponds to the late Dorsal gradient formation. However, iB-07888 knockdown embryos do not express *Tc-sog* (Figure 22). Interestingly, iB-07888 is zygotically activated by Toll signaling during early blastoderm stage (Figure 19), which indicates the presence of another self-enhancing positive feedback loop in *Tribolium*. Collectively, the knockdown results of iB-09824 and iB-07888 suggest that these newly identified genes likely act upstream of Toll signaling within the protease cascade to activate the Toll ligand Spaetzle (Figure 44).

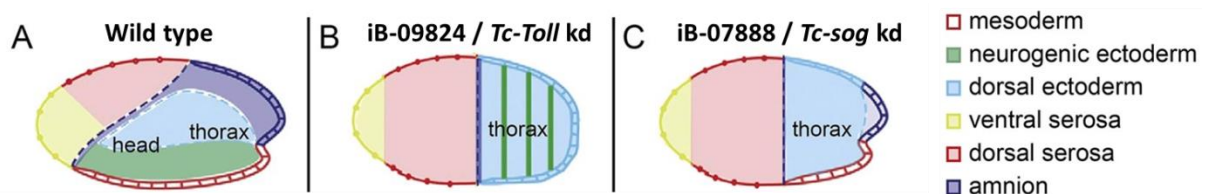


**Figure 43. Schematic drawings of wild-type and iB-09824 and iB-07888 knockdown embryos fate maps.**

(A) wild-type embryo, (B) iB-09824 KD embryo and (C) iB-07888 KD embryo. iB-09824 knockdown produces complete dorsalized phenotype. Similarly like *Tc-Toll* knockdown, the border between serosa and germ rudiment becomes straight while mesoderm and neurogenic ectoderm is lost. iB-07888 knockdown produces *Tc-sog*-like dorsalized phenotype. Like *Tc-sog* knockdown, the border between serosa and germ rudiment is straight and neurogenic ectoderm is absent. Modified from Stappert et al., 2016.

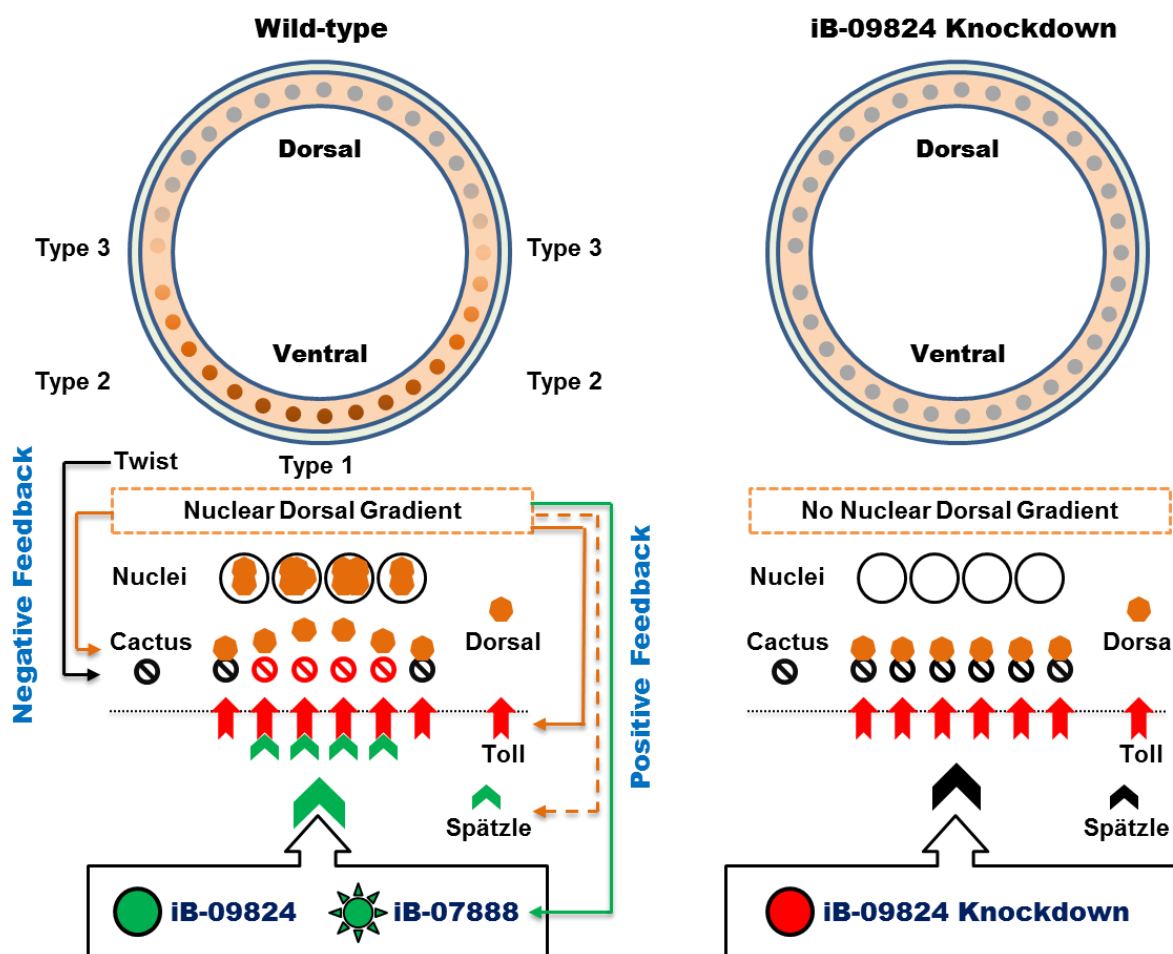


**Figure 44. iB-09824 and iB-07888 act upstream of Toll signaling in *Tribolium castaneum*.**

Schematic drawing of Toll signaling in wild-type and iB-09824 knockdown embryos. In wild-type embryos, serine proteases (iB-09824 indicated by a green filled circle and iB-07888 indicated by a green filled star) process the Toll ligand Spätzle and subsequently activate Toll signaling on the ventral side of the embryo. The activation of Toll signaling leads to NF- $\kappa$ B/Dorsal nuclear gradient formation and ultimately to the activation of zygotic target genes. Zygotic expression of iB-07888 by Toll signaling suggests another positive feedback loop (indicated by a green arrow). After iB-09824 knockdown, Toll signaling is not present. In the absence of Toll signaling (indicated by a red filled circle) Cactus binds to NF- $\kappa$ B transcription factor Dorsal which restricts their activity and translocation into the nuclei thereby no nuclear dorsal gradient is formed and produced completely *Toll*-like dorsalized phenotype.

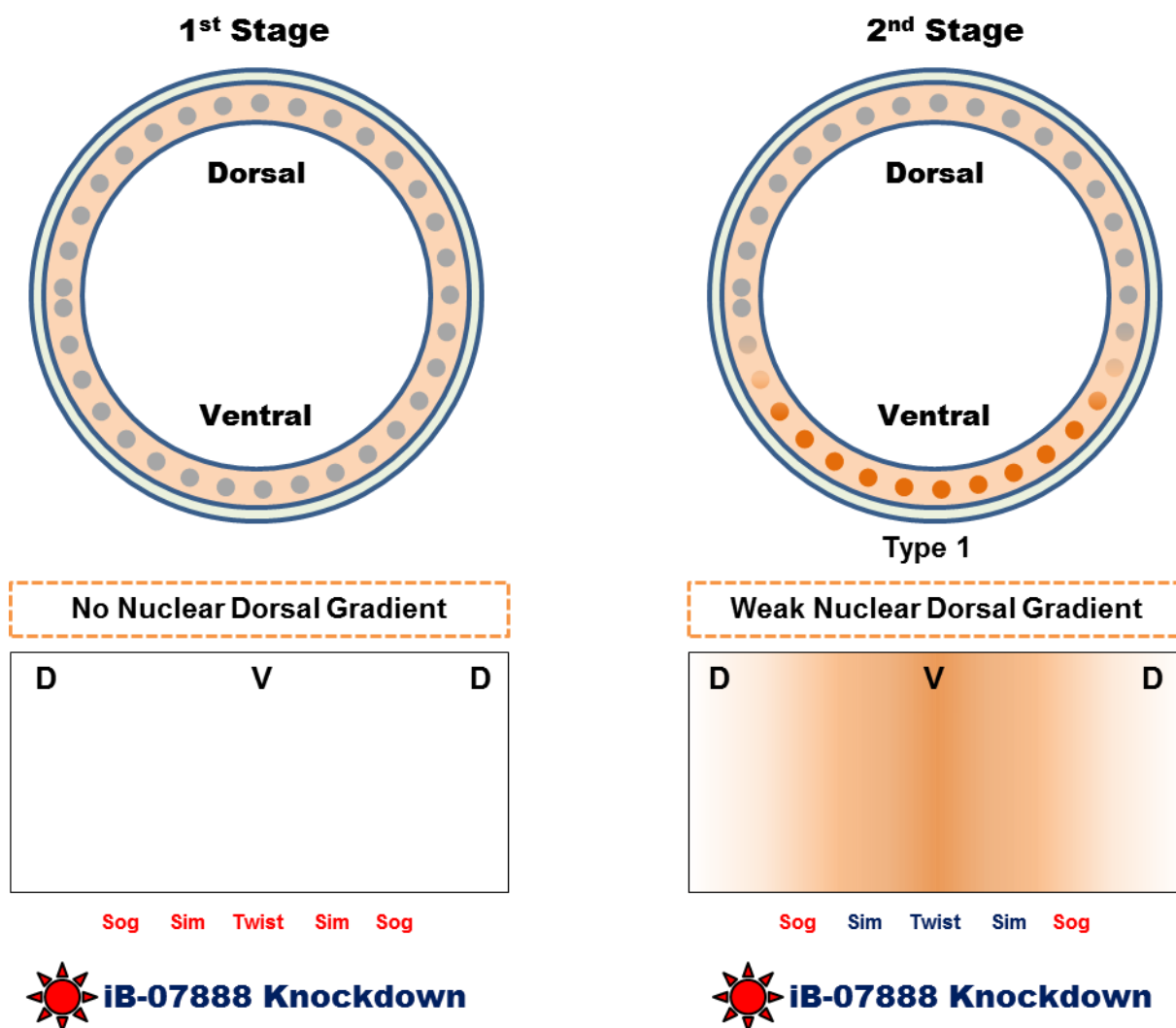


**Figure 45. iB-07888 knockdown delays the nuclear Dorsal gradient formation in *Tribolium castaneum*.** NF- $\kappa$ B nuclear Dorsal gradient formation in iB-07888 knockdown at blastoderm stage (1<sup>st</sup> stage) and at the primitive pit stage (2<sup>nd</sup> stage) embryos. After iB-07888 knockdown, the nuclear Dorsal gradient formation and refinement were absent at the blastoderm stage (1<sup>st</sup> stage). However, later at the primitive pit stage (2<sup>nd</sup> stage) weak nuclear Dorsal gradient was formed in broad ventral domain. No zygotic Dorsal target genes are expressed during the 1<sup>st</sup> stage. However, later at the primitive pit stage (2<sup>nd</sup> stage), the weak nuclear Dorsal gradient expresses genes such as *Tc-twist*, *Tc-snail* and *Tc-sim*, while the expression of *Tc-sog* was absent.



## 7.4 iB-06699 regulates the activity of the protease cascade

The serine protease cascade that activates the Toll signaling pathway to establish the dorsoventral polarity of the *Drosophila* embryo is regulated by a serine protease inhibitor of the serpin family. Serpins inhibitors function as suicide substrates which are cleaved by their target proteases and form irreversible 1:1 complex of serpin and protease (Hashimoto et al., 2003; Ligoxygakis et al., 2003). In *Drosophila*, the activated Easter activity is spatially restricted to the ventral side of the perivitelline space by the serine protease inhibitor *serpin27A*. Loss of *serpin27A* leads to a completely ventralized phenotype in *Drosophila* which demonstrates that it controls the activity of the serine protease cascade, thereby restricting the activation of Toll signaling to the ventral side of the embryo (Stein and Stevens, 2014; Moussian and Roth, 2005; Hashimoto et al., 2003; Ligoxygakis et al., 2003).

The dynamic behavior of nuclear Dorsal gradient formation and activation of Dorsal target genes in *Tribolium* suggests the involvement of protease inhibitor activities in the process of DV pattern formation. However, no functional serpin inhibitor has been identified by candidate gene approaches in *Tribolium*. With the help of the iBeetle RNAi screen, we identified a new serpin inhibitor iB-06699 (TC034678, Leukocyte elastase inhibitor). iB-06699 knockdown embryos showed lateral expansion of the *Tc-sog* expression domain in *Tribolium* (Figure 47D-F). In *Drosophila*, reduced *serpin27A* expression leads to the expansion of the ventral region with high levels of nuclear Dorsal, while the lateral region with low levels of nuclear Dorsal are shifted towards the dorsal side (Figure 46) (Ligoxygakis et al., 2003). However, after iB-06699 knockdown in *Tribolium*, no obvious *Tc-twist* or nuclear Dorsal expansion was detected in most knockdown embryos (Figure 33 and 34). This phenotype indicates that iB-06699 knockdown has only minimal effects on the nuclear Dorsal gradient which could be potentially undetectable with Dorsal antibody staining, but is sufficient to express *Tc-sog* with expanded domain. Furthermore, the phenotypic recovery of the iB-06699 knockdown embryos (Figure 31) could be due to the presence of self-organizing mechanisms of DV axis formation in *Tribolium* which may rescue the phenotype and thus enable normal development of the embryo (Nunes da Fonseca et al., 2008). Taken together, it is likely that the serpin inhibitor iB-06699 acts upstream of Toll signaling to regulate the activity of the proteases cascade to the ventral side of the perivitelline space.

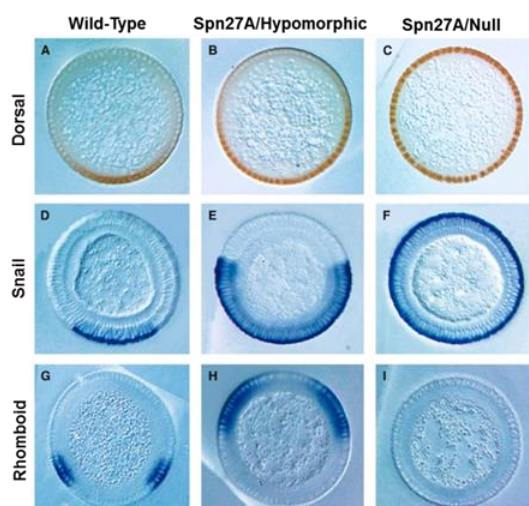


**Figure 46. Loss of *serpin27A* leads to a completely ventralized phenotype in *Drosophila melanogaster*.** (A-C) Dorsal protein, (D-F) *snail* mRNA and (G-I) *rhomboid* mRNA. The dorsal side of the embryo points upwards. Partial loss of *serpin27A* (hypomorphic phenotype) leads to partial ventralization of the embryo. The ventral region with high nuclear Dorsal levels and the corresponding *snail* expression domain is expanded while the lateral region with low nuclear Dorsal levels and the corresponding *rhomboid* expression domain is shifted to the dorsal side. Null mutant of *serpin27A* results to a complete ventralization of the embryo. Modified from Ligoxygakis et al., 2003



## 7.5 Spatial and temporal regulation of Dorsal target genes

The DV patterning of the *Drosophila* embryo is established by the nuclear concentration gradient of the NF- $\kappa$ B Dorsal transcription factor (Roth et al., 1989). High levels of the nuclear Dorsal protein are present in the ventral region of the embryo and get progressively reduced in more lateral positions. At the dorsal side of the embryo, the nuclear localization of the Dorsal transcription factor is inhibited by *cactus* and the protein remains in the cytoplasm. In *Drosophila*, the NF- $\kappa$ B nuclear Dorsal gradient regulates multiple zygotic target genes in a concentration-dependent manner to specify different cell fates along the DV axis (Moussian and Roth, 2005; Roth et al., 1989). High levels of nuclear Dorsal express Type-I genes such as *twist* and *snail*, whereas intermediate and low levels of nuclear Dorsal regulate Type-II (i.e. *ventral nervous system defective* and *rhomboid*) and Type-III (i.e. *short gastrulation*) genes, respectively (Reeves and Stathopoulos, 2009; Moussian and Roth, 2005). Moreover, combinatorial interactions of Dorsal with additional transcription factors and signaling pathways is essential for differential regulation and spatial patterning of different zygotic target genes along the DV axis (Rushlow and Shvartsman, 2012; Liberman et al., 2009; Reeves and Stathopoulos, 2009; Hong et al., 2008).

In contrast to *Drosophila*, the NF- $\kappa$ B nuclear Dorsal gradient formation in *Tribolium* is highly dynamic. The nuclear Dorsal uptake is initiated around the DV axis and subsequently refines to the ventral most region of the embryo (Lynch and Roth, 2011; Chen et al., 2000). The presence of a self-regulatory circuit of Dorsal target genes in *Tribolium* regulates the dynamic behavior of the nuclear Dorsal gradient formation. In *Tribolium*, both *Toll* receptor and *cactus* inhibitor are zygotically expressed by Toll signaling, leading to positive and negative feedback loops, respectively. (Lynch and Roth, 2011; Nunes da Fonseca et al., 2008).

Functional analysis of iB-07888 (serine protease P125) revealed its requirement for activation of Toll signaling and nuclear Dorsal gradient formation in *Tribolium*. Knockdown of iB-07888 delays the nuclear Dorsal gradient formation and the expression of their corresponding target genes (Figure 47G-I). Importantly, iB-07888 itself is expressed zygotically by Toll signaling in a narrow ventral domain (Figure 19). Like *Tc-Toll*, low level proteolytic activity of iB-07888 might initiate the nuclear uptake of Dorsal. This will subsequently up-regulate iB-07888 zygotically for local self-enhancement of Toll signaling and ultimately refine Dorsal gradient formation (Nunes da Fonseca et al., 2008; Chen et al., 2000). These results indicate that iB-07888 acts as a positive feedback loop which functions for spatial and temporal control of the nuclear Dorsal gradient dynamics in *Tribolium*. Moreover, a self-enhancing positive feedback mechanism is often counterbalanced by inhibitory processes for stable and spatial pattern formation (Nunes da Fonseca et al., 2008). Knockdown embryos of iB-06699 (Leukocyte elastase inhibitor) showed a lateral expansion of the *Tc-sog* expression domain (Figure 47D-F). Collectively, these results suggest that a combinatorial function of activators and inhibitors is required for defining the spatial expression pattern of Dorsal target genes in *Tribolium*.

Interestingly, knockdown embryos of iB-07888 lack *Tc-sog* expression but they still activate *Tc-twist* and *Tc-snail* in a broad ventral domain at the primitive pit stage (Figure 22 and Figure 23). The late expression of *Tc-twist* and *Tc-snail* corresponds to the delayed weak nuclear Dorsal gradient formation (Figure 26). This is contrary to *Drosophila*, where low levels of nuclear Dorsal protein activate *sog* while high levels are required to express genes such as *twist* and *snail* (Reeves and Stathopoulos, 2009; Moussian and Roth, 2005). These results suggest that NF- $\kappa$ B nuclear Dorsal gradient in *Tribolium* plays a less direct role in DV cell fates determination compared to *Drosophila* (Chen et al., 2000). Taken together, the new serine protease (iB-07888) affects the timing of nuclear Dorsal gradient formation and ultimately the expression of its zygotic target genes. Importantly, these observations also propose that the Dorsal target genes in *Tribolium* have to be activated in a temporal sequence to define their spatial expression domains at different time points (Figure 48). We assume that in contrast to *Drosophila*, where several Dorsal target genes are simultaneously activated based on different nuclear Dorsal concentrations, the *Tribolium* NF- $\kappa$ B Dorsal gradient acts by a temporal shift to activate its zygotic target genes in a time-dependent manner.

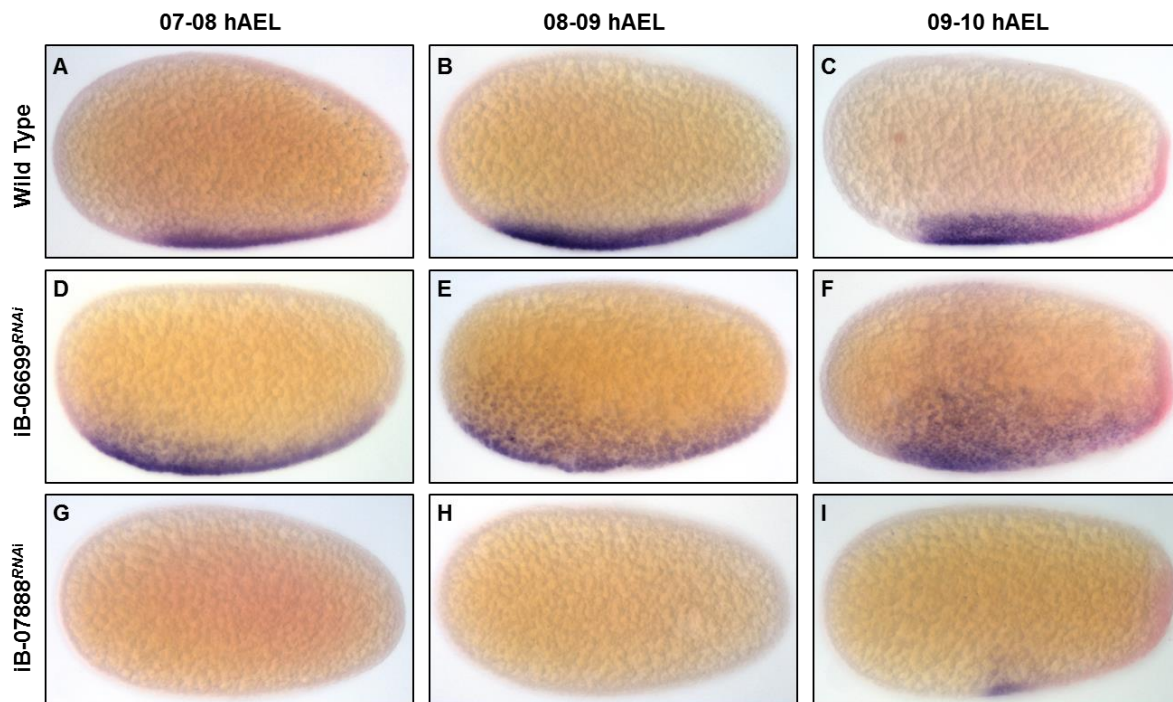


**Figure 47. Double *in-situ* hybridization of *Tc-sog*+*Tc-twist* after iB-06699 and iB-07888 knockdown.**

(A-I) Whole-mount double *in-situ* hybridization of blastoderm stage embryos at different developmental stages. The anterior of the embryo points to the left and the dorsal side of the embryos points upwards. (A-C) Expression of *Tc-sog*+*Tc-twist* in wild-type embryos, (D-F) expression of *Tc-sog*+*Tc-twist* in iB-06699 knockdown embryos and (G-I) expression of *Tc-sog*+*Tc-twist* in iB-07888 knockdown embryos. Blue staining indicates *Tc-sog* expression pattern, while pink staining indicates *Tc-twist* expression pattern. Both *Tc-sog* and *Tc-twist* expression start at early blastoderm stage (7-8 hAEL) in wild-type embryos (A). After iB-06699 knockdown, the *Tc-twist* expression pattern did not show any significant difference compared to wild-type, but *Tc-sog* expression domain is extended to the anterior along the AP axis and later expanded laterally (D-F). After iB-07888 knockdown, the expression of *Tc-sog* was completely absent except few embryos which showed weak lateral expression at 9-10 h AEL (I), while *Tc-twist* expression was delayed (G-H) and the expression starts later in a broad ventral domain (I).

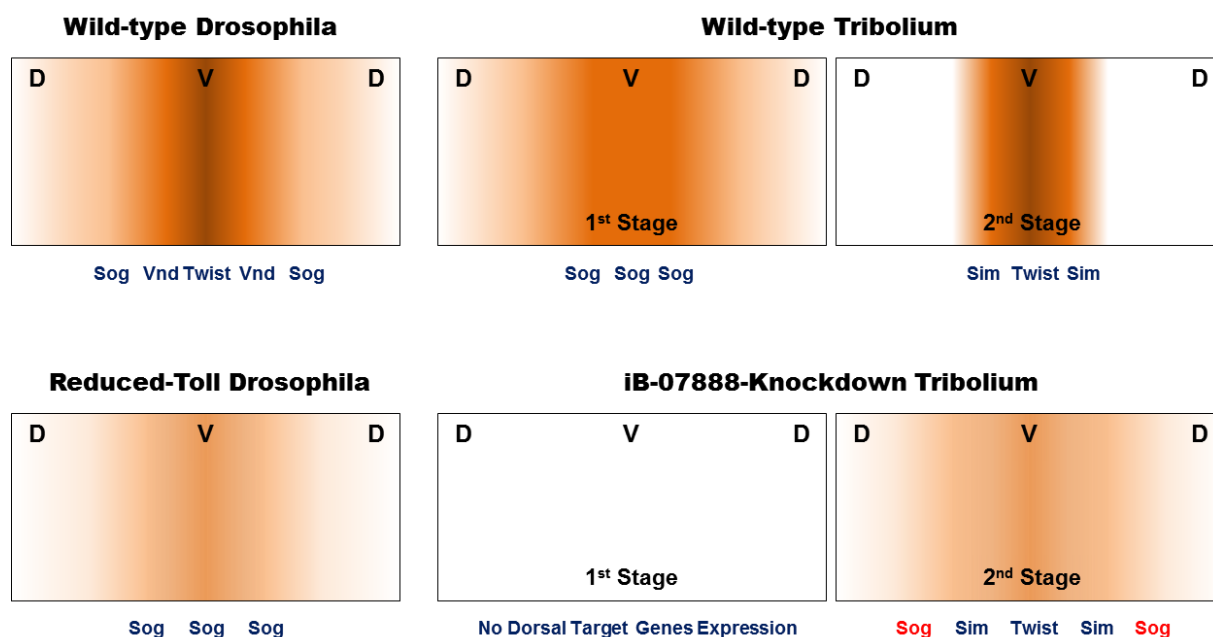


**Figure 48. Model for temporal and spatial NF-kB Dorsal target genes activation in *Tribolium castaneum*.**

The schematic drawing represents comparative analysis of the nuclear Dorsal gradient formation and regulation of their target genes between *Drosophila* and *Tribolium*. In *Drosophila*, the stable nuclear Dorsal concentration gradient regulates their target genes simultaneously in a concentration dependent manner. However, the nuclear Dorsal gradient formation in *Tribolium* is dynamic and their target genes are activated in a temporal sequence. Our model suggests that in *Tribolium*, the broad nuclear Dorsal (1<sup>st</sup> stage) express *sog* while later during the refined nuclear Dorsal gradient (2<sup>nd</sup> stage), genes such as *twist*, *sim* and *snail* are activated. Knockdown phenotype of iB-07888 supports this model. After iB-07888 knockdown, the nuclear Dorsal gradient formation and their corresponding target genes activation is delayed (1<sup>st</sup> stage). However, during early gastrulation stage (2<sup>nd</sup> stage), weak nuclear Dorsal gradient forms and only activates genes such as *Tc-twist* and *Tc-sim* in a broad ventral domain. This is contrary to *Drosophila*, where low level of nuclear Dorsal (reduced Toll signaling) activates *sog* while high level is required to express genes such as *twist*. These data suggest that the Dorsal target genes in *Tribolium* are activated in a temporal sequence to define their spatial expression domains at different time points along the DV axis.

## 8. Conclusion and Future Outlook

---

The aim of my PhD thesis was to identify novel DV patterning genes in *Tribolium castaneum* by overcoming the limitations of a candidate gene approach. The analysis of previously unknown DV patterning genes, which were identified in the unbiased iBeetle RNAi screen, provided new insights into the DV patterning network of *T. castaneum*, which is radically different from *Drosophila melanogaster*. Our results suggest that the nuclear NF- $\kappa$ B/Dorsal gradient in *T. castaneum* has a less direct role in the specification of the expression domains of its zygotic target genes than in *D. melanogaster*. We propose that in *T. castaneum* the NF- $\kappa$ B/Dorsal gradient acts by a temporal shift to regulate its zygotic target genes in a time-dependent manner rather than by a stable morphogenetic mechanism as in *D. melanogaster*.

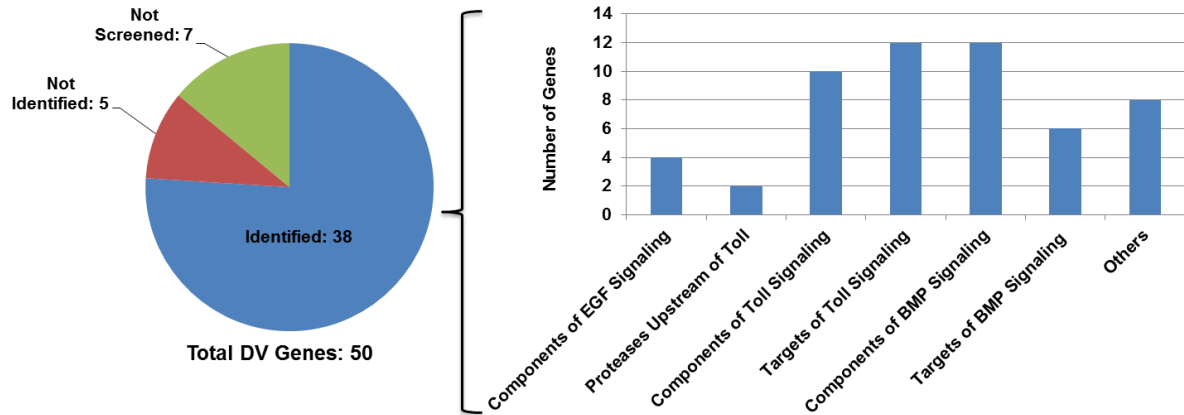
To further investigate the temporal regulation of NF- $\kappa$ B/Dorsal target genes in *T. castaneum*, I will do multiplexed (e.g. *Tc-sog* and *Tc-twist*) *in situ* amplification based on the mechanism of hybridization chain reaction (HCR) (Choi et al., 2016). Furthermore, I will perform ovarian *in situ* hybridization of iB-07888 (serine protease P125) to investigate if iB-07888 also provides maternal positional cues to the future embryo. Epistasis analysis and rescue experiments will also be important in order to confirm that the newly identified serine proteases (iB-07888 and iB-09824) are acting upstream of Toll signaling. Additionally, functional analyses of iB-09592 (*exostosin*) and iB-02234 (*sulfateless*) are necessary to analyze their potential role in DV pattern formation in *T. castaneum*.

## 9. Supplementary Information

**Supp. Table 1. The iBeetle large scale RNAi screen and DV patterning genes.**

Nr.	Gene Name	Tc-identifier	iB-number	iBeetle screen	Signaling Pathway
1	<i>Tc-ind</i>	TC006888	iB_04233	Not identified	Target of BMP Signaling
2	<i>Tc-doc</i>	TC012346	iB_05219	Identified	Target of BMP Signaling
3	<i>Tc-twist</i>	TC014598	iB_09112	Identified	Target of Toll Signaling
4	<i>Tc-sim</i>	TC016205	iB_05974	Identified	Target of Toll Signaling
5	<i>Tc-vnd</i>	TC007014	iB_04254	Identified	Target of Toll Signaling
6	<i>Tc-snail</i>	TC014474	iB_05637	Identified	Target of Toll Signaling
7	<i>Tc-msh (drop)</i>	TC012748	iB_05308	Identified	Target of BMP Signaling
8	<i>Tc-zen1</i>	TC000921	iB_03104	Identified	Others
9	<i>Tc-zen2</i>	TC000922	/	Not Present	Others
10	<i>Tc-pannier</i>	TC010407	iB_09082	Identified	Target of BMP Signaling
11	<i>Tc-sog</i>	TC012650	iB_10751	Identified	Target of Toll Signaling/Component of BMP Signaling
12	<i>Tc-iroquois (arauca)</i>	TC031040	iB_03594	Identified	Target of BMP Signaling
13	<i>Tc-cactus</i>	TC002003	iB_00322	Identified	Target of Toll Signaling/Component of Toll Signaling
14	<i>Tc-rhomboid</i>	TC034043	/	Not Present	Components of EGF Signaling
15	<i>Tc-Dorsal</i>	TC007697	/	Not Present	Component of Toll Signaling
16	<i>Tc-Toll</i>	TC000176	/	Not Present	Component of Toll Signaling
17	<i>Tc-neuralized</i>	TC000216	iB_07911	Identified	Notch Signaling/Target of Toll Signaling
18	<i>Tc-delta</i>	TC004114	iB_03691	Identified	Notch Signaling/Target of Toll Signaling
19	<i>Tc-dpp</i>	TC008466	iB_04497	Identified	Target of Toll Signaling/Component of BMP Signaling
20	<i>Tc-otd</i>	TC003354	iB_07391	Identified	Others
21	<i>Tc-achaete-scute (asc)</i>	TC008433	iB_04489	Identified	Target of BMP Signaling
22	<i>Tc-dan</i>	TC016383	iB_06366	Identified	Component of BMP Signaling
23	<i>Tc-mad</i>	TC033446	iB_05723	Identified	Component of BMP Signaling
24	<i>Tc-pelle</i>	TC015365	iB_02469	Identified	Component of Toll Signaling
25	<i>Tc-tolloid</i>	TC034615	iB_01822	Identified	Component of BMP Signaling
26	<i>Tc-twisted gastrulation</i>	TC003620	iB_00592	Identified	Component of BMP Signaling
27	<i>Tc-bambi</i>	TC012274	iB_06409	Not identified	Component of BMP Signaling
28	<i>Tc-maverick</i>	TC004299	iB_06649	Identified	TGF Signaling/Others
29	<i>Tc-myoglianin</i>	TC015805	iB_05899	Not identified	TGF Signaling/Others
30	<i>Tc-glass bottom boat</i>	TC014017	iB_05543	Identified	Component of BMP Signaling
31	<i>Tc-gremlin</i>	TC007044	iB_04261	Identified	Component of BMP Signaling
32	<i>Tc-saxophone</i>	TC015948	iB_02534	Identified	Component of BMP Signaling
33	<i>Tc-crossveinless 2</i>	TC012674	/	Not Present	Component of BMP Signaling
34	<i>Tc-myd88</i>	TC003185	/	Not Present	Component of Toll Signaling
35	<i>Tc-tartan</i>	TC014658	/	Not Present	Target of Toll Signaling
36	<i>Tc-uninflatable</i>	TC000871	iB_06402	Identified	Notch Signaling/Others
37	<i>Tc-htl heartless</i>	TC004713	iB_03821	Identified	FGF Signaling/Others
38	<i>Tc-dof/stumps</i>	TC011323	iB_02631	Identified	FGF Signaling/Others
39	<i>Tc-zfh1</i>	TC011114	iB_01805	Identified	Target of Toll Signaling
40	<i>Tc-spatzle</i>	TC016006	iB_06774	Identified	Component of Toll Signaling/Target of Toll Signaling
41	<i>Tc-tgf-alpha/Gurken</i>	TC003429	iB_03555	Identified	Components of EGF Signaling
42	<i>Tc-egfr/Torpedo</i>	TC003986	iB_00647	Identified	Components of EGF Signaling
43	<i>Tc-star</i>	TC012408	iB_02916	Not identified	Components of EGF Signaling
44	<i>Tc-easter</i>	TC002112	iB_07073	Identified	Proteases Upstream of Toll
45	<i>Tc-nudel</i>	TC000870	iB_03095	Identified	Proteases Upstream of Toll
46	<i>Tc-tube</i>	TC011895	iB_01901	Identified	Component of Toll Signaling
47	<i>Tc-windbeutel</i>	TC006116	iB_04068	Identified	Component of Toll Signaling
48	<i>Tc-seele</i>	TC009499	iB_02831	Identified	Component of Toll Signaling
49	<i>Tc-weckle</i>	TC014974	iB_05734	Not identified	Component of Toll Signaling
50	<i>Tc-punt</i>	TC011357	iB_01844	Identified	Component of BMP Signaling





### Supp. Figure 1. The iBeetle large scale RNAi screen and DV patterning genes.

Previously known components and targets of DV patterning pathways (EGF signaling, protease cascade, Toll signaling and BMP signaling) were checked in the iBeetle data set. 38 out of 50 genes showed the respective DV phenotypes, while 5 genes showed no phenotype and 7 were not present in the iBeetle RNAi screen.

### Supp. Table 2. Summary of the iBeetle re-screening.

#	iB-Numbers	iB-Fragments in PBA19 Strain	iB-Fragments in SB Strain	NOFs in PBA19 Strain	NOFs in SB Strain
1	iB_09689	Partially reproduced	Partially reproduced	Not reproduced	Not reproduced
2	iB_09592	Reproduced	Reproduced	Reproduced	Reproduced
3	iB_08587	Reproduced	Reproduced	Partially reproduced	Partially reproduced
4	iB_08599	Not reproduced	Not reproduced	Not reproduced	Not reproduced
5	iB_02234	Reproduced	Reproduced	Reproduced	Reproduced
6	iB_04132	Partially reproduced	Partially reproduced	Partially reproduced	Partially reproduced
7	iB_04537	Partially reproduced	Partially reproduced	Partially reproduced	Partially reproduced
8	iB_05227	Not reproduced	Partially reproduced	Not reproduced	Not reproduced
9	iB_05893	Reproduced	Partially reproduced	Not reproduced	Not reproduced
10	iB_07239	Partially reproduced	Reproduced	Not reproduced	Not reproduced
11	iB_08051	Reproduced	Partially reproduced	Not reproduced	Not reproduced
12	iB_10091	Partially reproduced	Partially reproduced	Not reproduced	Not reproduced
13	iB_10511	Reproduced	Reproduced	Not reproduced	Not reproduced
14	iB_10751	Reproduced	Reproduced	Not reproduced	Not reproduced
15	iB_07888	Reproduced	Reproduced	Reproduced	Reproduced
16	iB_07949	Reproduced	Not reproduced	Reproduced/NOF3 PR	Reproduced/NOF3 PR
17	iB_09824	Reproduced	Partially reproduced	Reproduced	Partially reproduced
18	iB_03355	Reproduced	Not reproduced	Not reproduced	Not reproduced
19	iB_06699	Not reproduced	Not reproduced	Reproduced	Partially reproduced
20	iB_05125	Reproduced	Partially reproduced	Reproduced	Partially reproduced
21	iB_06402	Reproduced	Reproduced	Reproduced	Reproduced
22	iB_07533	Reproduced	Reproduced	Not reproduced	Not reproduced
23	iB_06907	Reproduced	Reproduced	Not reproduced NOF2&3	Not reproduced NOF2&3
24	iB_08660	Reproduced	Reproduced	Reproduced	Partially reproduced
25	iB_03234	Partially reproduced	Not reproduced	Not reproduced	Not reproduced
26	iB_05958	Not reproduced	Not reproduced	Not reproduced	Not reproduced
27	iB_07911	Reproduced	Reproduced	Not reproduced	Not reproduced
28	iB_02326	Partially reproduced	Not reproduced	Partially reproduced	Not reproduced
29	iB_02993	Partially reproduced	Not reproduced	Not reproduced	Not reproduced
30	iB_03084	Reproduced	Reproduced	Not reproduced	Not reproduced

**Supp. Table 3. Re-screening of iB-fragments in pBA19 strain.**

#	iB-Numbers	Cuticle Analysis	Penetrance
1	iB_09689	Complete everted (only 12-15 Larvae present on slide)	more than 80%
2	iB_09592	Partially (abdomen) everted, head and thorax segments shape irregular	more than 80%
3	iB_08587	Potentially complete everted, pantagmatic defects and cuticle remnants	more than 80%
4	iB_08599	70-100% hatched	
5	iB_02234	Partially potentially everted, pantagmatic defects and cuticle remnants	more than 80%
6	iB_04132	Partially and complete everted, Pantagmatic defects	50%-80%
7	iB_04537	No almost no eggs	
8	iB_05227	70-100% hatched	
9	iB_05893	Partially and complete everted, Pantagmatic defects	more than 80%
10	iB_07239	Empty eggs and cuticle remnants	more than 80%
11	iB_08051	Complete everted, pantagmatic defects and empty eggs	more than 80%
12	iB_10091	Complete everted and empty eggs	50%-80%
13	iB_10511	Partially and complete everted, Pantagmatic defects and empty eggs	more than 80%
14	iB_10751	Larvae partially (anterior) and complete everted (inside-out)	more than 80%
15	iB_07888	Partially and complete everted, head appendiges random not present	more than 80%
16	iB_07949	Partially and complete everted and pantagmatic defects	50%-80%
17	iB_09824	Potentially everted, cuticle remnants/crumbs and empty eggs	more than 80%
18	iB_03355	Partially and complete everted and pantagmatic defects	50%-80%
19	iB_06699	70-100% hatched	
20	iB_05125	Abdomen partially everted and pantagmatic defects	more than 80%
21	iB_06402	Abdomen posterior segments everted, leg and head phenotypes	more than 80%
22	iB_07533	Abdomen posterior segments everted/not present	more than 80%
23	iB_06907	Abdomen everted, Abdomen segments not present and cuticle remnants	more than 80%
24	iB_08660	Abdomen posterior circumference decreased, empty eggs	30%-50%
25	iB_03234	Head capsule shape irregular/not present, 3-4 abdomen constriction	50%-80%
26	iB_05958	Pantagmatic defects, head appendiges position irregular/not present	50%-80%
27	iB_07911	Larvae ventral not closed, head appendiges position irregular, pantagmatic	more than 80%
28	iB_02326	Pantagmatic defects, dorsal not closed, everted and empty eggs	more than 80%
29	iB_02993	Empty eggs, cuticle remnants, ventral not closed and pantagmatic defects	50%-80%
30	iB_03084	Dorsal not closed, Head thorax and abdomen segment random not present	50%-80%

**Supp. Table 4. Re-screening of iB-fragments in SB strain.**

#	iB-Numbers	Cuticle Analysis	Penetrance
1	iB_09689	Pantagmatic defects, partially and complete everted and empty eggs	more than 80%
2	iB_09592	Partially (abdomen) everted, head and thorax segments shape irregular	more than 80%
3	iB_08587	Potentially complete everted, pantagmatic defects and cuticle remnants	more than 80%
4	iB_08599	Empty eggs and pantagmatic defects	50%-80%
5	iB_02234	Partially potentially everted, pantagmatic defects and cuticle remnants	more than 80%
6	iB_04132	Partially and complete everted, Pantagmatic defects	more than 80%
7	iB_04537	No almost no eggs	
8	iB_05227	Empty eggs and pantagmatic defects	50%-80%
9	iB_05893	Pantagmatic defects, partially and complete everted and empty eggs	50%-80%
10	iB_07239	Partially everted, Larva fragmented/constricted, Pantagmatic defects	more than 80%
11	iB_08051	Pantagmatic defects, few everted and empty eggs	more than 80%
12	iB_10091	Pantagmatic defects, few everted and empty eggs	50%-80%
13	iB_10511	Partially and complete everted and empty eggs	more than 80%
14	iB_10751	Larvae complete everted (inside-out) and few empty eggs	more than 80%
15	iB_07888	Complete everted, head capsule (appendiges ) random not present	more than 80%
16	iB_07949	70-100% hatched	
17	iB_09824	Empty eggs and cuticle remnants/crumbs	more than 80%
18	iB_03355	70-100% hatched	
19	iB_06699	70-100% hatched	
20	iB_05125	Head capsule/appendiges position irregular, no abdomen everted	50%-80%
21	iB_06402	Abdomen posterior segments everted, leg and head phenotypes	more than 80%
22	iB_07533	Abdomen posterior segments everted/not present	50%-80%
23	iB_06907	Abdomen everted, Abdomen segments not present	more than 80%
24	iB_08660	Abdomen posterior circumference decreased, abdomen everted	30%-50%
25	iB_03234	Empty eggs, three abdomen everted larvae and one abdomen constricted	30%-50%
26	iB_05958	Pantagmatic defects, head appendiges position irregular/not present	50%-80%
27	iB_07911	Larvae ventral not closed, head appendiges position irregular, pantagmatic	more than 80%
28	iB_02326	Pantagmatic defects, cuticle remnants and empty eggs	50%-80%
29	iB_02993	Empty eggs and few pantagmatic defects	30%-50%
30	iB_03084	Empty eggs, pantagmatic defects and few dorsal not closed	50%-80%

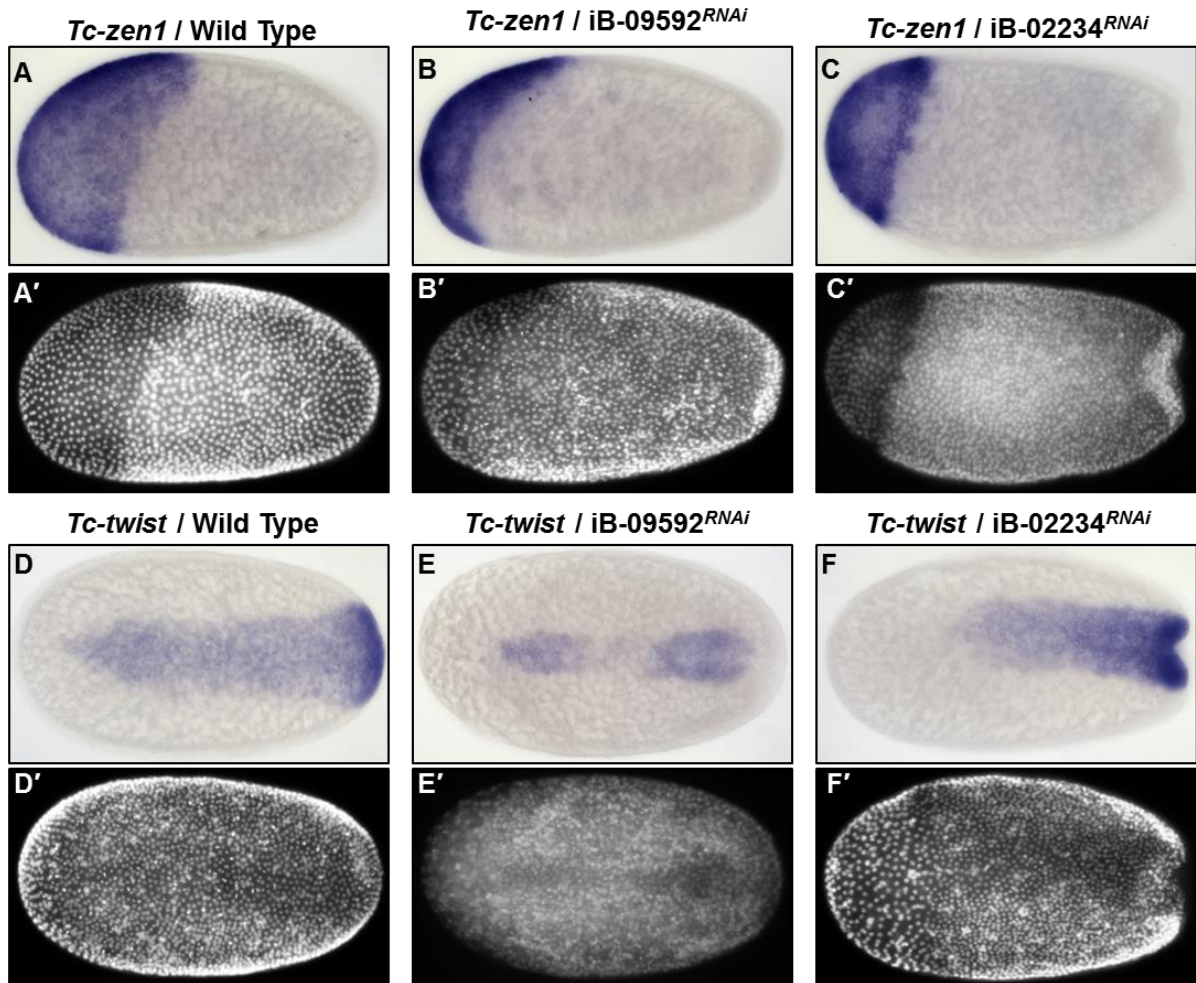
**Supp. Table 5. Re-screening of NOF in pBA19 strain.**

#	iB-Numbers	Cuticle Analysis	Penetrance
1	iB_09689-2	No almost no eggs	
2	iB_09592-2	Partially (abdomen) everted, Head and thorax segments shape irregular	more than 80%
3	iB_08587-2	Empty eggs and cuticle remnants/crumbs	more than 80%
4	iB_08599-2	70-100% hatched	
5	iB_02234-2	Partially potentially everted, pantagmatic defects and cuticle remnants	more than 80%
6	iB_04132-2	Partially and complete everted, Pantagmatic defects	50%-80%
7	iB_04537-2	No almost no eggs	
8	iB_05227-2	70-100%	
9	iB_05893-2	70-100%	
10	iB_07239-2	Empty eggs and pantagmatic defects	50%-80%
11	iB_08051-2	70-100%	
12	iB_10091-2	Empty eggs, pantagmatic defects and only two everted phenotypes	50%-80%
13	iB_10511-2	70-100%	
14	iB_10751-2	Head appendiges (capsule) position irregular and random not present	more than 80%
15	iB_07888-2	Partially and complete everted, head appendiges random not present	more than 80%
16	iB_07949-2	Partially and complete everted and pantagmatic defects	more than 80%
17	iB_07949-3	few everted and pantagmatic defects	30%-50%
18	iB_09824-2	Potentially everted, cuticle remnants/crumbs and empty eggs	more than 80%
19	iB_03355-2	70-100%	
20	iB_06699-2	Larva partially everted, abdomen segments decrease and pantagmatic	more than 80%
21	iB_05125-2	Abdomen partially everted, complete everted and pantagmatic defects	more than 80%
22	iB_06402-2	Abdomen posterior segments everted, leg and head phenotypes	more than 80%
23	iB_07533-2	Few pantagmatic defects and empty eggs	30%-50%
24	iB_06907-2	70-100%	
25	iB_06907-3	Mostly empty eggs and 2-3 cuticle remnants	more than 80%
26	iB_08660-2	Legs are bent, No everted/abdomen circumference decreased phenotypes	50%-80%
27	iB_03234-2	Empty eggs	more than 80%
28	iB_05958-2	No almost no eggs	
29	iB_07911-2	Head capsule dorasal cuticle not present, head appendiges not present	Less than 30%
30	iB_02326-2	Pantagmatic defects, dorsal not closed, everted and empty eggs	50%-80%
31	iB_02993-2	Mostly wild type only 3-4 larva showed ventral not closed phenotype	
32	iB_03084-2	Empty eggs	more than 80%

**Supp. Table 6. Re-screening of NOF in SB strain.**

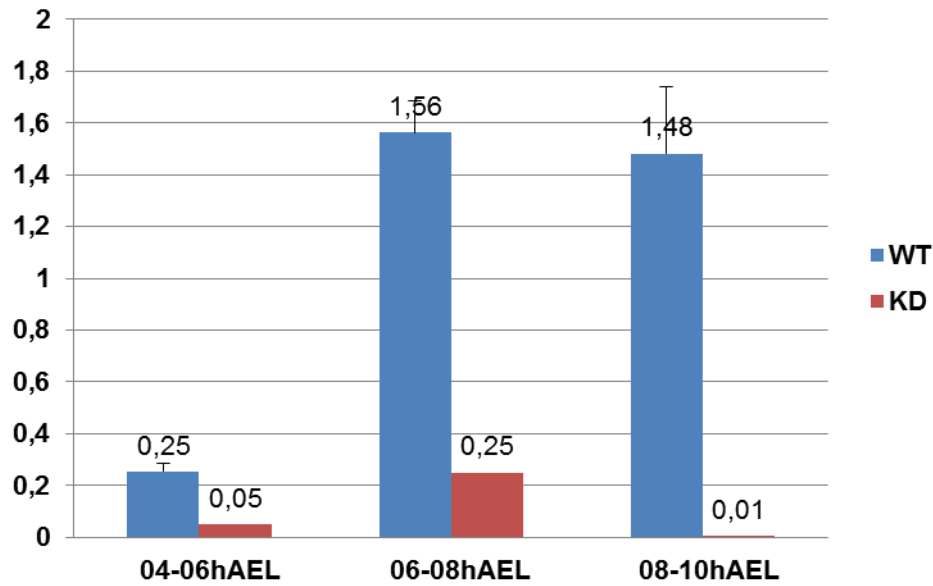
#	iB-Numbers	Cuticle Analysis	Penetrance
1	iB_09689-2	No almost no eggs	
2	iB_09592-2	Partially (abdomen) everted, Head and thorax segments shape irregular	more than 80%
3	iB_08587-2	Empty eggs and cuticle remnants/crumbs	more than 80%
4	iB_08599-2	Empty eggs and pantagmatic defects	50-80%
5	iB_02234-2	Partially potentially everted, pantagmatic defects and cuticle remnants	more than 80%
6	iB_04132-2	Partially and complete everted, Pantagmatic defects	50-80%
7	iB_04537-2	No almost no eggs	
8	iB_05227-2	70-100% hatched	
9	iB_05893-2	70-100% hatched	
10	iB_07239-2	70-100% hatched	
11	iB_08051-2	70-100% hatched	
12	iB_10091-2	Empty eggs and few pantagmatic defects	50-80%
13	iB_10511-2	70-100% hatched	
14	iB_10751-2	Head appendiges position irregular and random (capsule) not present	more than 80%
15	iB_07888-2	Partially and complete everted, head appendiges random not present	more than 80%
16	iB_07949-2	Partially and complete everted and pantagmatic defects	more than 80%
17	iB_07949-3	few everted and pantagmatic defects	50-80%
18	iB_09824-2	Empty eggs and cuticle remnants/crumbs	more than 80%
19	iB_03355-2	70-100% hatched	
20	iB_06699-2	No everted phenotypes only pantagmatic defects	30-50%
21	iB_05125-2	Head capsule/appendiges position irregular, no abdomen everted	50-80%
22	iB_06402-2	Abdomen posterior segments everted, leg and head phenotypes	more than 80%
23	iB_07533-2	Pantagmatic defects and head appendiges random not present	30-50%
24	iB_06907-2	Empty eggs and pantagmatic defects	more than 80%
25	iB_06907-3	Mostly empty eggs, 2-3 cuticle remnants and 1-2 abdomen everted	more than 80%
26	iB_08660-2	Legs are bent, abdomen posterior circumference decreased	30-50%
27	iB_03234-2	Empty eggs	more than 80%
28	iB_05958-2	No almost no eggs	
29	iB_07911-2	70-100% hatched	
30	iB_02326-2	Pantagmatic defects and empty eggs	50-80%
31	iB_02993-2	Mostly wild type larvae, only 1-2 larva showed ventral not closed	
32	iB_03084-2	Empty eggs	more than 80%





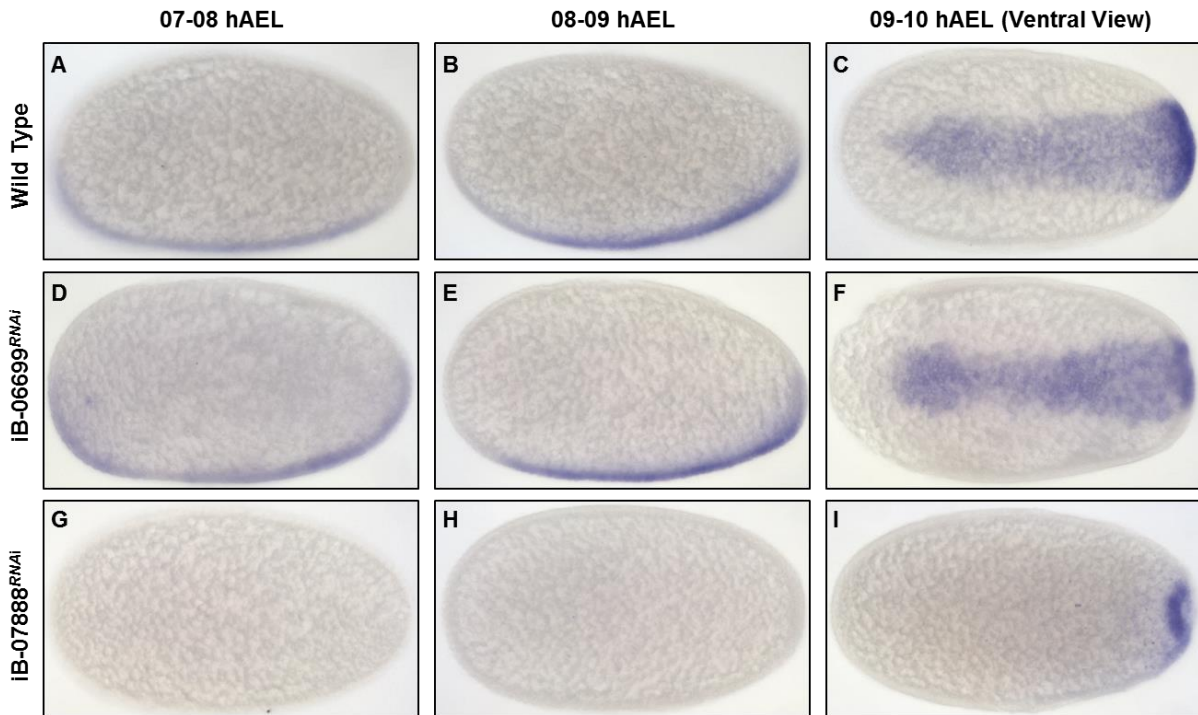
**Supp. Figure 2. Expression pattern of *Tc-zen1* and *Tc-twist* after iB-09592 and iB-02234 knockdown.**

(A-F) Whole-mount *in-situ* hybridization of blastoderm stage embryos. (A-C) *Tc-zen1* expression pattern, (D-F) *Tc-twist* expression pattern. (A-C) lateral view of the embryos and (D-F) ventral view of the embryos. The anterior of the embryos points to the left. A'-F' nuclear staining (DAPI) of the respective embryos. (A) In wild-type embryos, *Tc-zen1* is expressed in the serosa during blastoderm stage, (B and C, respectively) the expression domain is reduced in iB-09592 and iB-02234 knockdown embryos. Furthermore, (D) *Tc-twist* which is expressed ventrally during early blastoderm stage, (E) the expression domain of *Tc-twist* is reduced in iB-09592 knockdown embryos, (F) while the expression of *Tc-twist* resembles with wild-type in iB-02234 knockdown embryos.



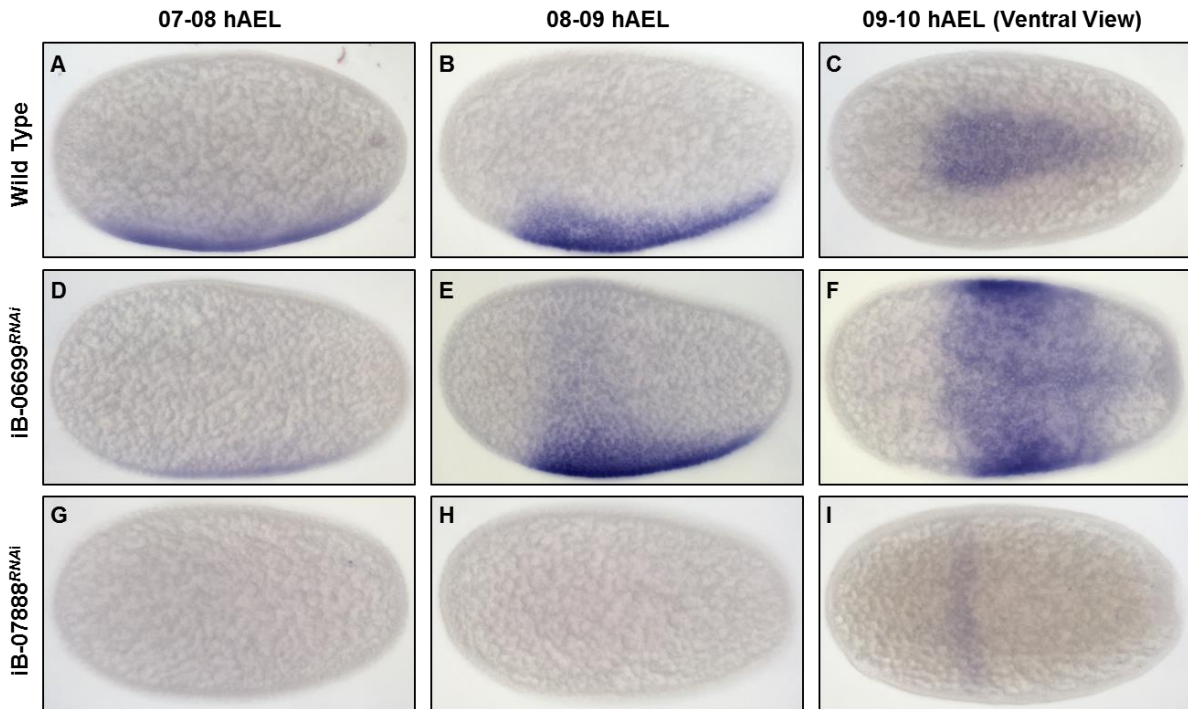
**Supp. Figure 3. Quantitative reverse transcription PCR (qRT-PCR) of iB-07888.**

The efficiency of iB-07888 knockdown was evaluated with qRT-PCR. Blue bars indicate the wild-type expression of iB-07888, while red bars indicate the expression of iB-07888 in iB-07888 knockdown embryos at different developmental stages (04-06 hAEL, 06-08 hAEL and 08-10 hAEL). Three biological replicates were used for wild-type expression analysis while only one biological replicate was used for iB-07888 knockdown embryos.



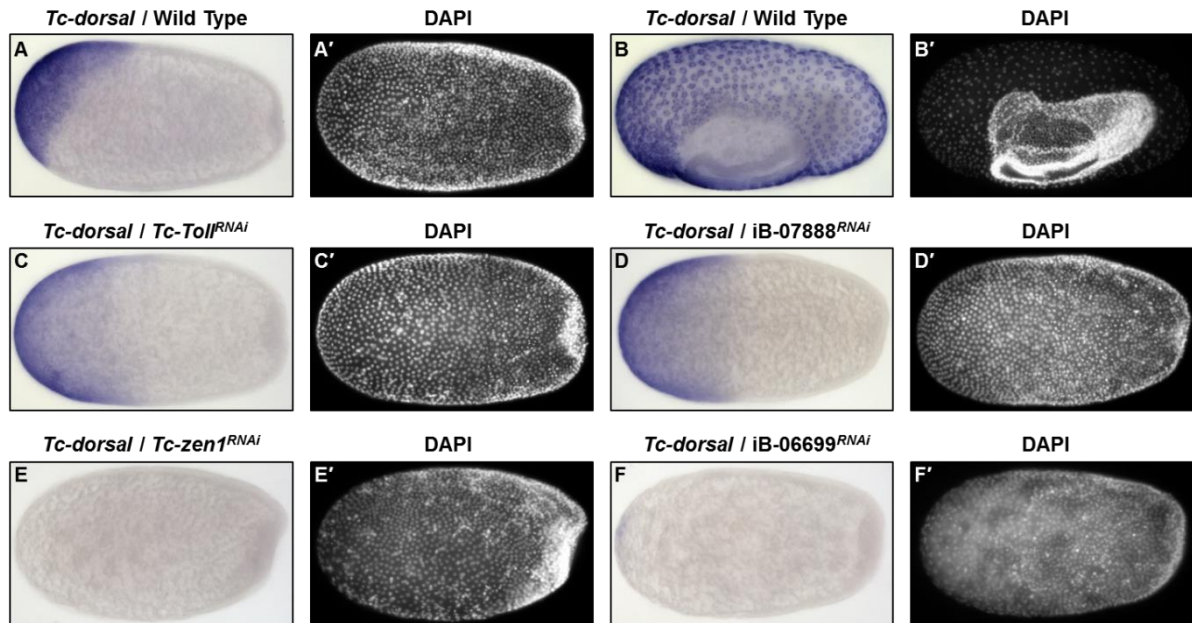
**Supp. Figure 4. Expression pattern of *Tc-twist* after iB-06699 and iB-07888 knockdown.**

(A-I) Whole-mount *in-situ* hybridization of *Tc-twist* at blastoderm stage embryos. The anterior of the embryos points to the left and the dorsal side of the embryos points upwards, except for (C, F and I) which shows the ventral surface view of the embryos. Whole mount *in-situ* hybridization of *Tc-twist* was performed in iB-06699 and iB-07888 knockdown embryos at different developmental stages. (A-C) *Tc-twist* expression in wild-type embryos, (D-F) *Tc-twist* expression in iB-06699 knockdown embryos and (G-I) *Tc-twist* expression in iB-07888 knockdown embryos. (F) *Tc-twist* expression domain is slightly broader at the anterior-most region in iB-06699 knockdown embryos. (G and H) the expression of *Tc-twist* is delayed (not present) till primitive pit stage e.g. 09 hAEL in iB-07888 knockdown embryos. However, (I) later the expression starts at the primitive pit stage in a broad ventral domain.



**Supp. Figure 5. Expression pattern of *Tc-sog* after iB-06699 and iB-07888 knockdown.**

(A-I) Whole-mount *in-situ* hybridization of *Tc-sog* at blastoderm stage embryos. The anterior of the embryos points to the left and the dorsal side of the embryos points upwards, except for (C, F and I) which shows the ventral surface view of the embryos. Whole mount *in-situ* hybridization of *Tc-sog* was performed in iB-06699 and iB-07888 knockdown embryos at different developmental stages. (A-C) *Tc-sog* expression in wild-type embryos, (D-F) *Tc-sog* expression in iB-06699 knockdown embryos and (G-I) *Tc-sog* expression in iB-07888 knockdown embryos. (E-F) *Tc-sog* expression is expanded in iB-06699 knockdown embryos (E lateral view and F ventral view of the same embryo). (G-H) *Tc-sog* expression is absent in iB-07888 knockdown embryos, but (I, ventral view) few knockdown embryos also show weak lateral expression at the primitive pit stage.





**Supp. Figure 6. Expression pattern of *Tc-dorsal* after different genes knockdowns.**

(A-F) Whole-mount *in-situ* hybridization of *Tc-dorsal* at blastoderm stage embryos except (B) at serosal window stage embryo. The anterior of the embryos points to the left and the dorsal side of the embryos points upwards. A'-F' DAPI staining of the respective embryos. Whole mount *in-situ* hybridization of *Tc-dorsal* was performed in *Tc-Toll*, iB-07888, *Tc-zen1* and iB-06699 knockdown embryos. (A-B) In wild-type embryos, *Tc-dorsal* is expressed in the serosa. (C-D) The expression of *Tc-dorsal* in *Tc-Toll* and iB-07888 knockdown embryos was expanded and dorsalized, (E-F) while it was completely absent in *Tc-zen1* and iB-06699 knockdown embryos.



Nr.	Tc-Numbers	Predicted Tc-gene in NCBI	iBeetle-Screen
1	TC000520	Spaetzle	iB_00116
2	TC001054	Protein spaetzle	iB_06737
3	TC030608	Spaetzle 3	iB_02896
4	TC006726	Uncharacterized	iB_04204
5	TC013304	Uncharacterized	iB_08356
6	TC016368	Spatzle 6	iB_06008
7	TC001053	Uncharacterized	iB_03126
8	TC016006	Spaetzle like	iB_06737, iB_06774, iB_09574
9	TC032150	Hypothetical protein	iB_09651
10	TC032149	Uncharacterized	/
11	TC031905	Spaetzle-like Protein	iB_06774
12	TC032151	Hypothetical protein	iB_06774
13	TC031906	Hypothetical protein	iB_06737, iB_06774, iB_09574
14	TC031010	Uncharacterized	iB_07446

 **No Phenotypes**
 **Potential DV Phenotypes**

**Supp. Figure 7. List of potential *spaetzle* candidates for the mini-screen.**

In total, 14 genes with *spaetzle* domains were identified and were checked in the iBeetle-Base for potential DV phenotypes. Only genes which showed potential DV phenotypes (highlighted in blue color) were selected for in-depth analysis.

```

TC032151      MWVKCVF--VCVYFMTEVSGIQASPAWQRNNHIVFPNSLEEHETFIAPKCSGNKTFCED
TC031905      -----
TC031906      MEVVSYYFFSLFLDFLIVFLVSIQASPAWQRNNHIVFPNSLEEHETFIAPKCSGNKTFCED

TC032151      VGHYPKNKFSVILENTTYGEDYFMPQSTAEESIKNRLYGVTEYYICNSHVQTQYPKVAQ
TC031905      -----
TC031906      VGHYPKNKFSVILENTTYGEDYFMPQSTAEESIKNRLYGVTEYYICNSHVQTQYPKVAQ

TC032151      NVRNEWKYVYNFDNYKQGVRTTEECVAETACRSFQGTPREVRTKCMQKYSMDLLVAD EYG
TC031905      -----
TC031906      NVRNEWKYVYNFDNYKQGVRTTEECVVRTCTCEDSTQPSVAVEE-MWVF-VLVFAVFKELG

TC032151      KPVWAFKPCHLIQPRWMIARVCTFPDSSEIGGDFLYETVVPNCQNHTYCEHLDRYPKELF
TC031905      -----MD-----DRKSLTFPDSSEIGGDFLYETVVPNCQNHTYCEHLDRYPKELF
TC031906      IQAMSFNPAKMD-----DRKGLTFPDSSEIGGDFLYETVVPNCQNHTYCEHLDRYPNELF
                :           : *****

TC032151      SKILKSREKEFSRYFQSMVIEPIMSRNQDTSCICASRKSIYPKAAYNIKNNLKFIYNF
TC031905      SKILKSREKEFSRYFQSMVIEPIMSRNQDTSCICASRKSIYPKAAYNIKNNLKFIYNF
TC031906      SKILKSREKEFSRYFQSMVIEPIMSRNQDTSCICASRKSIYPKAAYNIKNNLKFIYNF
                *****

TC032151      DGYKQGVSV EVCVIWVTAE-----
TC031905      DGYKQGVSV EVCVIKQMKFY EKVRKLKTRCQKFVEKLLLADENGRPYADRYRFP SA
TC031906      DGYKQGVSV EVCVIKQMKFY EKVRKLKTRCQKFVEKLLLADENGRPYADSWVTAE-
                *****

TC032151      -----
TC031905      CVCSYKIISNVFFT
TC031906      -----

```

**Supp. Figure 8. Multiple sequence alignment of TC031905, TC031906 and TC032151.**

Multiple sequence alignment of TC031905, TC031906 and TC032151 was performed by clustal omega shows strong protein sequence conservation.

## 10. References

---

- Anderson, Kathryn; Irvine, Kenneth (2009): Developmental biology moves forward in the 21st century. In *Current opinion in genetics & development* 19 (4), pp. 299–301. DOI: 10.1016/j.gde.2009.07.001.
- Arakane, Y.; Muthukrishnan, S.; Kramer, K. J.; Specht, C. A.; Tomoyasu, Y.; Lorenzen, M. D. et al. (2005): The *Tribolium* chitin synthase genes TcCHS1 and TcCHS2 are specialized for synthesis of epidermal cuticle and midgut peritrophic matrix. In *Insect molecular biology* 14 (5), pp. 453–463. DOI: 10.1111/j.1365-2583.2005.00576.x.
- Benton, Matthew A.; Akam, Michael; Pavlopoulos, Anastasios (2013): Cell and tissue dynamics during *Tribolium* embryogenesis revealed by versatile fluorescence labeling approaches. In *Development (Cambridge, England)* 140 (15), pp. 3210–3220. DOI: 10.1242/dev.096271.
- Bucher, Gregor; Scholten, Johannes; Klingler, Martin (2002): Parental RNAi in *Tribolium* (Coleoptera). In *Current Biology* 12 (3), R85–R86. DOI: 10.1016/S0960-9822(02)00666-8.
- Cardoso, Maira Arruda; Fontenele, Marcio; Lim, Bomyi; Bisch, Paulo Mascarello; Shvartsman, Stanislav Y.; Araujo, Helena Marcolla (2017): A novel function for the I $\kappa$ B inhibitor Cactus in promoting Dorsal nuclear localization and activity in the *Drosophila* embryo. In *Development (Cambridge, England)* 144 (16), pp. 2907–2913. DOI: 10.1242/dev.145557.
- Chen, Gang; Handel, Klaus; Roth, Siegfried (2000): The maternal NF- $\kappa$ B/Dorsal gradient of *Tribolium castaneum*: dynamics of early dorsoventral patterning in a short-germ beetle. In *Development*.
- Cho, Yong Suk; Stevens, Leslie M.; Stein, David (2010): Pipe-dependent ventral processing of Easter by Snake is the defining step in *Drosophila* embryo DV axis formation. In *Current biology : CB* 20 (12), pp. 1133–1137. DOI: 10.1016/j.cub.2010.04.056.
- Choi, Harry M. T.; Calvert, Colby R.; Husain, Naeem; Huss, David; Barsi, Julius C.; Deverman, Benjamin E. et al. (2016): Mapping a multiplexed zoo of mRNA expression. In *Development (Cambridge, England)* 143 (19), pp. 3632–3637. DOI: 10.1242/dev.140137.
- Dao, Van-Anh (2014): Genome-wide RNAi screening and the analysis of candidate genes for dorsoventral patterning in *Tribolium castaneum*. *PhD Thesis*.
- DeLotto, Yvonne; DeLotto, Robert (1998): Proteolytic processing of the *Drosophila* Spätzle protein by Easter generates a dimeric NGF-like molecule with ventralising activity. In *Mechanisms of Development* 72 (1-2), pp. 141–148. DOI: 10.1016/S0925-4773(98)00024-0.
- Dönitz, Jürgen; Grossmann, Daniela; Schild, Inga; Schmitt-Engel, Christian; Bradler, Sven; Prpic, Nikola-Michael; Bucher, Gregor (2013): TrOn. An anatomical ontology for the beetle *Tribolium castaneum*. In *PloS one* 8 (7), e70695. DOI: 10.1371/journal.pone.0070695.

- Dönitz, Jürgen; Schmitt-Engel, Christian; Grossmann, Daniela; Gerischer, Lizzy; Tech, Maïke; Schoppmeier, Michael et al. (2015): iBeetle-Base. A database for RNAi phenotypes in the red flour beetle *Tribolium castaneum*. In *Nucleic acids research* 43 (Database issue), D720-5. DOI: 10.1093/nar/gku1054.
- Hashimoto, Carl; Kim, Dong Ryoung; Weiss, Linnea A.; Miller, Jingjing W.; Morisato, Donald (2003): Spatial Regulation of Developmental Signaling by a Serpin. In *Developmental Cell* 5 (6), pp. 945–950. DOI: 10.1016/S1534-5807(03)00338-1.
- Hong, Jounge-Woo; Hendrix, David A.; Papatsenko, Dmitri; Levine, Michael S. (2008): How the Dorsal gradient works. Insights from postgenome technologies. In *Proceedings of the National Academy of Sciences of the United States of America* 105 (51), pp. 20072–20076. DOI: 10.1073/pnas.0806476105.
- Kanodia, Jitendra S.; Rikhy, Richa; Kim, Yoosik; Lund, Viktor K.; DeLotto, Robert; Lippincott-Schwartz, Jennifer; Shvartsman, Stanislav Y. (2009): Dynamics of the Dorsal morphogen gradient. In *Proceedings of the National Academy of Sciences of the United States of America* 106 (51), pp. 21707–21712. DOI: 10.1073/pnas.0912395106.
- Kitzmann, Peter; Schwirz, Jonas; Schmitt-Engel, Christian; Bucher, Gregor (2013): RNAi phenotypes are influenced by the genetic background of the injected strain. In *BMC genomics* 14, p. 5. DOI: 10.1186/1471-2164-14-5.
- Langdon, Yvette G.; Mullins, Mary C. (2011): Maternal and zygotic control of zebrafish dorsoventral axial patterning. In *Annual review of genetics* 45, pp. 357–377. DOI: 10.1146/annurev-genet-110410-132517.
- Liberman, Louisa M.; Reeves, Gregory T.; Stathopoulos, Angelike (2009): Quantitative imaging of the Dorsal nuclear gradient reveals limitations to threshold-dependent patterning in *Drosophila*. In *Proceedings of the National Academy of Sciences of the United States of America* 106 (52), pp. 22317–22322. DOI: 10.1073/pnas.0906227106.
- Ligoxygakis, Petros; Roth, Siegfried; Reichhart, Jean-Marc (2003): A Serpin Regulates Dorsal-Ventral Axis Formation in the *Drosophila* Embryo. In *Current Biology* 13 (23), pp. 2097–2102. DOI: 10.1016/j.cub.2003.10.062.
- Lynch, Jeremy A.; Peel, Andrew D.; Drechsler, Axel; Averof, Michalis; Roth, Siegfried (2010): EGF signaling and the origin of axial polarity among the insects. In *Current biology : CB* 20 (11), pp. 1042–1047. DOI: 10.1016/j.cub.2010.04.023.
- Lynch, Jeremy A.; Roth, Siegfried (2011): The evolution of dorsal-ventral patterning mechanisms in insects. In *Genes & development* 25 (2), pp. 107–118. DOI: 10.1101/gad.2010711.
- Maxton-Küchenmeister, Jörg; Handel, Klaus; Schmidt-Ott, Urs; Roth, Siegfried; Jäckle, Herbert (1999): Toll homolog expression in the beetle *Tribolium* suggests a different mode of dorsoventral patterning than in *Drosophila* embryos. In *Mechanisms of Development* 83 (1-2), pp. 107–114. DOI: 10.1016/S0925-4773(99)00041-6.

- Montell, D.; Keshishian, H.; Spradling, A. (1991): Laser ablation studies of the role of the *Drosophila* oocyte nucleus in pattern formation. In *Science* 254 (5029), pp. 290–293. DOI: 10.1126/science.1925585.
- Morisato, Donald; Anderson, Kathryn V. (1994): The *spätzle* gene encodes a component of the extracellular signaling pathway establishing the dorsal-ventral pattern of the *Drosophila* embryo. In *Cell* 76 (4), pp. 677–688. DOI: 10.1016/0092-8674(94)90507-X.
- Moussian, Bernard; Roth, Siegfried (2005): Dorsoventral axis formation in the *Drosophila* embryo--shaping and transducing a morphogen gradient. In *Current Biology* 15 (21), R887–99. DOI: 10.1016/j.cub.2005.10.026.
- Nunes da Fonseca, Rodrigo; Levetzow, Cornelia von; Kalscheuer, Patrick; Basal, Abidin; van der Zee, Maurijn; Roth, Siegfried (2008): Self-regulatory circuits in dorsoventral axis formation of the short-germ beetle *Tribolium castaneum*. In *Developmental Cell* 14 (4), pp. 605–615. DOI: 10.1016/j.devcel.2008.02.011.
- Nüsslein-Volhard, Christiane; Wieschaus, Eric (1980): Mutations affecting segment number and polarity in *Drosophila*. In *Nature* 287 (5785), pp. 795–801. DOI: 10.1038/287795a0.
- O'Connor, Michael B.; Umulis, David; Othmer, Hans G.; Blair, Seth S. (2006): Shaping BMP morphogen gradients in the *Drosophila* embryo and pupal wing. In *Development (Cambridge, England)* 133 (2), pp. 183–193. DOI: 10.1242/dev.02214.
- Reeves, Gregory T.; Stathopoulos, Angelike (2009): Graded dorsal and differential gene regulation in the *Drosophila* embryo. In *Cold Spring Harbor perspectives in biology* 1 (4), a000836. DOI: 10.1101/cshperspect.a000836.
- Reeves, Gregory T.; Trisnadi, Nathanie; Truong, Thai V.; Nahmad, Marcos; Katz, Sophie; Stathopoulos, Angelike (2012): Dorsal-ventral gene expression in the *Drosophila* embryo reflects the dynamics and precision of the dorsal nuclear gradient. In *Developmental Cell* 22 (3), pp. 544–557. DOI: 10.1016/j.devcel.2011.12.007.
- Richards, Stephen; Gibbs, Richard A.; Weinstock, George M.; Brown, Susan J.; Denell, Robin; Beeman, Richard W. et al. (2008): The genome of the model beetle and pest *Tribolium castaneum*. In *Nature* 452 (7190), pp. 949–955. DOI: 10.1038/nature06784.
- Robertis, E. M. de (2008): Evo-devo. Variations on ancestral themes. In *Cell* 132 (2), pp. 185–195. DOI: 10.1016/j.cell.2008.01.003.
- Rosenberg, Miriam I.; Desplan, Claude (2008): Patterning lessons from a dorsalized embryo. In *Developmental Cell* 14 (4), pp. 455–456. DOI: 10.1016/j.devcel.2008.03.019.
- Roth, Siegfried (2003): The origin of dorsoventral polarity in *Drosophila*. In *Philosophical transactions of the Royal Society of London. Series B, Biological sciences* 358 (1436), 1317–29; discussion 1329. DOI: 10.1098/rstb.2003.1325.



- Roth, Siegfried; Jordan, Pascale; Karess, Roger (1999): Binuclear Drosophila oocytes: consequences and implications for dorsal-ventral patterning in oogenesis and embryogenesis. In *Development*.
- Roth, Siegfried; Lynch, Jeremy A. (2009): Symmetry breaking during Drosophila oogenesis. In *Cold Spring Harbor perspectives in biology* 1 (2), a001891. DOI: 10.1101/cshperspect.a001891.
- Roth, Siegfried; Stein, David; Nüsslein-Volhard, Christiane (1989): A gradient of nuclear localization of the dorsal protein determines dorsoventral pattern in the Drosophila embryo. In *Cell* 59 (6), pp. 1189–1202. DOI: 10.1016/0092-8674(89)90774-5.
- Ruijter, J. M.; Ramakers, C.; Hoogaars, W. M. H.; Karlen, Y.; Bakker, O.; van den Hoff, M. J. B.; Moorman, A. F. M. (2009): Amplification efficiency. Linking baseline and bias in the analysis of quantitative PCR data. In *Nucleic acids research* 37 (6), e45. DOI: 10.1093/nar/gkp045.
- Rushlow, Christine A.; Shvartsman, Stanislav Y. (2012): Temporal dynamics, spatial range, and transcriptional interpretation of the Dorsal morphogen gradient. In *Current opinion in genetics & development* 22 (6), pp. 542–546. DOI: 10.1016/j.gde.2012.08.005.
- Sachs, Lena; Chen, Yen-Ta; Drechsler, Axel; Lynch, Jeremy A.; Panfilio, Kristen A.; Lässig, Michael et al. (2015): Dynamic BMP signaling polarized by Toll patterns the dorsoventral axis in a hemimetabolous insect. In *eLife* 4, e05502. DOI: 10.7554/eLife.05502.
- Schmitt-Engel, Christian; Schultheis, Dorothea; Schwirz, Jonas; Ströhlein, Nadi; Troelenberg, Nicole; Majumdar, Upalparna et al. (2015): The iBeetle large-scale RNAi screen reveals gene functions for insect development and physiology. In *Nature communications* 6, p. 7822. DOI: 10.1038/ncomms8822.
- Sommer, Ralf J. (2009): The future of evo-devo. Model systems and evolutionary theory. In *Nature reviews. Genetics* 10 (6), pp. 416–422. DOI: 10.1038/nrg2567.
- Stappert, Dominik; Frey, Nadine; Levetzow, Cornelia von; Roth, Siegfried (2016): Genome-wide identification of Tribolium dorsoventral patterning genes. In *Development (Cambridge, England)* 143 (13), pp. 2443–2454. DOI: 10.1242/dev.130641.
- Steen, Pamela W.; Tian, Sufang; Tully, Sarah E.; Cravatt, Benjamin F.; LeMosy, Ellen K. (2010): Activation of Snake in a serine protease cascade that defines the dorsoventral axis is atypical and pipe-independent in Drosophila embryos. In *FEBS letters* 584 (16), pp. 3557–3560. DOI: 10.1016/j.febslet.2010.07.020.
- Stein, David; Cho, Yong Suk; Stevens, Leslie M. (2013): Localized serine protease activity and the establishment of Drosophila embryonic dorsoventral polarity. In *Fly* 7 (3), pp. 161–167. DOI: 10.4161/fly.25141.

- Stein, David S.; Stevens, Leslie M. (2014): Maternal control of the *Drosophila* dorsal-ventral body axis. In *Wiley interdisciplinary reviews. Developmental biology* 3 (5), pp. 301–330. DOI: 10.1002/wdev.138.
- Trauner, Jochen; Schinko, Johannes; Lorenzen, Marcé D.; Shippy, Teresa D.; Wimmer, Ernst A.; Beeman, Richard W. et al. (2009): Large-scale insertional mutagenesis of a coleopteran stored grain pest, the red flour beetle *Tribolium castaneum*, identifies embryonic lethal mutations and enhancer traps. In *BMC biology* 7, p. 73. DOI: 10.1186/1741-7007-7-73.
- Tuomi, Jari Michael; Voorbraak, Frans; Jones, Douglas L.; Ruijter, Jan M. (2010): Bias in the Cq value observed with hydrolysis probe based quantitative PCR can be corrected with the estimated PCR efficiency value. In *Methods (San Diego, Calif.)* 50 (4), pp. 313–322. DOI: 10.1016/j.ymeth.2010.02.003.
- Valanne, Susanna; Wang, Jing-Huan; Rämet, Mika (2011): The *Drosophila* Toll signaling pathway. In *Journal of immunology (Baltimore, Md. : 1950)* 186 (2), pp. 649–656. DOI: 10.4049/jimmunol.1002302.
- van der Zee, Maurijn; Berns, Nicola; Roth, Siegfried (2005): Distinct functions of the *Tribolium* *zerknüllt* genes in serosa specification and dorsal closure. In *Current Biology* 15 (7), pp. 624–636. DOI: 10.1016/j.cub.2005.02.057.
- van der Zee, Maurijn; Stockhammer, Oliver; Levetzow, Cornelia von; Nunes da Fonseca, Rodrigo; Roth, Siegfried (2006): Sog/Chordin is required for ventral-to-dorsal Dpp/BMP transport and head formation in a short germ insect. In *Proceedings of the National Academy of Sciences of the United States of America* 103 (44), pp. 16307–16312. DOI: 10.1073/pnas.0605154103.
- Weber, Alexander N. R.; Tauszig-Delamasure, Servane; Hoffmann, Jules A.; Lelièvre, Eric; Gascan, Hugues; Ray, Keith P. et al. (2003): Binding of the *Drosophila* cytokine Spätzle to Toll is direct and establishes signaling. In *Nature immunology* 4 (8), pp. 794–800. DOI: 10.1038/ni955.
- Zou, Zhen; Evans, Jay D.; Lu, Zhiqiang; Zhao, Picheng; Williams, Michael; Sumathipala, Niranjani et al. (2007): Comparative genomic analysis of the *Tribolium* immune system. In *Genome biology* 8 (8), R177. DOI: 10.1186/gb-2007-8-8-r177.

## 11. Acknowledgements

---

First of all, I would like to express my sincere gratitude and appreciation to Prof. Dr. Siegfried Roth for his support, valuable suggestions and motivational guidance throughout my PhD research. His guidance and constant support helped me in all the time to complete this journey. Besides my supervisor, I would like to extend my gratitude to the rest of my thesis and examination committee: PD Dr. Michael Kroiher and Prof. Dr. Ute Höcker. I also extend my gratitude to the whole iBeetle screening members (iBeetle consortium), especially to Prof. Dr. Gregor Bucher (Georg-August-Universität Göttingen), who provided me the great opportunity to join the iBeetle large scale RNAi screening team in Göttingen. I am very much thankful to Dr. Daniela Grossmann and my screening buddy Dr. Salim Ansari for their support and lovely time during the entire screening phase in Göttingen. I would like to thank my colleagues Dr. Kristen Panfilio, Dr. Matthias Pechmann, Dr. Matt Benton and Matthias Teuscher for all support, encouragement and scientific discussions. I have gained a lot from your scientific experiences and your kind suggestions. Special thanks to my cool office-mates and colleagues, Dr. Dankina, Dr. Nadina and future-Dr. Kai. You are not only my colleagues but my all-time friends now. Thank you very much for taking care of me and for answering all my extremely focused scientific and unscientific questions. You guys have made my life very beautiful, charming and joyful in this lab and I am very lucky to have you all in my life. I am also very much thankful to my current and former fellow colleagues and lab-mates especially Stefan Koelzer, Dr. Thorsten Horn, Dr. Waldemar Wojciech, Fabian Pridoehl, Oliver Karst and little sweet Buru (Vielen Dank). I am also grateful to DFG for providing funding to my PhD research. Last but not least, I am very much thankful to my lovely parents, brothers, sister, all family members and friends who give me not only their excellent cooperation but also a lot of support, love and enjoyable moments throughout my studies.

Thanks for all your encouragement!

## 12. Erklärung

---

Ich versichere, dass ich die von mir vorgelegte Dissertation selbständig angefertigt, die benutzten Quellen und Hilfsmittel vollständig angegeben und die Stellen der Arbeit - einschließlich Tabellen, Karten und Abbildungen -, die anderen Werken im Wortlaut oder dem Sinn nach entnommen sind, in jedem Einzelfall als Entlehnung kenntlich gemacht habe; dass diese Dissertation noch keiner anderen Fakultät oder Universität zur Prüfung vorgelegen hat; dass sie - abgesehen von unten angegebenen Teilpublikationen – noch nicht veröffentlicht worden ist sowie, dass ich eine solche Veröffentlichung vor Abschluss des Promotionsverfahrens nicht vornehmen werde. Die Bestimmungen der Promotionsordnung sind mir bekannt. Die von mir vorgelegte Dissertation ist von Prof. Dr. Siegfried Roth betreut worden.

.....  
(Ort, Datum)

.....  
(Muhammad Salim Din Muhammad)

## 13. Curriculum Vitae

---

**Name:** Muhammad Salim Din Muhammad

**Date of birth:** 15.04.1989

**Nationality:** Afghan

### Educational History:

September 2013 - Continue

**Ph.D. Evolutionary Developmental Biology**

Department of Developmental Biology,

**University of Cologne, Germany**

Laboratory of Prof. Dr. Siegfried Roth

Thesis project:

Large scale RNAi screen in *Tribolium* reveals novel genes involved in dorsoventral pattern formation.

October 2011 - September 2013

**MSc International Horticulture**

Major: Genetics and Plant Breeding

**Leibniz University Hannover, Germany**

Laboratory of Prof. Dr. Edgar Maiß

Thesis project:

Molecular characterization and generation of an infectious full-length clone of a potyvirus from *Melissa officinalis* tentatively named Melissa mosaic virus

September 2007 - June 2011

**B.Sc (Hons) Agriculture**

Major: Plant Breeding and Genetics

**University of Agriculture Faisalabad, Pakistan**

2005 - 2007

**F.Sc (Pre-Medical)**

Major: Biology

**Govt. Post Graduate College Mardan, Pakistan**

2003 – 2005

**Secondary School Certificate**

Major: Biology

**Govt. High School Jalala Mardan, Pakistan**